Design and Development of a Novel Fast Pilot Protection System for Future Renewable Electric Energy Distribution Management Project

by

Xing Liu

A Thesis Presented in Partial Fulfillment
of the Requirements for the Degree
Master of Science

Approved on February 2012 by the
Graduate Supervisory Committee:

George Karady, Chair
Richard Farmer
Raja Ayyannar

ARIZONA STATE UNIVERSITY

May 2012

ABSTRACT

In the future electrical distribution system, it can be predicted that local power generators such as photovoltaic panels or wind turbines will play an important role in local distribution network. The local energy generation and local energy storage device can cause indeterminable power flow, and this could cause severe protection problems to existing simple overcurrent coordinated distribution protection system. An accurate, fast and reliable protection system based on pilot protection concept is proposed in this thesis. A comprehensive protection design specialized for the FREEDM system - the intelligent fault management (IFM) is presented in detail. In IFM, the pilot-differential protective method is employed as primary protection while the overcurrent protective method is employed as a backup protection. The IFM has been implemented by a real time monitoring program on LabVIEW. A complete sensitivity and selectivity analysis based on simulation is performed to evaluate the protection program performance under various system operating conditions. Followed by the sensitivity analysis, a case study of multiple-terminal model is presented with the possible challenges and potential limitation of the proposed protection system. Furthermore, a micro controller based on a protection system as hardware implementation is studied on a scaled physical test bed. The communication block and signal processing block are accomplished to establish cooperation between the micro-controller hardware and the IFM program. Various fault cases are tested. The result obtained shows that the proposed protection system successfully identifies faults on the test bed and the response time is approximately 1 cycle which is fast compared to the existing commercial protection systems and satisfies the FREEDM system requirement. In the end, an advanced system with faster, dedicated communication media is accomplished. By verifying with the virtual FREEDM system on RTDS, the correctness and the advantages of the proposed method are verified. An

ultra fast protection system response time of 4ms is achieved, which is the fastest protection system for a distribution level electrical system.

ACKNOWLEDGMENTS

I would like to express my heartfelt gratitude to my research advisor and mentor Dr. George G. Karady for advising on my research as well as continuing support. His rigorous, meticulous and expertise, have been influential in performing this research work, and also been a great inspiration throughout my entire Master tenure. I would also like to thank my supervisory committee members, Prof. Raja Ayannar and Prof. Richard Farmer for their valuable suggestions and for being on the supervisory committee. I am obliged to the entire faculty of the power systems group at Arizona State University for their guidance inside and outside the classroom.

I am also very grateful to NSF and FREEDM project for providing me this great opportunity to perform research work. I would thank Jim Blake at Alstom, Michael Bryner at National Instrument and Dan Morman at SEL for their generous help towards this research.

My sincere thanks also to my lab mates and all members in our research group for always supporting me. I would like to thank my parents deeply for their support and encouragement during the hard moments. Without you, this couldn't be possible.

TABLE OF CONTENTS

Page

CHAPTER Page

LIST OF TABLES

LIST OF FIGURES

Figure Page

Figure Page

Figure Page

NOMENCLATURE

A	Ampere
A/D	Analog to Digital Converter
AC	Alternating Current
ARP	Address Resolution Protocol
CT	Current Transformer
$\frac{dv}{dt}$	Voltage gradient with respect to time
D/A	Digital to Analog Converter
DAQ	Data Acquisition System
DC	Direct Current
DESD	Distributed Energy Storage Device
DRER	Distributed Renewable Energy Resource
DGI	Distributed Grid Intelligence
DHCP	Dynamic Host Control Protocol
ESD	Energy Storage Device
FCL	Fault Current Limiter
FID	Fault Isolation Device
FREEDM	Future Renewable Electric Energy Delivery and Management
GPS	Global Positioning Satellite
GTO	Gate turn-off Thyristor
HEX2DEC	Hexadecimal to Decimal Converter
HTS	High Temperature Superconductor
ICMP	Internet Control Message Protocol
IEC	International Electrotechnical Commission

IEEE	Institute of Electrical and Electronics Engineers
IEM	Intelligent Energy Management
IFM	Intelligent Fault Management
IGBT	Insulated-gate Bipolar Transistor
IP	Internet Protocol
IRIG	Inter-range Instrumentation Group
J_c	Critical Current density of Superconductor
k	Kilo ($1x10^3$)
kA	Kilo Ampere
kbyte	Kilo Byte
kOhm	Kilo Ohm
kV	Kilo Volt
kVA	Kilo Volt Ampere
K	Kelvin
m	Milli (1x10-3)
mH	Milli Henry
ms	Milli Second
mV	Milli Volt
M	Mega (1x106)
Mbps	Mega bits per second
MHz	Mega Hertz
MS	Microsoft
MVA	Mega Volt Ampere
MW	Mega Watt
n	Nano (1x10-9)

ns	Nano Second
NSF	National Science Foundation
OP AMP	Operational Amplifier
p.u.	Per unit
rms	Root mean square
RC	Resistor-Capacitor
RSC	Reliable and Secured Communication
SFCL	Superconducting Fault Current Limiter
SSFCL	Solid State Fault Current Limiter
SSCB	Solid State Circuit Breaker
SNTP	Simple Network Time Protocol
s	Seconds
SEL	Schweitzer Engineering Laboratories Company
SST	Solid State Transformer
TCP	Transmission Control Protocol
u	Micro (1x10-6)
uF	Micro Farad
uH	Micro Henry
US	United States of America
V	Volt
W	Watt

CHAPTER 1

INTRODUCTION

1.1 Problem Description

Renewable energy is a hot research field and is comprehensively studied by people both from academia and industry in recent years. As the costs of renewable energy have dropped significantly in the past decade, the rapid growing of renewable energy has now become possible. The U.S. Federal government has declared its ambitious goal of the development of the new electric energy, and several radical acts are passed recently in states such as California, Arizona and Texas. All these effects direct to one goal, which is to increase the ratio and the position of green energy amongst the total power production. However, due to the cost and other constraints, it is not likely to build a separate grid independently for the green energy. One common approach is to integrate the renewable generators and their associate devices together with the existing distribution grid and share the same network. When renewable generation resources, like photovoltaic, wind generators and affiliated power electronic devices are integrated to the existing distribution networks, new issues and challenges into the protection system and the reliability of the distribution systems will be encountered.

However, compared with the renewable generation systems, little attention has been paid to the impact of the integration of the renewable devices to the distribution protection system, in which only typical components like electromagnetic transformers and induction machines have been considered. Due to the presence of the power electronic devices, the response of the system under fault condition could be quite different from the existing distribution system. The magnitude of fault current will be limited by power electronic devices, i.e. the maximum current capability of IGBT, and

growing harmonics in the current waveforms can be an issue due to the uses of power electronic switches.

1.2 Future Renewable Energy Distribution Management (FREEDM) Project

This thesis is a part of the FREEDM [1] project. The main objective of the FREEDM project is to develop a smart grid infrastructure that will aid the large scale integration of renewable energy generation into the power grid. The system provides breakthrough technologies in energy storage, distributed control and power semiconductor devices. To demonstrate the various developments, a 1 MW green energy hub supplied by renewable energy resources is under development. The FREEDM system is aimed at enabling the customers to plug-and-generate, plug-and-store energy devices at homes as well as in the factories. Moreover, the FREEDM system also has the ability to manage energy consumption through the load management system [2].

1.3 Motivation and Objective

The typical distribution system is structured in a tree-branch topology and is protected by the traditional 3-segment overcurrent protection: The main feeder is protected by a circuit breaker at the substation terminator. A re-closer is inserted in the middle of the main feeder. The branch feeders are protected by expulsion or current limiting fuses. With current-time coordination, the higher segment will provide backup protection for the lower segment .The major disadvantage of this protection scheme is that if the main feeder fails due to a fault, the whole distribution system will have to be shut down.

Another reason why the traditional protection system will not work for the FREEDM system is that the system topology is completely different. The FREEDM

system is a loop system instead of the typical tree-branch structure. The overcurrent protection coordination will be very difficult to achieve for this loop system.

Another issue is the operation speed of the protection system. The existing power distribution protection system is designed to detect and interrupt possible faults in the system in more than a second. This is because the traditional mechanical circuit breakers, which can only switch off the circuits at current zero crossing point, needs at least a cycle to interrupt the circuit. The development of solid state technology provides another solution of interrupting a fault: the solid state circuit breaker (SSCB) is based on a fast switching solid state switch. With a speed of thousands of switches per second, SSCB is capable of interrupting the fault current within a millisecond. However, unlike the traditional mechanical devices, the solid state devices are fragile and may fail with large fault current for a long time. Moreover, by increasing the speed of the protection system, one can reduce the energy storage requirements of each SST to facilitate load ride through capacity. In that sense, the fast protection aims at minimizing the energy storage requirement and increasing system stability and reliability. Hence, a novel smart protection system specified for FREEDM is needed. This is the main motivation of the research.

The objective of this thesis is to design and implement a protection system which satisfies the fast operation and precise fault isolation requirements of the FREEDM loop system.

1.4 Thesis Outline

The principal content of this thesis has been partitioned into 7 Chapters. Chapter 1 provides an introduction to the problem and presents the objective of the project and the major work of this thesis. The thesis background – FREEDM system is also explained. In

Chapter 2, a comprehensive literature survey consists of stating problems and its mitigation strategies are studied. Common protection schemes are described. The pros and cons of the proposed scheme are then compared. Immediately followed is the development of a novel pilot protection method as a solution, as well as a statement why the existing protection method is not feasible. Chapter 3 presents a zonal protection concept as well as a differential protection scheme, which are the foundations of the following chapters. Chapter 4 presents the feasibility of the differential protection concept with a test of the existing industrial relay by setting up a scaled model of a protective zone and applying one of the fastest commercial relay that has been used widely in industry for transformer protections the SEL387 current differential relay. A complete study of the percentage differential protection both literately and practically is done to demonstrate how a differential scheme works and its feasibility for the FREEDM loop subzone protection. The test results are displayed at the end this chapter to increase the speed over existing methods. Chapter 5 extends the study proposed in Chapter 4 for FREEDM loops intelligent fault managements. A faster and more accurate protection algorithm which uses the differential unit as the primary protection and current as the back-up protection is presented. This system is an implementation of the proposed protection scheme. In Chapter 5, a real time protection program is developed based on Labview. Its performance and response to various situations are analyzed and discussed in detail. Chapter 6 continues with the development of IFM algorithms by extending the protection system simulation to a scaled, physical test bed with the analog merging unit (AMU), which does the data acquisition and digitization job. Preliminary protection results are presented. For Chapter 7, a new system, which successfully solves the communication and synchronization issue, as an improved hardware implementation, is discussed. The final result is presented. An ultra-fast protection system response time of

4ms is achieved, which is the fastest protection system for distribution level electrical systems. In the end, the conclusions and possible extensions of future work are shown in Chapter 8.

Appendices A-C provides supplemental information on the studies carried out in this research. Appendix A is the relay code that is used for chapter III experiment. Appendix B presents the IFM protective algorithm. Appendix C shows the full IFM software with data communication and data processing blocks that help the IFM program cooperates with the AMU.

CHAPTER 2

LITERATURE REVIEW

This chapter gives a comprehensive summary of the previous work that has been done by researchers on protection system techniques, integration of renewable energy and its impact on the protection system.

2.1 Development of Renewable Energy

Renewable energy, including solar photovoltaic, wind generator, biomass and others have been studied ever since the early 1960s. Hughes, W. L.; Summers, C. S.; Allison, H. J published their concept of “Energy System For The Future” [3]. In which the feasible new source of energy including solar, wind, tide and fusion were presented as accessorial source to the existing power system. After that, during the past few decades, a large volume of research has been conducted and many papers have been published. In the early 1980s, the economic and socioeconomic aspects of the application of renewable (solar) energy sources for rural development in resource-poor, population-rich, developing countries in order to accelerate the use of local renewable energy sources were investigated [4]. The author claims that if such possible sources were effectively used, the cumulative impact of even small amounts of intermittently available energy in rural areas can be considerable.

Renewable energy systems [5] provide a viable way to obtain green, sustainable and environment friendly energy. The two major renewable energy sources, wind and solar, are considered as key components and are included in the FREEDM system.

2.2 FREEDM System

The envisioned FREEDM System is a revolutionary power grid based on power electronics, high bandwidth digital communication, and distributed control technology [6]. There are 2 features that made the FREEDM system radically different from today's

grid: One is that it replaces electromagnetic transformers with solid state transformers. Another feature in this system is that the solid state based protection devices will replace conventional mechanical switches. The power flow control provided by the solid state transformer allows the plug-and-play of the distributed generation and also allows for the addition of storage and loads to the grid with no adverse effects on nearby users. The solid state transformer will provide unmatched power quality improvement to residential users and industry customers. In this way, the total energy efficiency of FREEDM is improved. In the FREEDM system, every energy user is not only limited to be a customer, but also can be able to act as a participator of energy production.

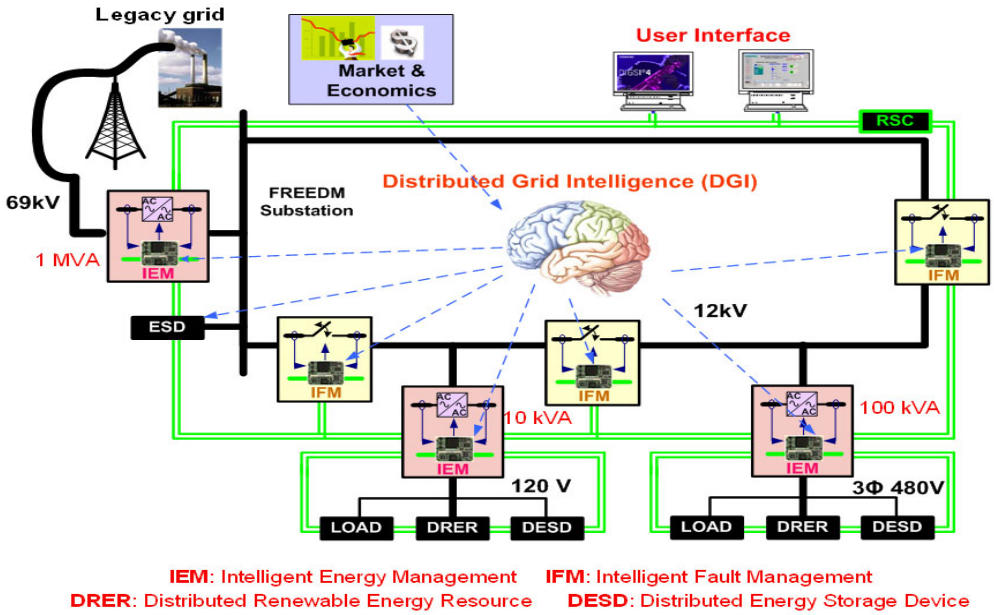

Fig. 2.1. FREEDM system [6]

Fig. 2.1 shows, the sensing, measurement and control devices with two-way communications to electricity production, transmission, distribution and consumption parts applied throughout the distribution network. In this way, the smart grid is established.

As a smart grid, the FREEDM system delivers electricity from suppliers to consumers using digital technology with two-way communications to control appliances

at consumers' homes to save energy, reduce cost and increase reliability and transparency.[7] Another proposed smart feature is the monitoring system - intelligent energy management (IEM), which keeps track of all power flow in the system. Renewable resources such as solar and wind are integrated by the intelligent energy management system. The idea is by monitoring the power flow status, the IEM can provide advisory operation command basic upon real time energy price.

In this system, low voltage smart loads are connected to a regulated 120VAC. Low voltage Distributed Renewable Energy Resource (DRER), Distributed Energy Storage Device (DESD) and loads are connected to the 12kV bus through a highly efficient, power electronics based Solid State Transformer (SST). A SST is a three port system (one AC in, one DC out, one AC out) which performs bi-directional energy flow control and other power management control functions.

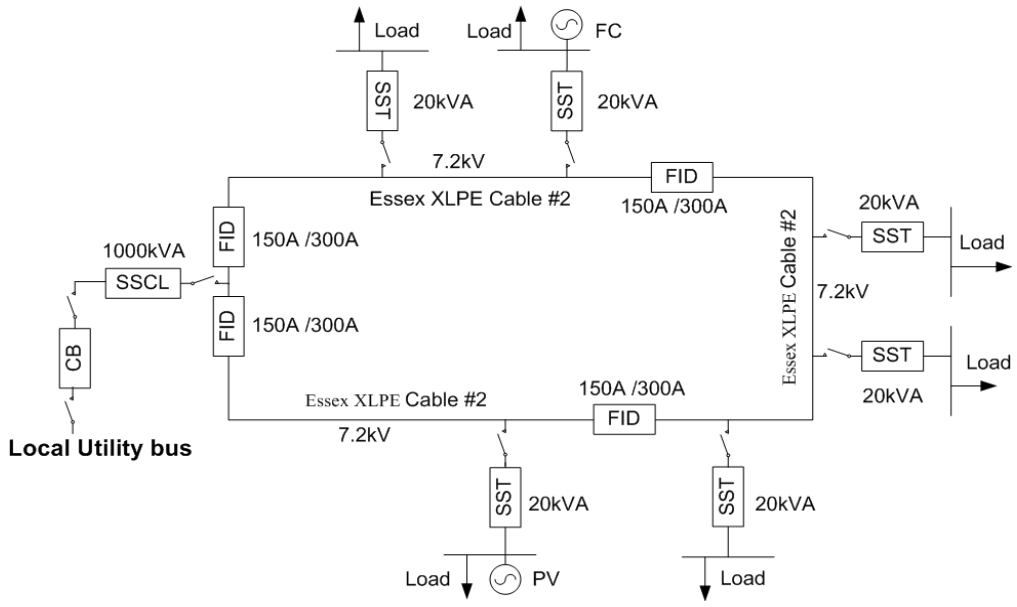

Fig. 2.2. Single line diagram of FREEDM system [8]

The 12kV main loop will connect to the existing, traditional power transmission grid through a higher rated regular transformer or SST. This improves system reliability in the event of failure or insufficient of any DSER or heavy load. On the other hand, in

the event of the unavailability of the power grid from transmission line fault or system failure, the FREEDM system can operate independently as a smart grid. Coordinated control of the FREEDM system is achieved through the Distributed Grid Intelligence (DGI) software programmed into each IEM and IFM. The DGI could be considered the brain of the whole FREEDM loop since it performs total energy management and power balancing functions inside the loop.

2.2.2 Solid State Transformer

The Solid State Transformer (SST) [9] is one of the key elements in the FREEDM systems. The SST converts the voltage just as the conventional transformer. However, the traditional 60Hz transformer is replaced by a high frequency transformer, which provides fault isolation and step up/down function plus the power electronics converters. This is the key component to achieve size and weight reduction and the power quality improvement. Each SST will have bi-directional energy flow control capability allowing it to control active and reactive power flow and to manage the fault currents. Fig. 2.3. shows a topology of SST applied in FREEDM. The SST also provides the plug-and-play feature for distributed resources to rapidly identify and respond to changes in the system.

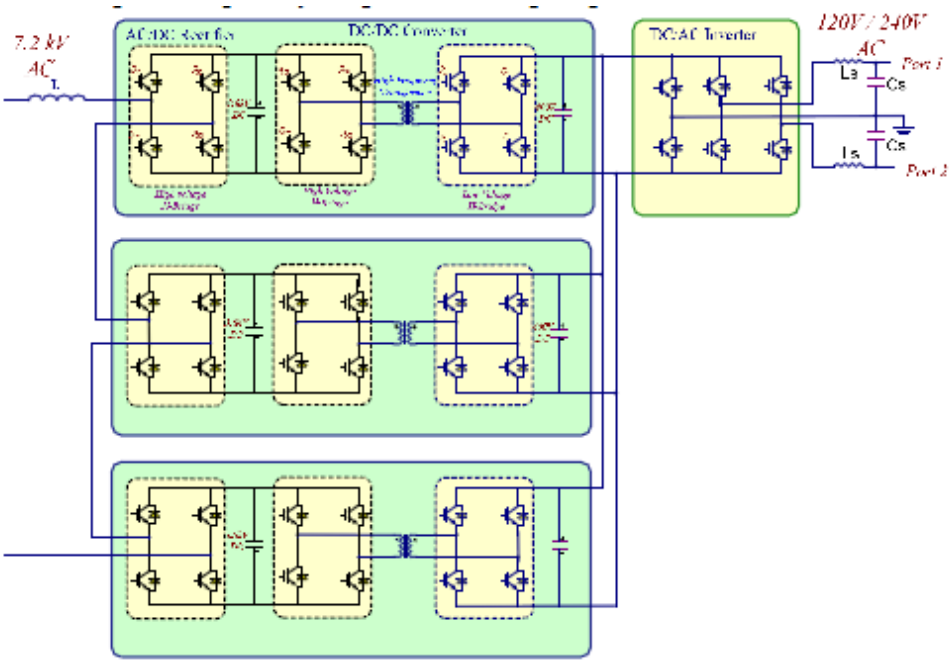

Fig. 2.3. Topology of proposed 20kVA Solid State Transformer [9]

2.2.3 Solid State Circuit Breaker

Solid-state circuit breakers (SSCBs) [10], based on modern high-power capability semiconductors, offers considerable advantages when compared to mechanical circuit breakers in both speed and life. Its topology is shown in Fig. 2.4. For instance, voltage quality of a power grid can be improved during a short circuit because the fault current is reduced. The interval over which voltage distortions occur, caused by a three-phase short circuit, can be limited to a few 100µs. In contrast, present circuit breaker technology requires at least 100ms to clear a fault. The major disadvantage that limits SSCB to wide employ are the cost and on-state losses.

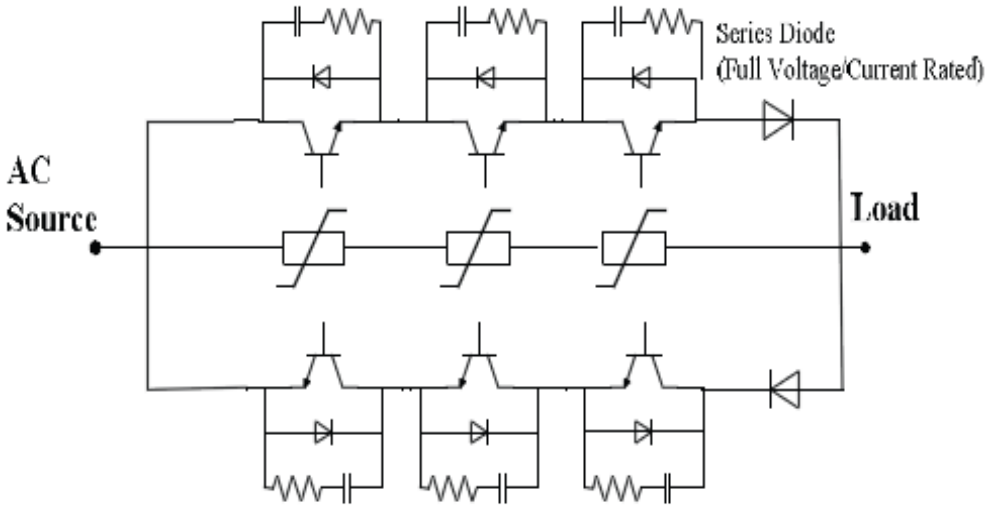

Fig. 2.4. SSFID Topology [10]

2.3 Development of Power Protection System

2.3.1 Introduction to Protection System

It's accepted that electric power system is the backbone of economic development [11]. And the protection system is the backbone of electric power system. In the event of an abnormality in any section of the power system network, it is essential to isolate the faulty section from the healthy sections, otherwise the spread of the high-magnitude current and voltage-collapse will adversely affect the healthy section and may result in a major blackout. The protection system is design to detect intolerable or undesirable conditions. Thus, the protection system must be reliable, fast in operation and easily maintainable.

2.3.2 Development of Protective Relays

Fig. 2.5 shows the brief development history of the protection system. It is generally divided into 4 stages: electron-magnetic relaying, static relaying, digital relaying and the novel intelligent relaying and network relaying for 21st century.

Around the 1980s, it was recognized that numerical devices have more powerful capabilities than electro-magnetic and semiconductor devices. And the new scheme should make an effort to remove the summation current transformer, and perform the current summation function by numerical technology.

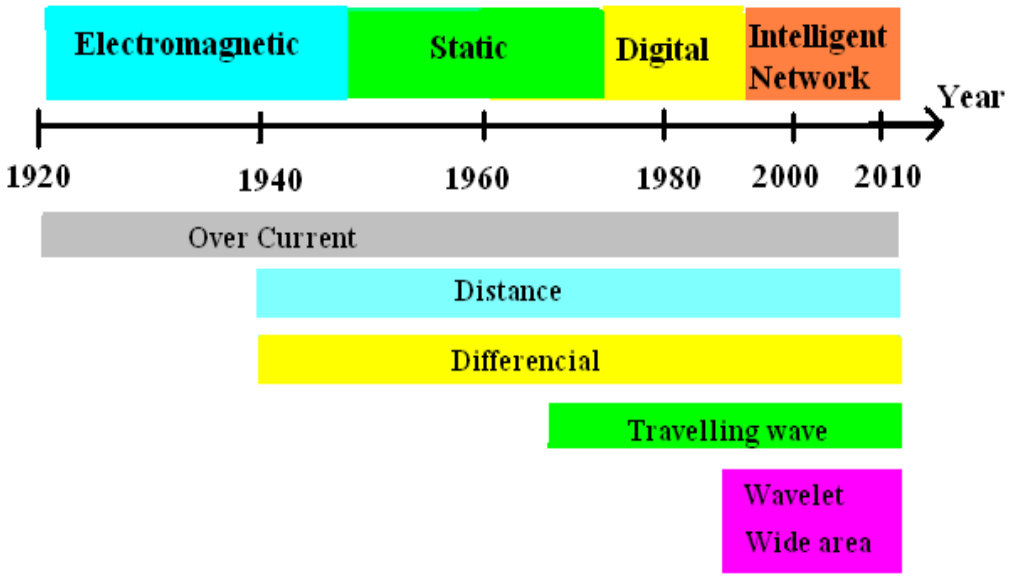

Fig. 2.5. Development of power system protection

With the rapid progression of technology, there has been a great development for power system protection since the first electro-mechanical over-current relay was applied at the beginning of the last century. The protection devices had evolved from electro-mechanical to semiconductor, to integrated circuit and to microprocessor technologies. Now, microprocessor based digital relays have gradually replaced old relays in power systems.

During the past two decades, the rapid development of digital computers makes more complicated numerical techniques become possible. For ultra-high-speed protection, transient wave protection schemes and wavelet analysis method became popular and started to come into use recently. Fault detection is performed by numerical relays which

consist of a Digital Signal Processor (DSP) with additional measuring circuits and output circuits. From the history of the protection system development, we can expect progressive improvement in protection schemes with increasing speed and processing power of computers in the future.

Novel integrated and intelligent network based protection schemes were proposed at the beginning of the 21st century and represents an attractive advancement for power system protection.

2.3.3 Operainge Quantities

Operating Quantities are these quantities which represents power system conditions directly and indirectly. The relay monitors one or several quantities and applies them to the protective algorithms, and then determines fault.

Table 2.1. Operating quantities

Magnitude	Frequency duration
Phase angle	Rate of magnitude change
Wave shape	

2.3.4 Faults

Typically, there are 4 kinds of faults which may occur in the power system:

Table 2.2. Types of fault

Balanced three-phase short circuit	Single phase-ground short circuit
Two-phase short circuit	High impedance

The operating quantities will be much different with different kinds of fault. The protection system is supposed to distinguish fault type and send the correct trip signal to the corresponding CB based on the type of fault.

2.3.5 Protection Zones

In reality, the power system is divided into different protective zones, such as generator protection, transformer protection, transmission line protection, motor protection, busbar protection and etc. Notice that the overlapping of zones avoids blind areas.

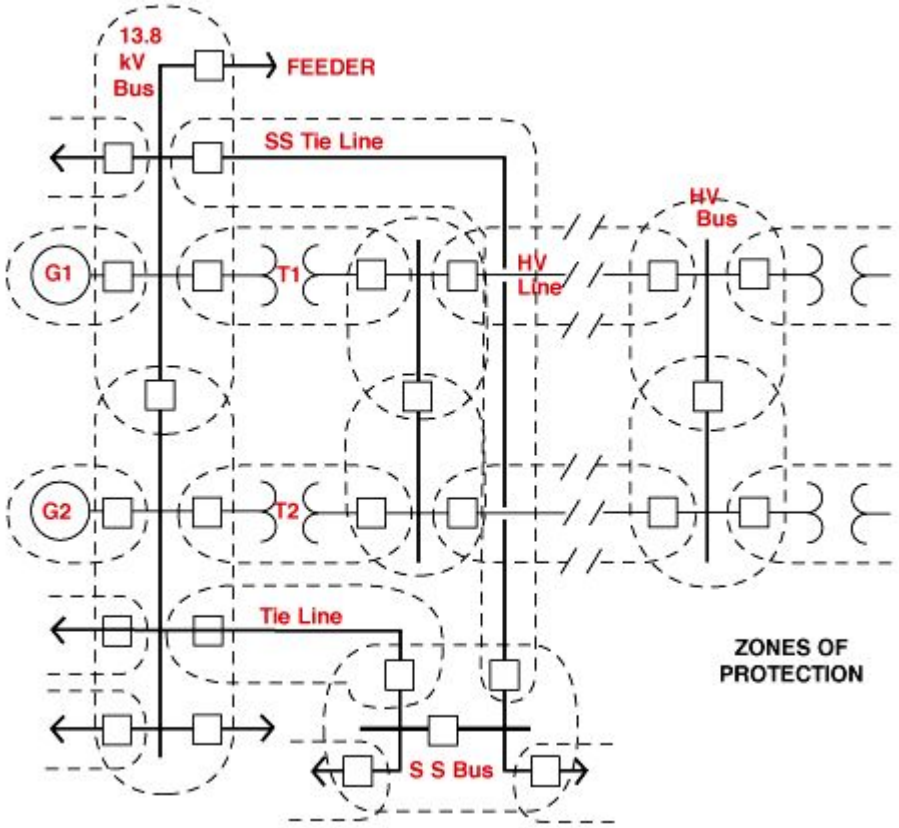

Fig. 2.6. Protection zone of an electrical power system [12]

The Fig. 2.6 above shows a portion of a typical small power grid system. Two generators feed power to a 13.8 kV generator bus. Two transformers deliver power from this bus to two transmission lines and ultimately to the remote loads. The generating station has high-voltage switchgear which feeds power to these transmission lines and routes that power over alternate paths during emergencies or during routine dispatching

operations. Circuit breakers are provided to permit any part of the system to be removed from service and still deliver power to the major loads. These circuit breakers are the devices which are controlled by the protective relays. The relay scheme may be quite elaborate, with various levels of back-up and overriding protection, covering all possible contingencies. Manual control of each breaker is provided as well. The compartmentalization of zones helps isolating faults as well as fast response.

2.3.6 Protection System Back up:

The reason for introducing protective back up is to increase the reliability of power systems. Generally, there are 6 kinds of backup for power system shown in the table below

Table 2.3. Protection back up system

Relay back up	duplicate device
Breaker back-up	duplicate CBs
Remote back-up	overlapping zone

2.4 Protection schemes

2.4.1 Over-current relays

Generally speaking, there are two kinds of overcurrent relays:

a. Instantaneous overcurrent relay: These relays work without intentional time delay. The logic unit trips directly when the current reaches the threshold (shown in Fig. 2.7). They are widely used in feeder's protection. The instantaneous overcurrent relay is also very useful for protecting electrical equipment against short circuits, especially for high fault current.

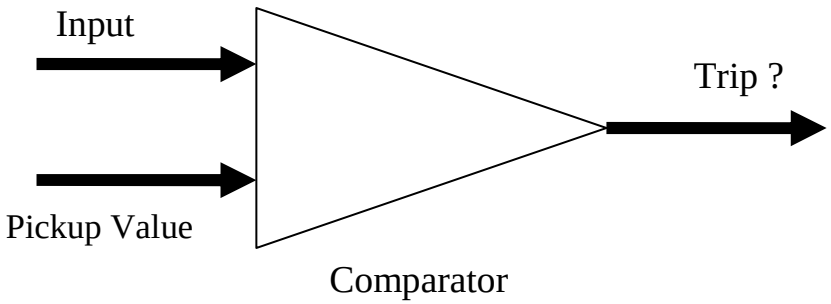

Fig. 2.7. Logic diagram of instantaneous overcurrent scheme [13]

b. Time-delayed overcurrent relays: a time-graded system is applied to implement the back-up protection. Time-current curve implies that the operation time is inversely proportional to the fault current. If the fault current is higher, the relay should operate faster. The general equation is:

$$\tau = \frac{K}{[(PSM)^n - 1]}$$

Where τ = operation time

PMS= plug multiplier setting

K,n= preset constants.

There are two settings that must be applied to all time-delay overcurrent relays: one is the pickup value, and another is the time delay. Time-delay overcurrent relays are designed to produce fast operation at high current and slow operation at low current. Hence, the curve follows an inverse time characteristic. Relays from different manufacturers may have different inverse time characteristics. Fig. 2.8 shows the IEEE standard pick up curves for overcurrents relays.

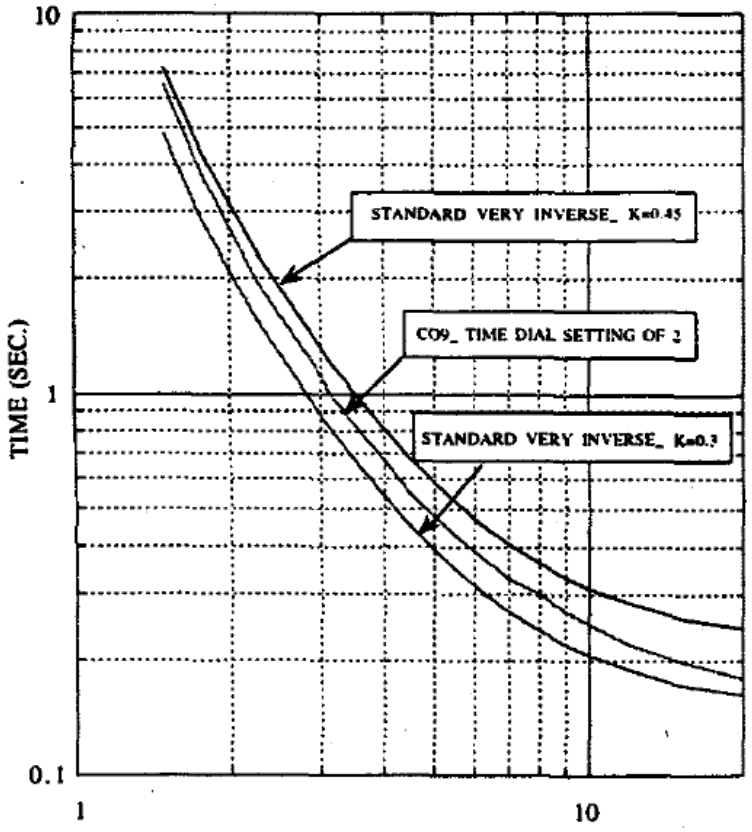

Fig. 2.8. IEEE Standard Inverse-Time Characteristic of overcurrent relays [14]

Overcurrent protection scheme is widely used in the conventional distribution protection system because it's simple, low cost, easy to coordinate and reliable. Fig. 2.9 below shows coordination of a typical overcurrent relay coordination system: in this system, relay 1 relay 2 and relay 3 are employed with different curves for coordination. Relay 2 provides backup for relay 3, relay 1 provides backup for relay 2 and relay 3. Its disadvantage is that it is not feasible for complex energy networks since it only measures current at one location, the pick-up time coordination will be very difficult to achieve.

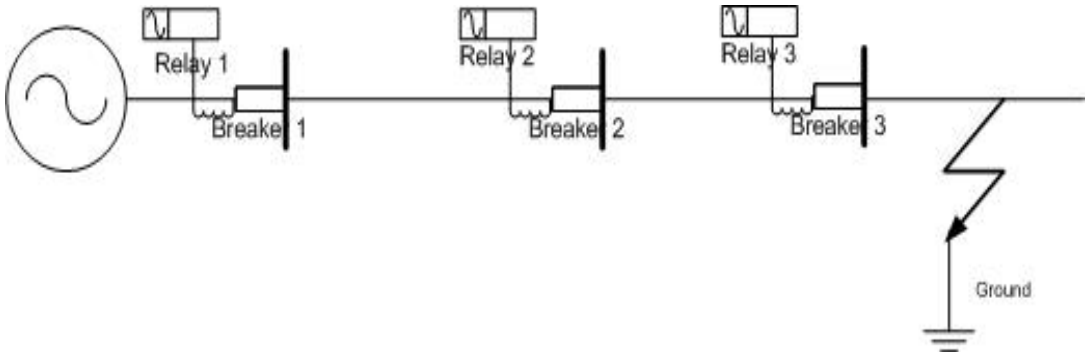

Fig. 2.9. Overcurrent relay coordination system [15]

2.4.2 Differential Relays

Differential protection scheme is one of the fastest schemes that is widely used for key component protection in power system for generators, transformers and buses.

2.4.2.1 Principle of current differential relay

The working principle of a conventional differential scheme is that the pick up current is equal to the difference of the currents coming to the operating coil, and its working principle is by Kirchhoff's current law.

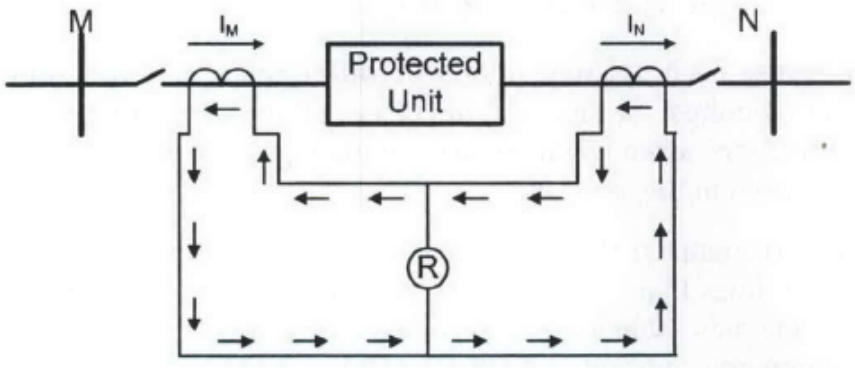

Fig. 2.10. Normal condition of a differential protection scheme[16]

For normal conditions, the currents at each side of the relay are exactly equal in magnitude and opposite in phase. As a result, there is no differential current through the relay as shown in Fig. 2.10.

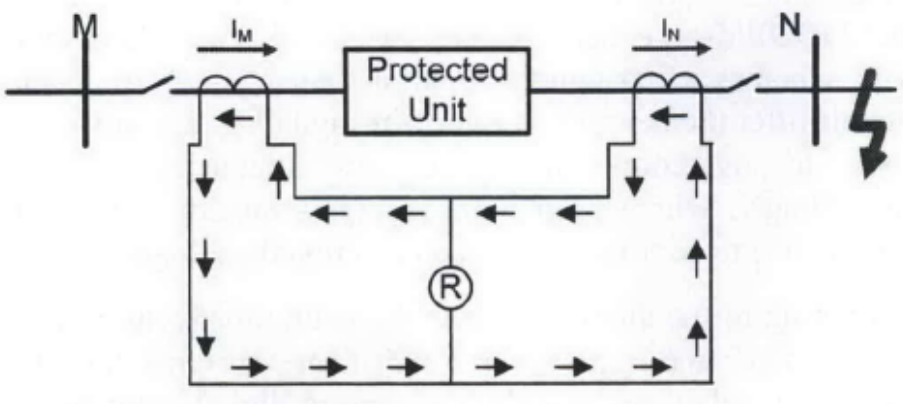

Fig. 2.11. External fault condition of a differential protection scheme[16]

When a fault happens out of the protective zone, there is still no current flowing into the relay since the current in both sensor increase equally, as shown in Fig. 2.11.

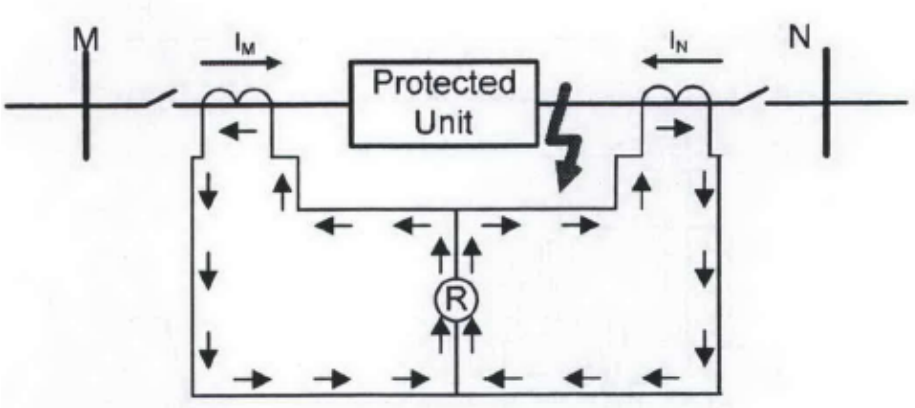

Fig. 2.12. Internal fault condition of a differential protection scheme[16]

When a fault happens within the protected zone, the current I_M will no longer equal to I_N. As a result, imbalance current is generated and the relay take actions, as shown in Fig. 2.12.

The differential scheme ensures absolute discrimination since the CTs employed are nearly identical and will have the same output under saturation.

2.4.2.2 Percentage Differential Relay

The conventional percentage differential has two coils: one is the restraining coil, while the other is the operating coil. The bias or percentage is defined as

$$Bias = \frac{(i1 - i2)}{(i1 + i2)/2}$$

The operation condition is

$$Iop = \frac{(i1 - i2)}{(i1 + i2)/2} > preset\ bias\ current$$

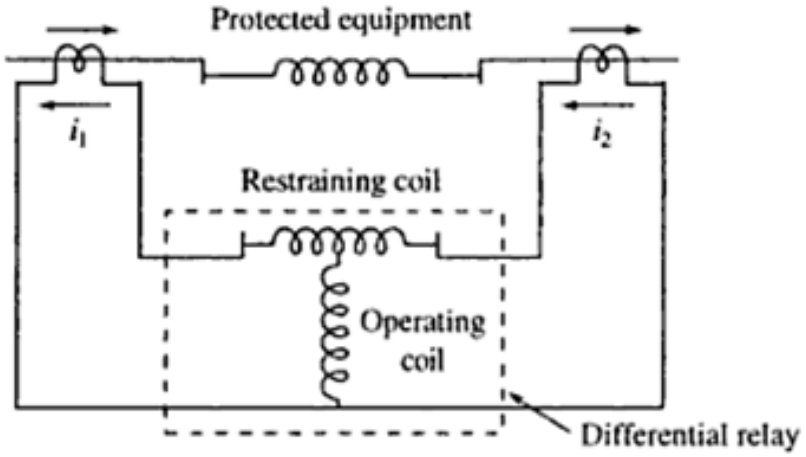

Fig. 2.13. Percentage differential relay [17]

The percentage differential relay is able to prevent unwanted mismatch. See Fig. 2.13.

2.4.2.3 Pilot Protection

The traditional protection solution is instructive to compare protective systems used for EHV transmission lines, all of which share some common characteristics. These systems utilize a communications path to send signals from the relaying system at one end of the line to that at the other end. The working principle is very simple: the two relays compare the current at each terminal of the transmission line. If the two currents are equal, which means there is no fault on the transmission line. When the two currents are not equal, there must be a fault in the transmission line. The pilot protection concept is shown in Fig. 2.14.

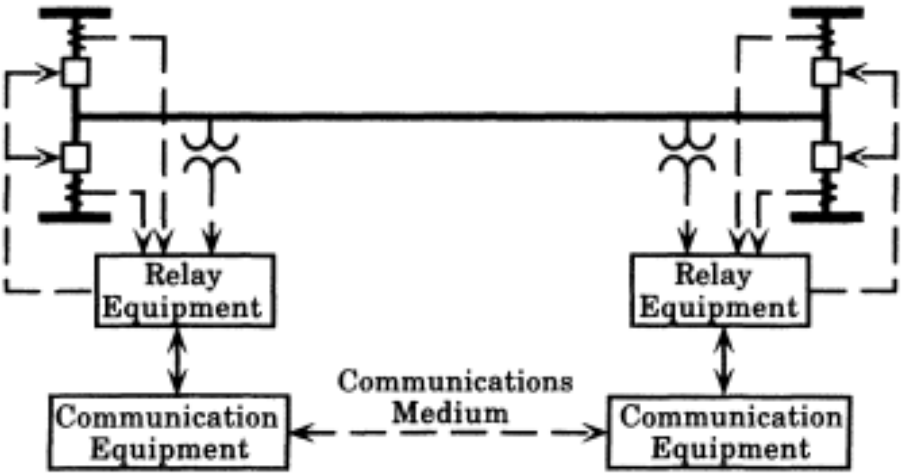

Fig. 2.14. General view of pilot protection [18]

Communication is the major challenge for pilot protection. Pilot-wire relaying is an analog system using only current measurements with the relays interconnected between each end using telephone-type copper cable. Recently, digital representation of analog currents can be sent between each end on a per-phase basis. According to the latest research, the IEC 61850 GOOSE message standard is a designated communication solution for substation automation as proposed by Richard Hunt, Mark Adamiak from GE Energy Inc.. As in Fig. 2.15. [20]

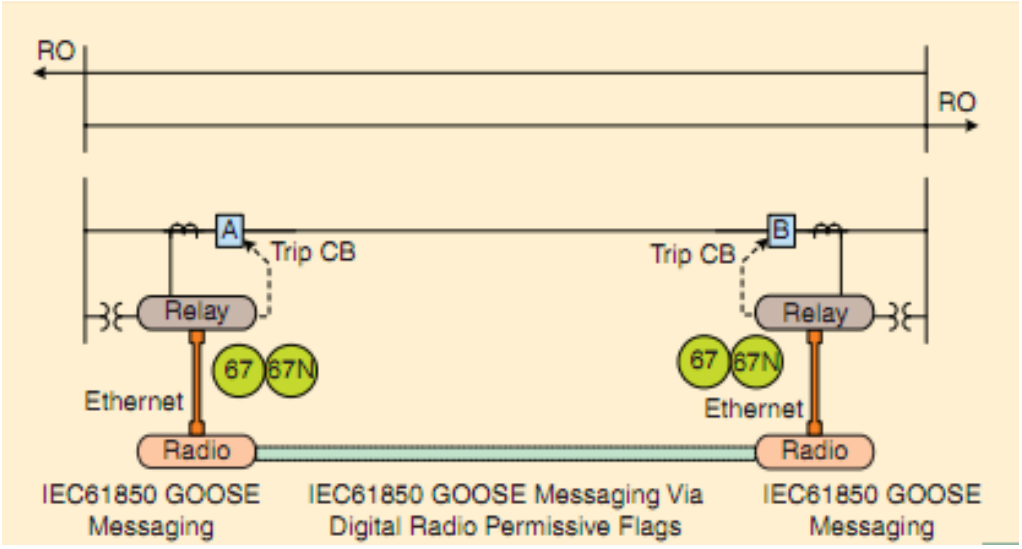

Fig. 2.15. pilot protection with IEC 61850 [19]

2.5 Directional overcurrent protection

For smart gird application, Abhisek Ukil and Bernhard from ABB proposed a directional overcurrent protection method as a solution to smart gird [20]. The nondirectional overcurrent relays are the widely used ones in power distribution side protection for radial and ring-main units. The directional overcurrent relays rely on a reference voltage phasor, for estimating the direction of the fault current. Considering a smart grid connecting an upstream power source to a downstream power distribution system, the forward fault happens between the relay and the line, and the backward or reverse direction between the source and the relay (shown in Fig. 2.16). When a fault occurs, the fault current has a characteristic phase angle relative to the voltage phasor. The fault direction is determined by judging the current phasor against the reference voltage phasor measured at a location on the power line. This requires measurement of both current and voltage, hence the cost is higher.

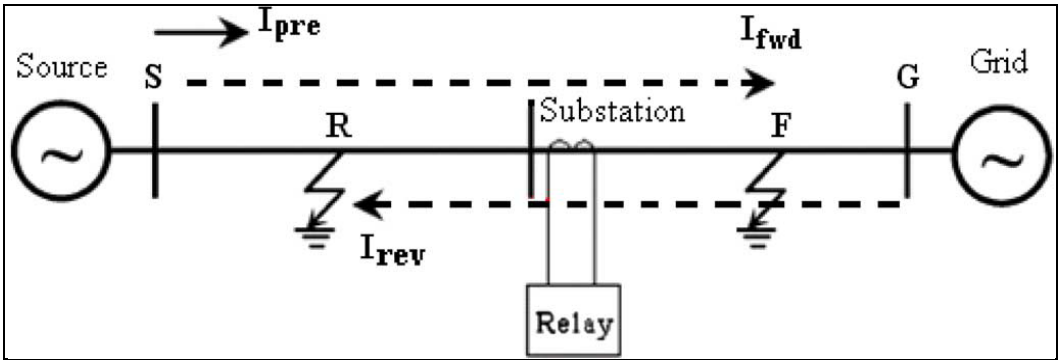

Fig. 2.16. Direction overcurrent relay: forward and reverse fault [20]

2.6 Protection scheme for FREEDM

From all protection methods discussed above, over-current protection is not feasible for the FREEDM system because of coordination issues and slow response. The

zonal division concept could help us to simplify the FREEDM topological structure. The pilot protection strategy is the choice for the FREEDM project for its precise fault identification feature and fast response. Therefore, the communication media needs to be determined. The differential protection scheme could be applied to solve the multiple input problem for complex networks. Thus, a pilot- differential hybrid protection scheme would be a good choice for the FREEDM system. Meanwhile, the directional overcurrent can be considered as a backup scheme.

CHAPTER 3

DESIGN OF THE FREEDM PROTECTION SYSTEM

In this chapter, fault cases that may happen in FREEDM system and features of FREEDM are analyzed in detail. The pilot protection system as well as zonal protection division concept is introduced. The percentage differential protection strategy as a key protection algorithm concept is also discussed in detail.

3.1 Fault Features of Solid State Device

With the presence of solid state power devices, such as SST and SSCB, the fault current waveform will no longer be the same as the fault waveform in traditional power systems. Fig 3.1 shows the simulation result of a short circuit current on the 7.2 kV single phase line. The current limiter produces a square shape current with about 130A amplitude. Without the current limiter, the short circuit current would be more than 1000A. The current limiter limits the fault current magnitude, but brings some issues to the protection system.

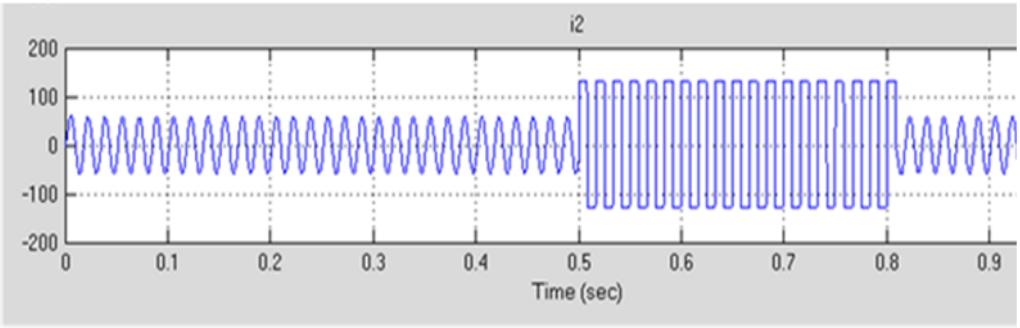

Fig. 3.1. Short circuit on the 7.2 kV line produced current [21]

From the Fig.3.1, we can obtain that with the FCL or SST the magnitude of the fault current is limited to approximately 2 times the normal current, which would be 5-10 times without solid state devices.

Typically, the total current is the sum of the large square wave current and much smaller sinusoidal components. The result is a distorted wave with high harmonic content.

3.2 FREEM System Faults and Solutions

Faults can happen in various locations of the FREEDM system (shown in Fig. 3.2 and Table 3.1).

Table 3.1. Possible faults in FREEDM

SST fault	Component failure in the solid state transformer
Distribution system fault	Short circuit in the loads
Local generation fault	Fault at distributed generators
Line fault	Short circuit to ground in the 7.2kV line

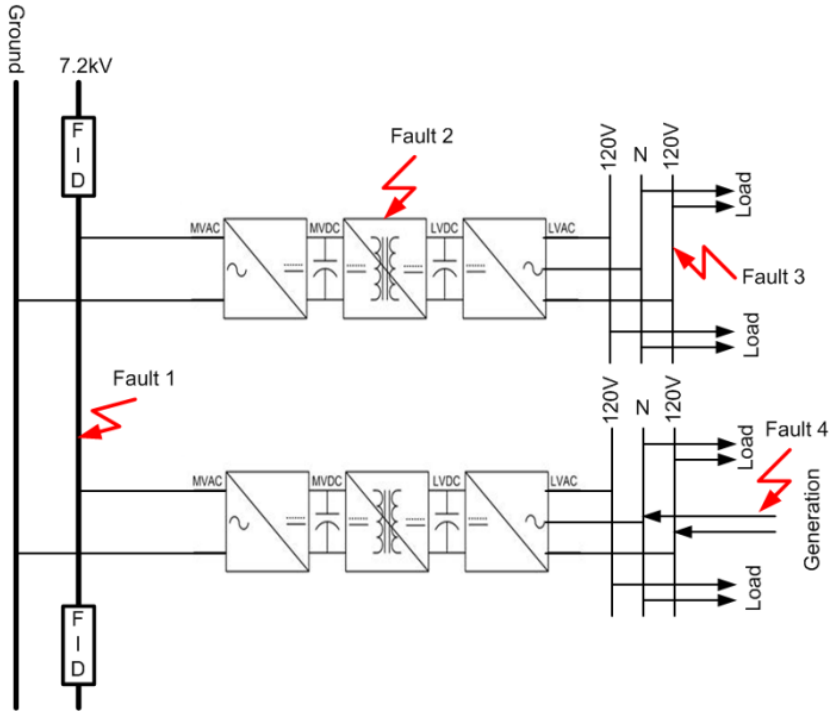

Fig. 3.2. Possible fault locations [21]

The solutions to different fault situations are shown below:

3.2.1 SST Fault

SST is equipped with internal sensors, which shuts down the converters by removing the gate signals in case of component fault. In addition, SST is equipped with

over current protection, which blocks the converters. This results in the reduction of SST produced current to zero and output voltage collapses. The adjusted fault current value for SST fault is 1.8-2 times the rated current.

The SST is also equipped with under voltage protection, which also blocks the converters when the high voltage supply voltage is reduced. The adjusted fault voltage value is 0.8 times the rated voltage.

3.2.2 Distribution System Fault

Loads, operating at 120V bus, are protected by conventional magnetic circuit breakers. The SST protection provides backup protection. The SST can sense the load fault but shutdowns with a delay. The SST short circuit current is limited to twice the rated current.

3.2.3 Local Generation Fault

Local generation has internal protection, which blocks the converters in case of internal fault. The internal fault reverses the current direction, which makes its detection easy. In addition, local generators have over-current protection which operates with a delay in case of load fault. It provides backup protection in case of a 7.2 kV line fault.

3.2.4 Line Fault

For the 7.2kV backbone line fault protection, the freedom loop is divided into sections. The number of sections depends on the loads/local generation. The section must be self supporting. If a fault occurs in the section, the two FIDs (electronic circuit breakers) must clear the fault immediately. Simultaneously an outside fault should not initiate FID operation.

3.3 FREEDM System Protection Scheme

3.3.1 Intelligent Fault Management (IFM) Program

IFM is a comprehensive protective program that is running continuously in the central computer. It is utilized to improve the reliability of the FREEDM system by isolating potential faults on the 12kV bus. The IFM is the brain of the FREEDM loop, it communicates with the IEM through a Reliable and Secured Communication (RSC) network and monitors the whole system. When a fault happens in the system, the IFM detects the fault location and sends the trip signal to the corresponding FID which will perform the function of isolating the fault.

3.3.2 Protective Zone Dividing

The FREEDM loop is divided into several zones in order to accomplish fast protection and fault isolation, refer to the protection zonal division concept discussed in Chapter 2. Each zone is isolated by a Fault Isolation Device (FID) on both terminals and the loads and distributed generators are connected to the main loop through the solid state transformer (SST). When a fault happens inside a zone, the FID at the two terminals will operate, thus the fault is isolated from the main loop. The SST will also turn off so that the load or local generator will not be affected. The compartmentalization of zones in FREEDM loop helps isolate faults as well as it gives a fast operation response.

A fast differential pilot protection scheme acts as the primary protection in each zone. The outer zone provides the back-up protection for the whole system. The analog merging units (AMU)[22] are distributed at the each terminal of the distribution line and the SST primary side, to measure the current magnitude information at every measurement point and send them back to the IFM. This protection system arrangement for a zone is shown in Fig.3.3.

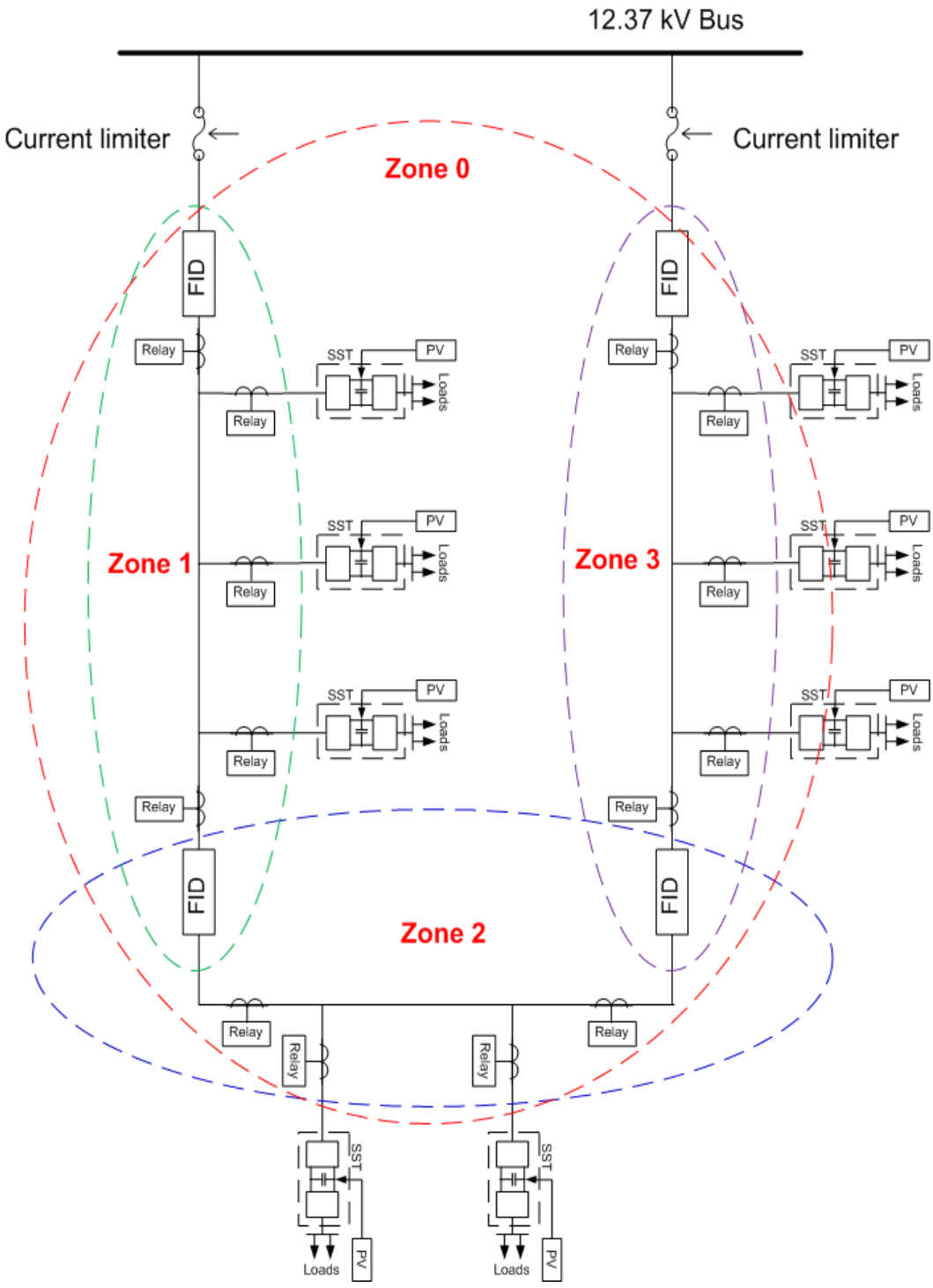

Fig. 3.3. FREEDM protection strategy [8]

3.3.3 Protection Concept of Zone

For every protective zone, the differential protection scheme is employed as the primary protection. The idea is that the IFM constantly exams all current in the zone, if

the sum of currents in a zone is zero, it implies that either there is no fault or the fault is outside the zone. Else, if there is a fault within the zone, the IFM will send a trip signal to FIDs and SSTs in this zone. FIDs are located at the terminals of the zone and response for isolate the fault in the zone, The SSTs, which is connected to the loads and local energy generations, will shut down the load in case of fault. Since the SST is a solid state device, there is very negligible switching time delay for the SST. The protection system for every single zone is shown in Fig. 3.4 blow:

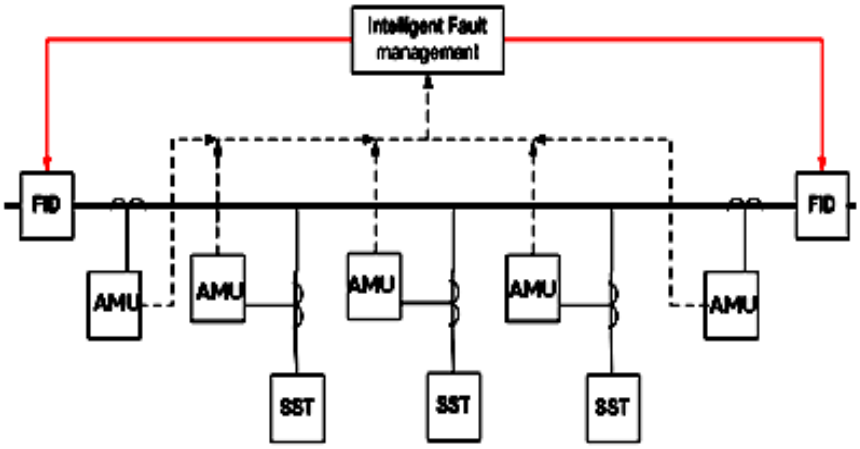

Fig. 3.4. IFM system and AMU[8]

The IFM program, which implements the protection schemes, is the brain of the protection system and running on a section computer for system monitoring, fault identification and trip signal generation. The AMU, composed of microcontroller, measures system current at the current transformer (CT), converts the analog value into digital form and sends the digital data to the section computer via digital communication system. GPS (Global Positioning System) [25] clock is added to implement the synchronization of data digitization between several AMUs.

Since the execution time of the IFM program is within milliseconds and can be neglected, The key point of the protection speed is very much depend on the AMU ability. This requires a high speed microcontroller and a very high speed communication medium.

Currently a microcontroller operating at a frequency of 25 MHz is considered and the proposed communication is through Ethernet [26]. The Ethernet cable connects the microcontroller to the computer, through an Ethernet switch. The medium of communication in the cable is regular 100Mb Ethernet cable. The full schematic of the proposed digital protection system is shown in Fig. 3.5.

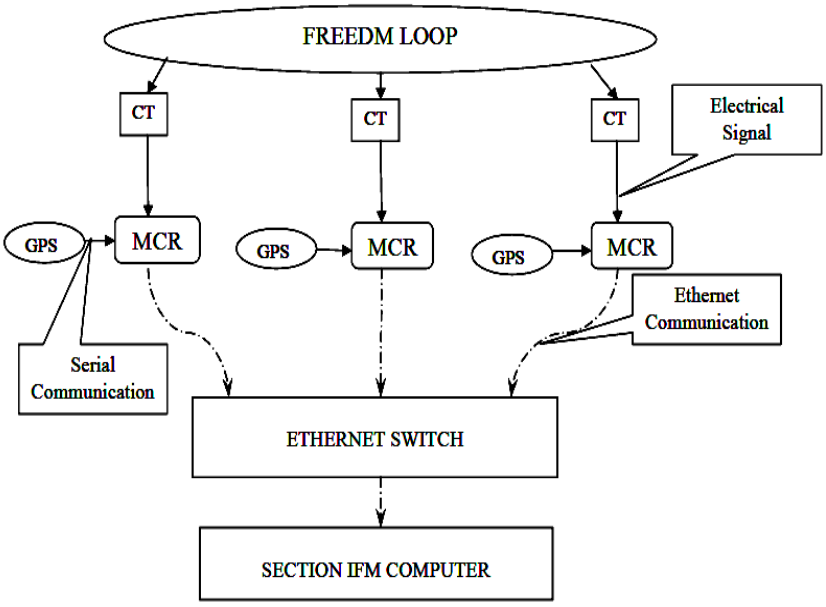

Fig. 3.5. Schematic of the proposed digital protection system

Moreover, as in Fig. 3.3, zone 0 acts as the backup protection zone for the zones 1, 2, and 3. The measured current values from these three zones are compared and the same difference of these values is calculated at the central IFM. The coordination between the outer zone IFM and zone 1, 2 and 3 IFM is done in a simple way: the outer zone has the longest fault evaluation time (5-10 times then the subzones). In this way, the zone 0 will only act when subzone fails, which provides backup protection for FREEDM loop.

3.3.4 Summary

A novel hybrid protection system as a solution for FREEDM system smart gridd is presented. From the concept, the loop system will be divided into sections. Each

section will be protected by a multi- terminal differential protection system, which employs the differential protection strategy as primary protection, overcurrent protection strategy as backup. And the outer zone provides the backup for every zone. The synchronization of distributed AMUs is implemented by the GPS clock. The GPS clock sends high frequency pulses (1k/s) to every AMU, and AMU makes every sample with a pulse.

3.4 Differential Protection Algorithm

3.4.1 Current polarity and vector sum calculation

The CT measured current signal is converted to a voltage signal with a small resistor. The reference directions for currents on the primary terminal and voltages at the secondary terminals are shown. If the primary input current is the same direction with the reference direction, the voltage signal at the secondary resistor is positive. Else, the secondary voltage signal will be negative.

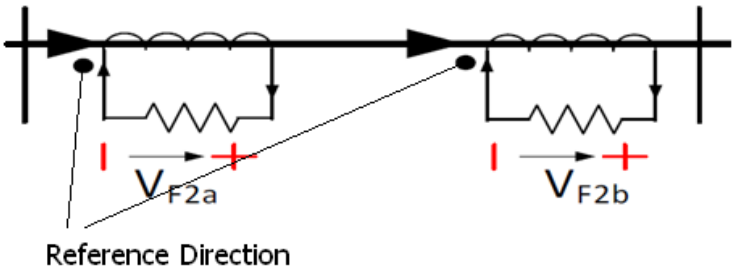

Fig. 3.6. CT reference direction

As the reference direction determined in the Fig. 3.6, according to the Kirchhoff's Current Law, we have

$$V_{F2b} - V_{F2b} = 0 \quad (1)$$

The simulation result is shown below. As in the Fig. 3.7, for the sample points with same time stamp, we have A1-A2=0 and B1-B2=0. The simulation result satisfies

the equation (1).

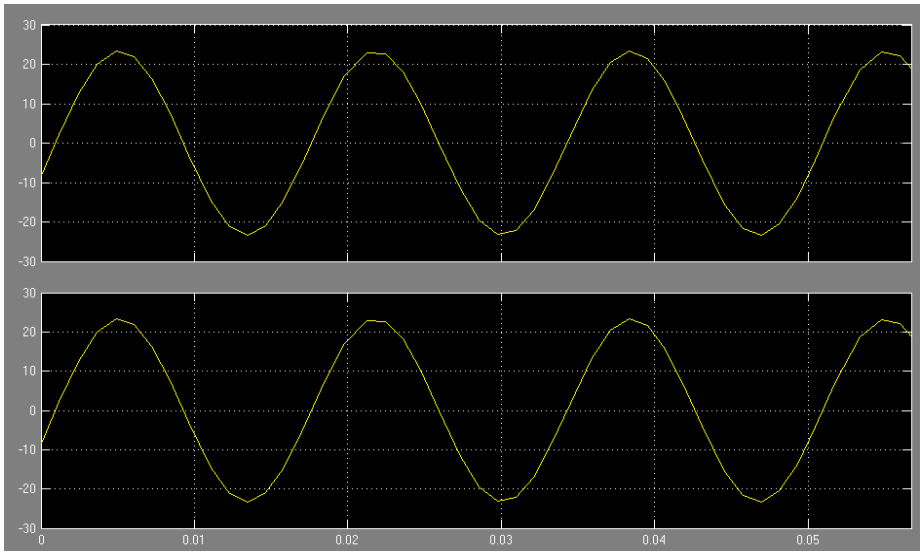

Fig. 3.7. Simulation result

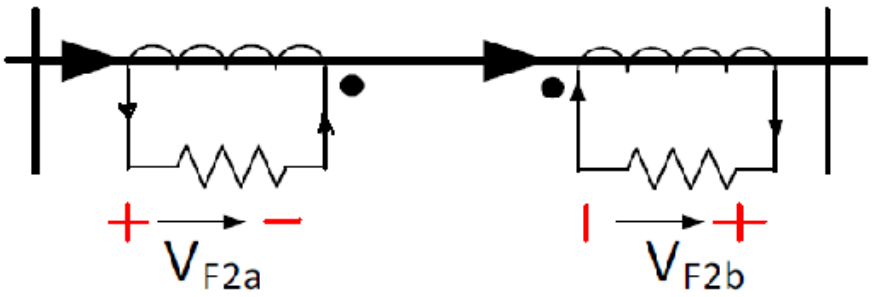

Fig. 3.8. Simulation result

In case that the reference direction changed in the Fig. 3.8, according to the Kirchhoff's Current Law, we have

$$V_{F2a} + V_{F2b} = 0 \qquad (2)$$

The simulation result is shown below. As in the Fig. 3.9, for the sample points with same time stamp, we have A1+A2=0 and B1+B2=0. The simulation result satisfies the equation (2).

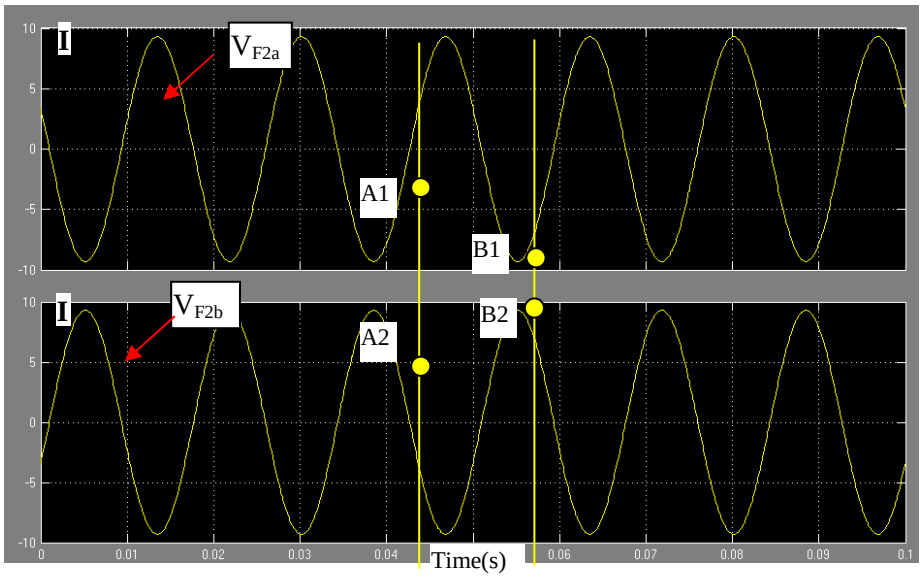

Fig. 3.9. Simulation result

Thus, together with Kirchhoff's Current Law, the reference direction determines the current vector sum calculation.

3.4.2 The Percent-slope Characteristic

For modern differential protection that are widely applied in the industrial areas, the differential elements and percent-slope characteristic [23] are employed to improve the selectivity and security of the current differential scheme. The differential element includes an operation quantity which is the summation of currents from all measurement points, a restraint quantity which is the absolute magnitude sum of all the currents, and a differential ratio (the slope) which is defined as the outcome of the operating quantity divided by the restraining quantity (Fig. 3.10).

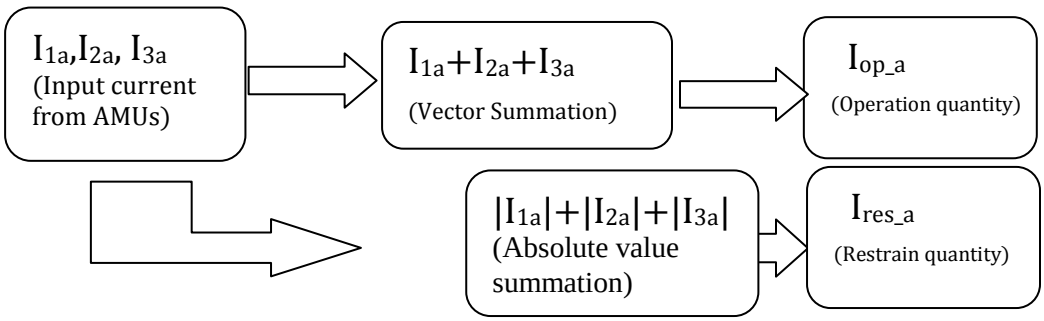

Fig. 3.10. Differential elements calculation procedure

Where $I_i a$ stands for the current value at the measurement point i, phase A;

Iop_a stands for the operation quantity, phase A;

Ires_a stands for the restrain quantity, phase A.

For input currents to the differential protective unit, it calculates the differential elements first, and then compares the result with the differential percent-slope characteristic (shown in Fig. 3.11). If the result is located in the operation region, the differential protection unit outputs a result “fault = true”, else, the output will be “fault = false”. In this way, the fault is determined.

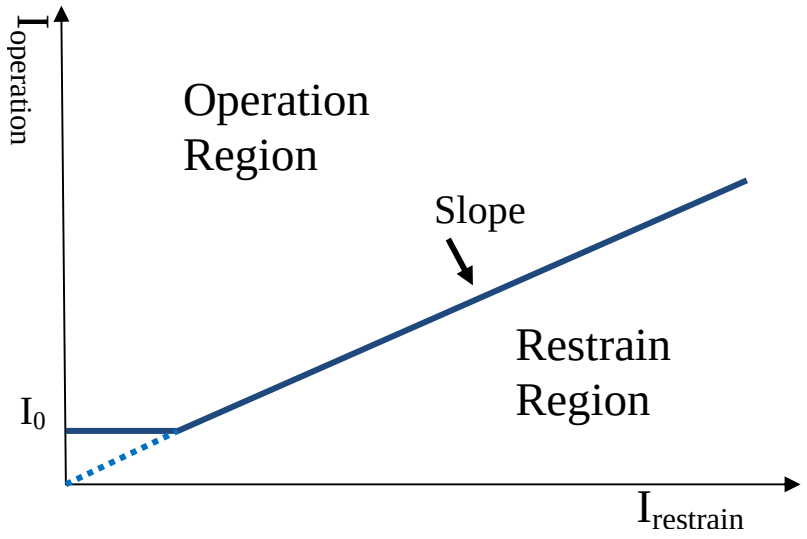

Fig. 3.11. Percent-slope characteristic

The criteria of Percent-slope characteristic can be expressed as:

$$I_{op} - S_0 \cdot I_{res} > 0 \quad (3.1) \quad \textit{and} \quad I_{op} > I_0 \quad (3.2)$$

Where $I_{op} = |\sum_{i=1}^{m} \dot{I}_i|$

$$I_{\mathrm{Res}} = \sum_{i=1}^{m} |\dot{I}_i|$$

m equates to the total number of measurement points,

I_i stands for the current value at each measurement point

S is the default slope coefficient

I_0 is the minimum operating current

Compared to Iop and Ires, I0 is relatively small, thus we can approximately have:

$$I_{op} - S_0 \cdot I_{res} - I_0 > 0 \qquad (3.3)$$

In equation 3.3, the criteria of 3.1 and 3.2 are both satisfied.

The differential algorithm judgment can be expressed as:

$$|\sum_{i=1}^{m} \dot{I}_i| - S_0 \cdot \sum_{i=1}^{m} |\dot{I}_i| > I_0 \qquad (3.4)$$

Introducing the equivalent slope *S*,

$$Let \quad S = \frac{|\sum_{i=1}^{m} \dot{I}_i| - I_0}{\sum_{i=1}^{m} |\dot{I}_i|} \quad £ 3.5£ ©$$

the differential protection criteria can be simplified as

$$S > S_0 \qquad £ 3.6£$$

which is convenient for numerical calculation.

The percent-slope characteristic helps prevent undesired relay operation resulting from abnormal power flow like load switching on/off, CT error and CT saturation under heavy external fault.

3.4.3 Case Study

The case study shows the detailed work process of differential algorithm and how it distinguishes faults. For the percentage differential protection algorithm, as defined in Fig. 3.10, the Iop stands for the operation quantity, which is the vector sum of all input current. Ires stands for the restrain quantity, which is the absolute value sum for all input currents. Notice that the Ires have multiplied a coefficient 20%. Typically, the recommended slope percentage value is between 10% - 30%. Then we can calculate the differential algorithm result under different situations that may occur during operations.

a. For the two terminal system, in case that a fault happens inside the zone, as shown in Fig. 3.12

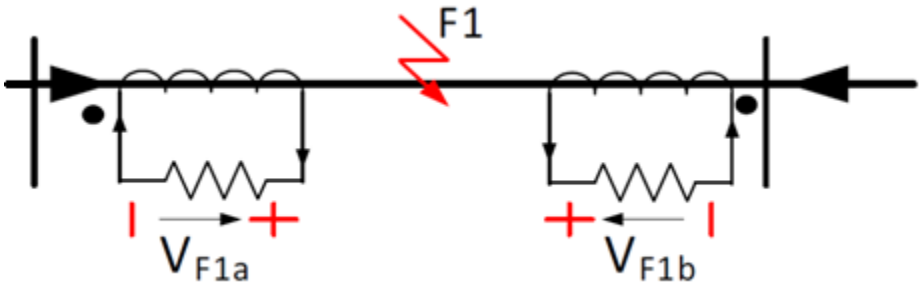

Fig. 3.12. Fault in the system

The simulation result is shown in Fig. 3.13, however, the results no longer satisfies the equation (1).

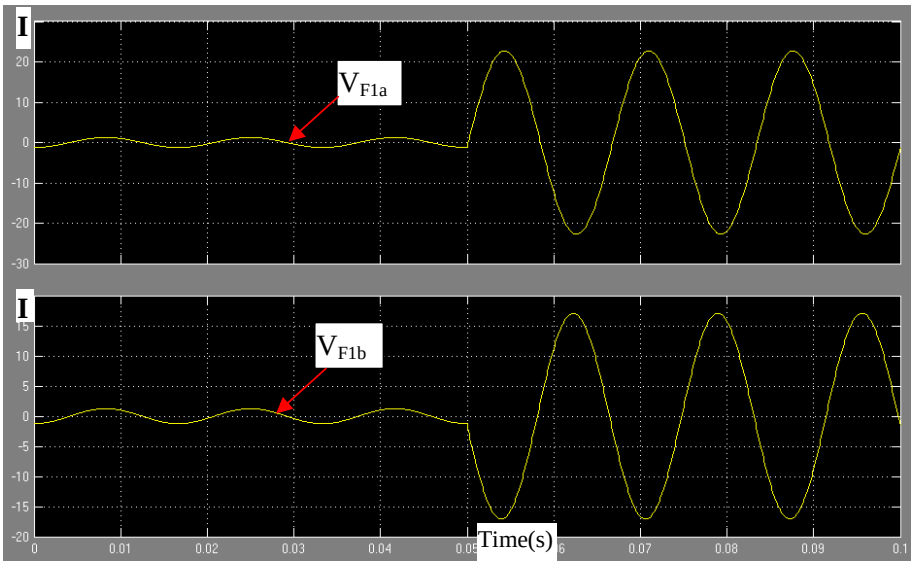

Fig. 3.13. Simulation results

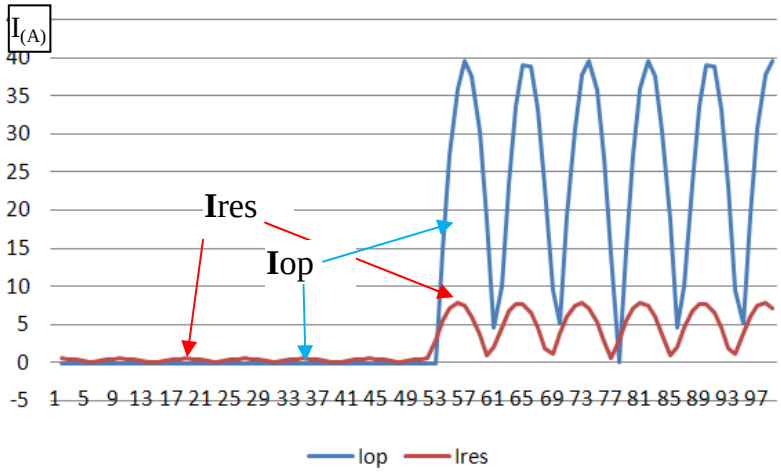

Fig. 3.14. Percentage differential calculation result

As in the Fig. 3.14, before the fault, the operation signal is small than the restrain signal. When a fault is initialed, the operation signal became larger than the restrain signal, which indicates the inside fault is inside the zone. As a result, a trip signal will be generated.

b. For the two terminal system, in case that a fault happens outside the zone as in Fig .3.15 below:

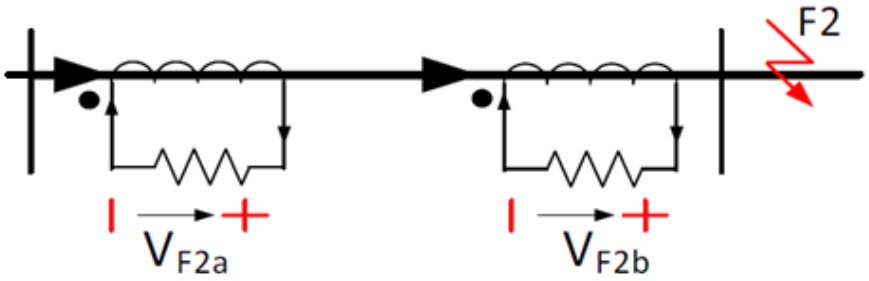

Fig. 3.15. Fault outside the system

The simulation result is shown is Fig. 3.16:

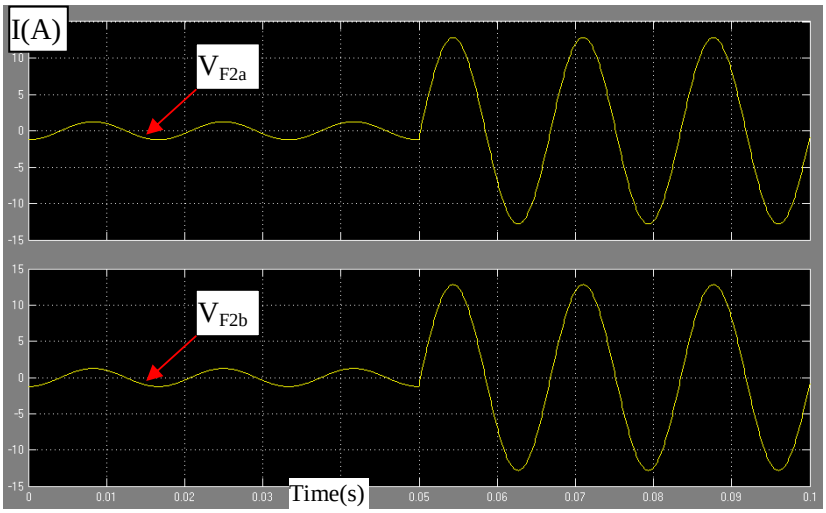

Fig. 3.16. Simulation result

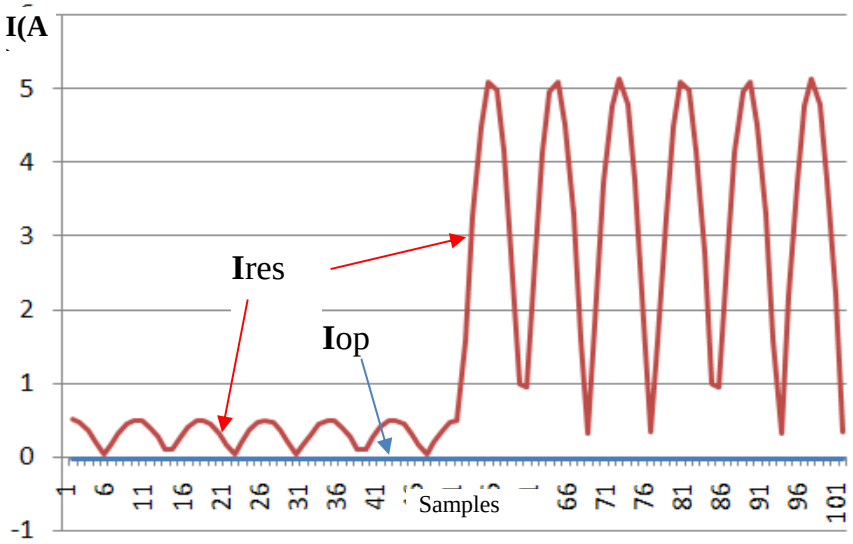

Fig. 3.17. Percentage differential calculation result

As in the Fig. 3.17, before the fault, the operation signal is smaller than the restrain signal. When a fault is initialed, the operation signal is still smaller than the restrain signal, which indicates the inside fault is outside the zone. As a result, no trip signal will be generated.

c. For the 3 terminal system, as show below, A simple single zone with 3 measuring point, two sources and a load, is analyzed in this case, as in Fig. 3.18.

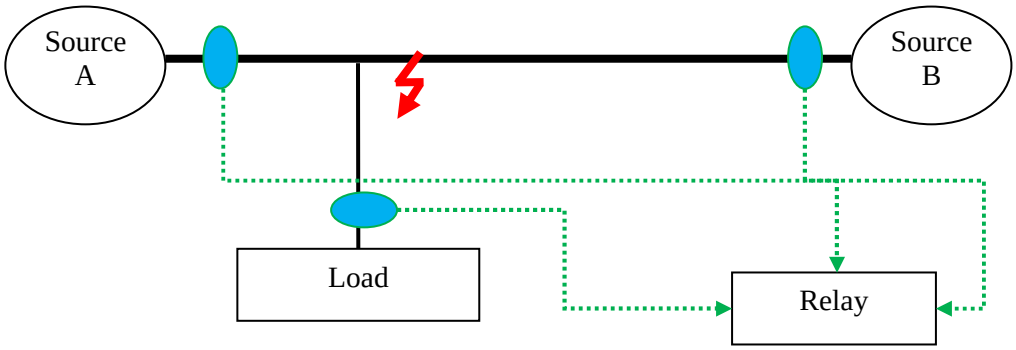

Fig. 3.18. Virtual single zone

The simulation result is shown below:

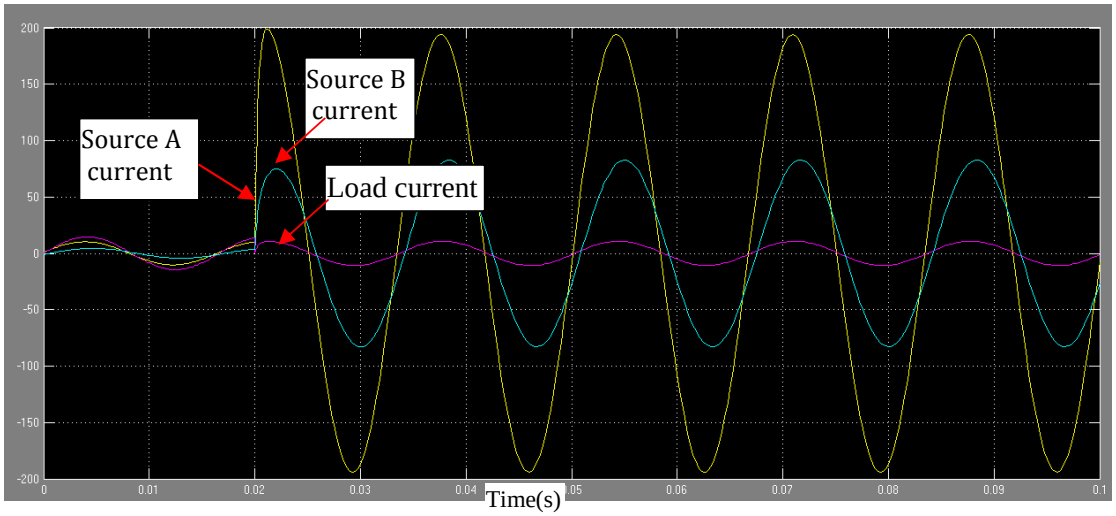

Fig. 3.19. Simulation result

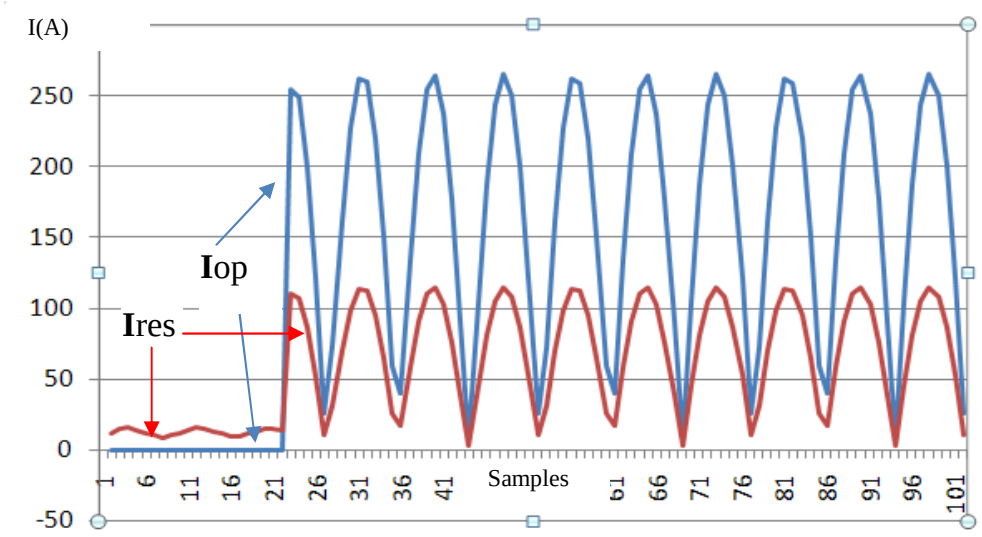

Fig. 3.20. Percentage differential calculation result

As in the Fig. 3.20, before the fault, the operation signal is small than the restrain signal. When a fault is initialed, the operation signal became larger than the restrain signal, which indicates the inside fault is inside the zone. As a result, a trip signal will be generated.

d. For 3 terminal system, when fault outside the zone at source B:

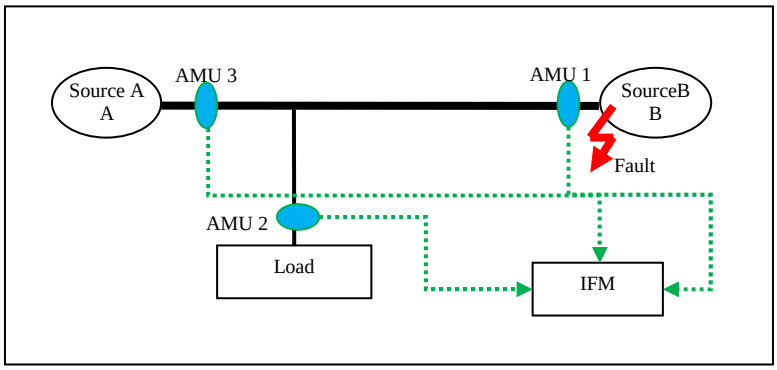

Fig. 3.21. Fault at Source B

The simulation result is shown below:

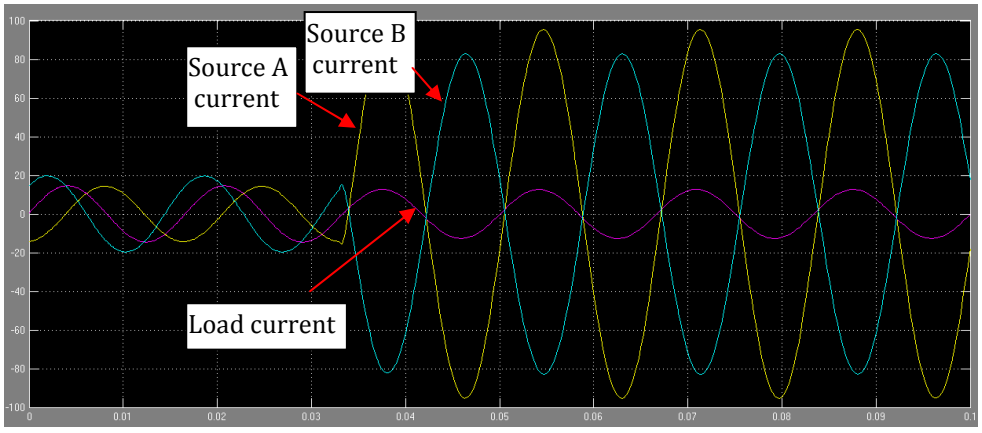

Fig. 3.22. Simulation result

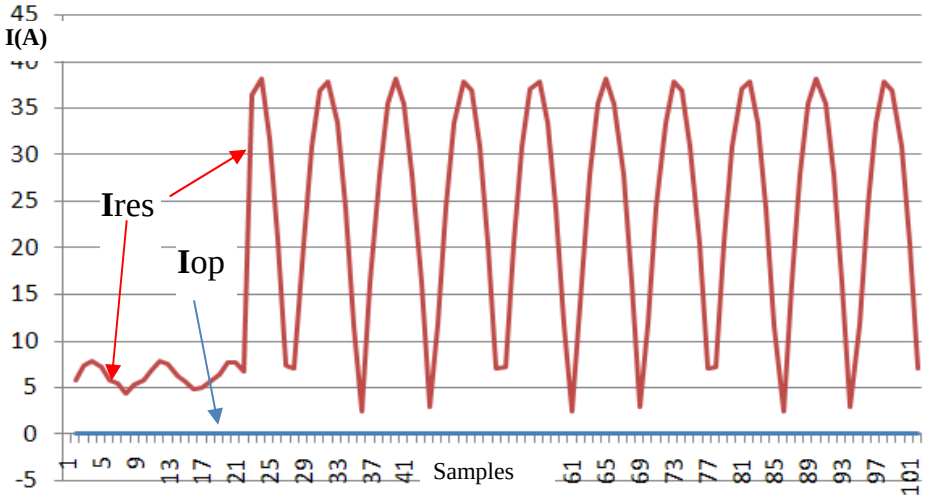

Fig. 3.23. Percentage differential calculation result

As in the Fig. above, the operation signal is always smaller than the restrain signal, which indicates either there is no fault or fault outside the zone. No trip signal will be generated.

e. When fault happens at the load:

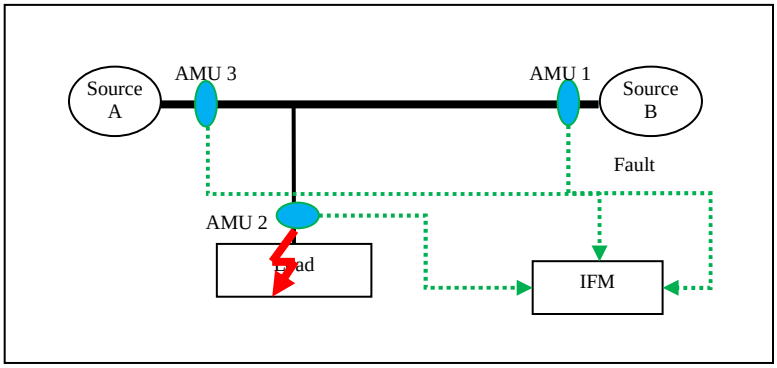

Fig. 3.24. Fault at Load

The simulation result is as in Fig. 3.25:

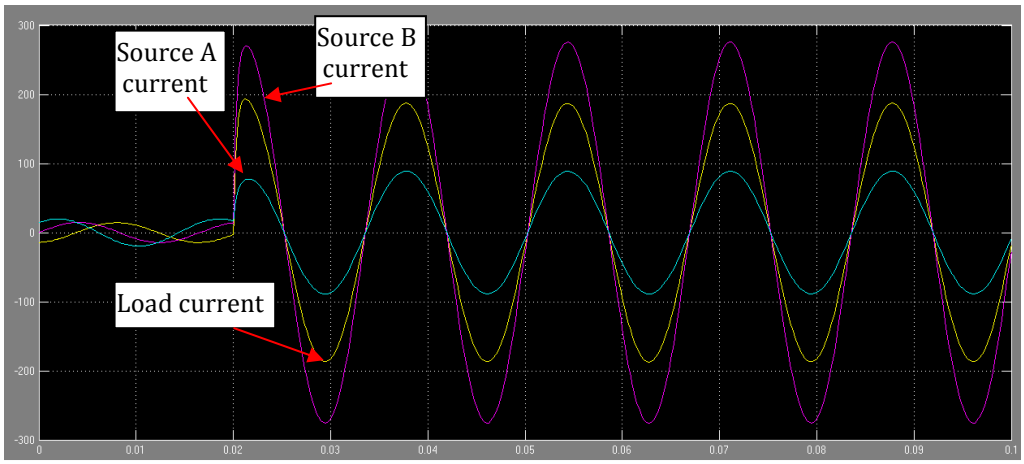

Fig. 3.25. Simulation result

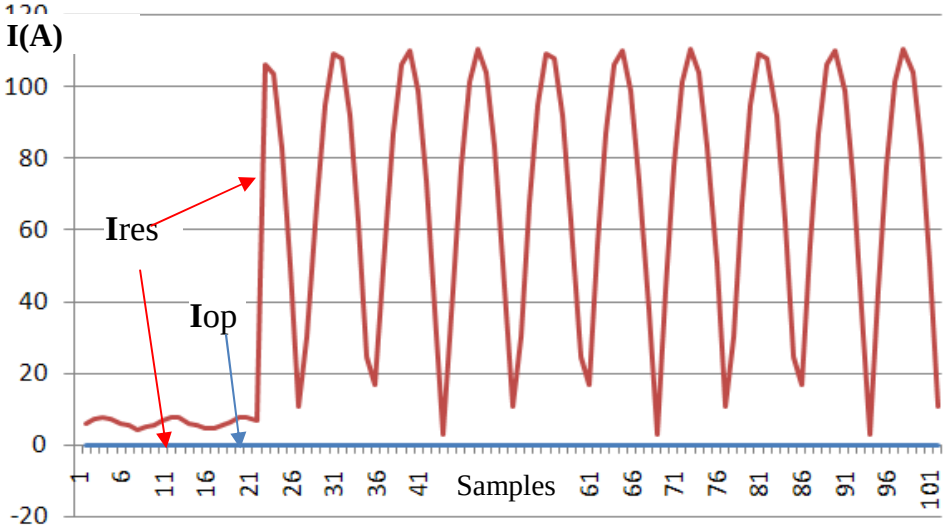

Fig. 3.26. Percentage differential calculation result

As in the Fig. 3.26, the operation signal is always smaller than the restrain signal, which indicates either there is no fault or fault outside the zone. No trip signal will be generated.

3.4.4 Summary

From the differential protection concept, we can see that the sensitivity of the percentage differential protection strategy is depending on the characteristic slope. The percent-slope characteristic helps prevent undesired relay operation and mismatch. And the percent-slope characteristic, unlike the over-current protection strategy, has no

magnitude-time curve relationship which will cause time delay. So fast, accurate protection is attainable.

CHAPTER 4

TEST OF COMMERCIAL DIFFERENTIAL AND OVER-CURRENT PROTECTION SYSTEM

This chapter presents an experimental test of the differential concept with a commercial relay and a test-bed which models a single FREEDM zone. The result proves the validity and feasibility of the proposed protection scheme and also gives an industrial benchmark.

4.1 Single Zone Physical Testing-bed

A scaled physical model of single FREEDM zone (Fig. 3.8) has been built, the full test-bed picture is shown in the Fig.4.1.

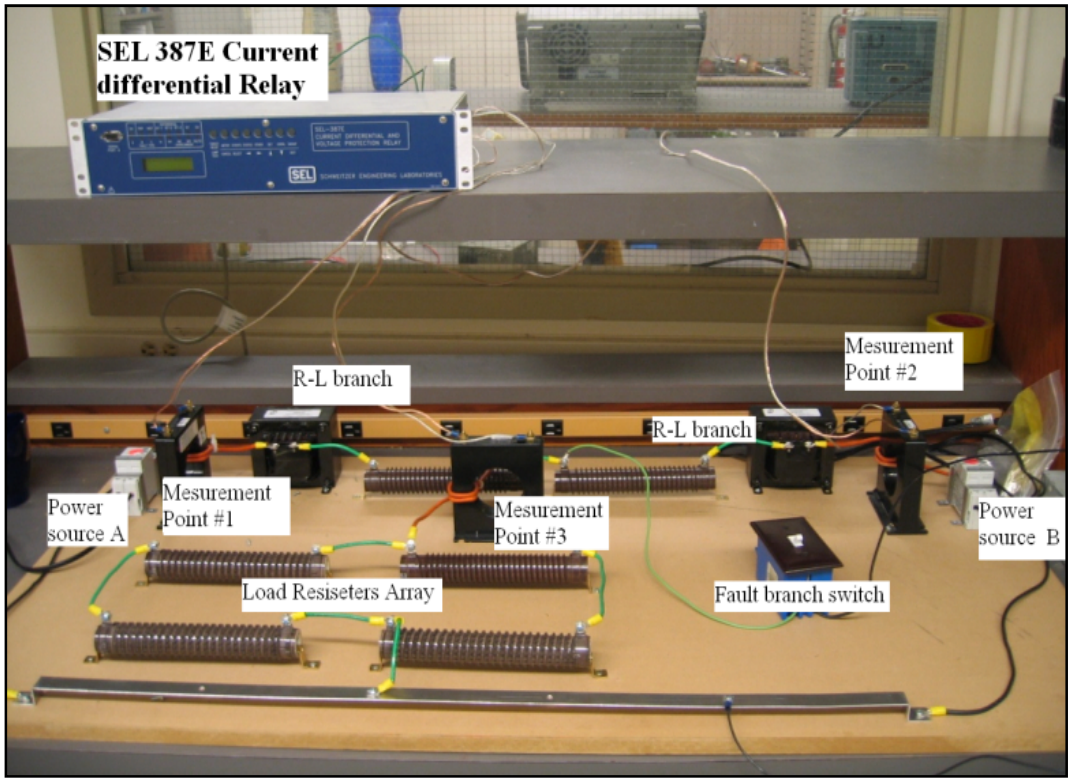

Fig. 4.1. Test bed photo

Fig. 4.2 shows the design diagram of the circuit: two standard 60Hz, 120V utility sources feed the single zone system from switch 1(SW1) and switch 2 (SW2). The

switches are connected to two symmetric R-L circuits that consist of a 2ohm resistor and a 5mH inductor which represents a 1 mile distribution lines and supplies the load. The load is rated at 1.2kW and 10ohm, modeled by 2x2 300W 10 ohm resistor array. The fault branch, a 2.5 ohm, 1kW resistor in series with switch 3 (SW3) is connected in parallel to simulate a shunt fault at the load. Three current transformers (CT) rating at 100:5 ratio are distributed at each source terminal and the load point of the test-bed in the purpose of measuring the current at the corresponding place. All primary sides of the CTs are double wound for the purpose of generating sufficient secondary current to the relay, thus the equivalent CT ratio is 50:5.

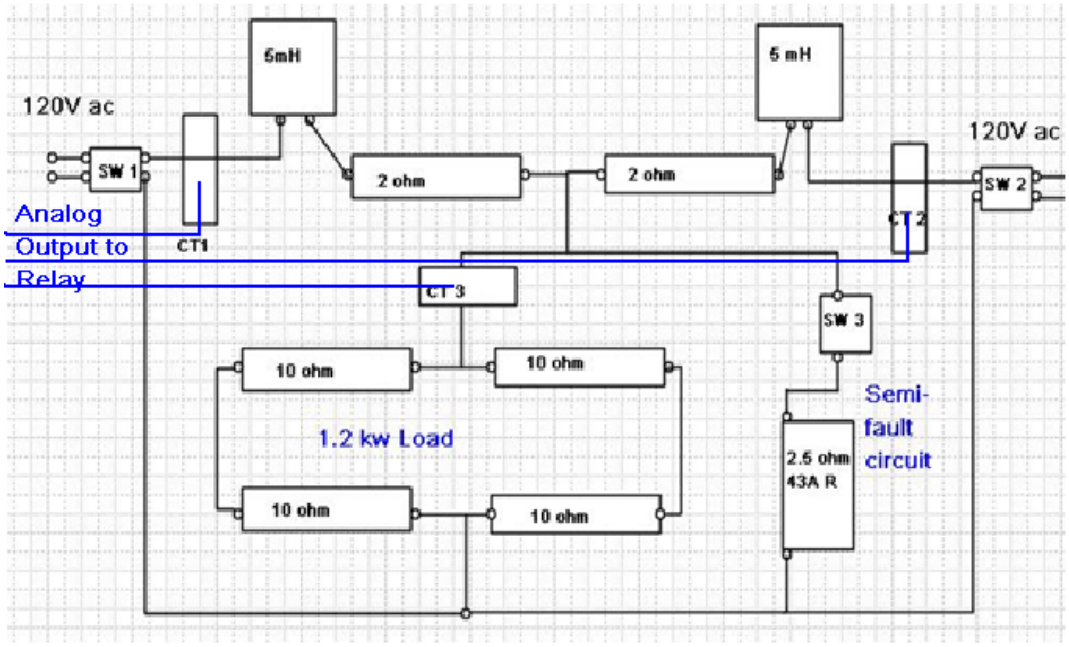

Fig. 4.2. Test bed design chart

Initially, SW1 and SW2 are closed and SW3 is open. The power flow starts from each of the sources and goes through the R-L circuit and feeds the load. The system is running in normal condition. The currents I1 measured from CT1, I2 measured from CT2

and I3 measured from CT3 are shown in table 4.1, row 1, satisfies the relationship: I1 + I2 = I3.

When SW3 closes, the currents at each CT are measured are shown in Table 4.1, row 2. The sum of I1 and I2 is no longer equal to I3. The fault current is approximately 3 times the normal current.

Table 4.1. Test bed current

	I1	I2	I3
Pre-fault	6.4A	6.4A	12.8A
Fault	16.7 A	16.7A	6.7A

From the current shown in Table 4.1, we can use the RMS value and the power flow direction for reference direction. From the CT equivalent ratio, the secondary current input to the relay is calculated and listed in table 4.2

Table 4.2. Relay input

	I1	I2	I3
Pre-fault	0.64A	0.64A	1.08A
Fault	1.67 A	1.67A	0.67A

4.2 SEL 387E Relay

The SEL-387E Current Differential and Overcurrent Relay provides protection, control, and metering for transformers, machines, buses, breakers, and feeders [23]. It is designed and specialized for transformer protection. There are four current input channels and each channel is 3 phase. For the test-bed zone with 3 current measurement points in Fig. 4.1, we simply connect the secondary of CT1, CT2 and CT3 to phase A of winding 1, winding 2 and winding 3 respectively, as shown in Fig. 4.3.

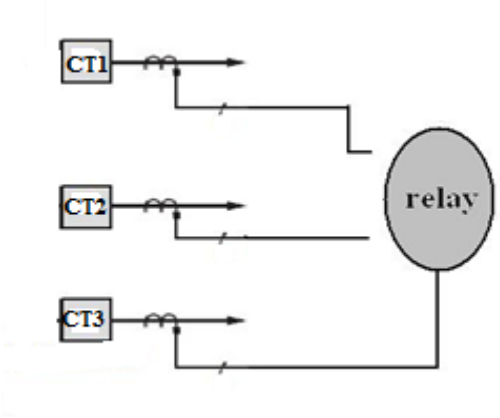

Fig. 4.3. Connection diagram

4.3 Differential Protection Unit Test

The differential protection method is proposed to provide primary protection to the zone system. The differential protection strategy is to measure the currents at secondary winding (CT1 and CT2) to the current at the primary winding (CT3), and calculate the differential elements with the threshold slope. In this case, I_0=1A, which is the minimum setting and a typical 25% percentage slope is applied. The response with fault is shown in Fig.4.4. The full relay setting and coding is listed in appendix A.

Before the fault, the equivalent differential slope

$$S = \frac{I_{op} - I_0}{I_{Res}} = \frac{0.64 + 0.64 - 1.28 - 1}{0.64 + 0.64 + 1.28} = \frac{-1}{2.56} = -0.39 < 0.25$$

This means that it is in the restraining region. Thus, no trip signal.

When the fault happens, the equivalent differential slope is:

$$S = \frac{I_{op} - I_0}{I_{Res}} = \frac{1.67 + 1.67 - 0.67 - 1}{1.67 + 1.67 + 0.67} = \frac{1.67}{4.01} = 0.46 > 0.25$$

This means that the result is in the operating region and a trip signal is generated as in Fig. 4.4.

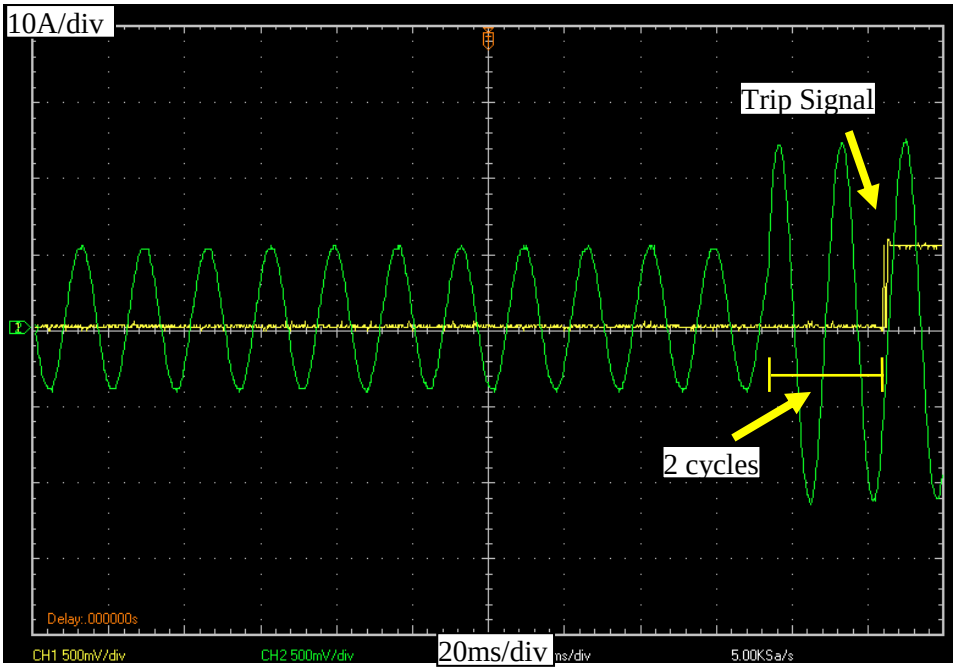

Fig. 4.4. Relay differential test result

The trip signal is the tripping command from the relay output mechanical switch, which causes transients during switching. In reality, the step up signal goes to a circuit breaker, but in the proposed FREEDM system, it will go to the FID at zone terminals.

Table 4.3. Repeating test

Test	1	2	3	4	5	average
Time: (cycle)	2.0	2.3	2.1	2.1	2.2	2.1

It can be observed that the relay response time is 2 cycle from Fig. 4.4. The test is repeated 5 times, as in Table 4.3. The average response time obtained is approximately 2.1 cycles. The 2 cycles operation time is the existing fastest protection method in the industry which is supposed to protect the key components such as large generators, transformers and buses.

An additional experiment is conducted to verify the differential algorithm selectivity. The fault circuit was relocated in this case: the connector of SW3 is connected to SW2 directly, to the right of CT2, thus the fault is outside the zone.

a. Before the fault, the circuit system is the same.

$$S' = \frac{I_{op} - I_0}{I_{Res}} = \frac{0.64 + 0.64 - 1.28 - 1}{0.64 + 0.64 + 1.28} = \frac{-1}{2.56} = -0.39 < 0.25$$

This means it's in the restraining region. Thus, no trip signal.

b. When the fault happens, the current is recorded as I1=1.45A, I2= -0.53A and I3= 0.93A, then, the equivalent differential slope:

$$S = \frac{I_{op} - I_0}{I_{Res}} = \frac{1.45 - 0.53 - 0.93 - 1}{1.45 + 0.53 + 0.93} = -\frac{1.01}{4.41} = -0.35 < 0.25$$

This means it's in restraining region. Thus, no trip signal.

In this way, the relay views that the fault is out of the monitoring zone and does not operate. This test shows the selectivity of differential protection.

4.5 Summary

This chapter provides a bench mark for the operating speed of existing commercial protection, the differential protection successfully identifies the fault in and out of the zone, which helps to locate and isolate the fault.

The commercial differential protection relay has a few drawbacks: First, the operation is not fast enough to match the fast operation of the novel FID system, which can interrupt a fault within micro seconds in the FREEDM system. Second, the relay is only capable of 4 inputs, which means that a zone with more than 2 loads is not possible. Third, the relay works independently and cannot communicate with other relays or intelligent devices in the FREEDM system. The last and most important problem is that the relay only accepts analog input which can only be transported in a very small range. Otherwise noise signals are introduced and cannot be eliminated. Thus, this method is typically used for small range application such as protection for transformers and buses, instead of protection for an entire distribution system.

To overcome these drawbacks, a novel protection system based on digital sampling and communication is proposed. The radical change from conventional analog protection to digital protection results in the fact that the signal transmitted between the distributed current measuring point and the relay should be digital. The solution is: an analog merging unit (AMU) that measures and digitizes current information will be installed at every CT to send the data to the central IFM through the high quality communication system. To implement this, both a low delay and high reliability communication system is required.

CHAPTER 5

DESIGN OF REAL-TIME INTELLIGENT FAULT MANAGEMENT PROGRAM

This chapter first presents the design details and working principle of the IFM real time protection program that is implemented on the LabVIEW platform. Following that, the performance of the IFM under various system operating conditions is tested and analyzed in detail.

5.1 LabVIEW Platfrom

LabVIEW is a graphical programming environment used by engineers and scientists all over the world to develop sophisticated measurement, test, and control systems [24]. The LabVIEW platform was introduced in 1986 by National Instrument (NI). The original idea is to provide program support for the NI hardware. The platform gradually becomes scalable across multiple targets and operating systems (OS). It has becomes more and more popular and now is the leading software that is widely used in both industry and academia. LabVIEW offers paramount integration with thousands of hardware devices by providing hundreds of built-in libraries for advanced analysis and data visualization. With these libraries, the hardware can be simply modeled as virtual instrumentation in LabVIEW. In this way, the program between different devices and the computers can be accomplished.

There are several reasons for choosing LabVIEW for the IFM platform. The first and fundamental reason is that LabVIEW provides a real time programming environment that is designed to run for a relatively long time. This satisfies the key requirement of the IFM protection implementation. The second reason is that among the various software, LabVIEW environment provides a very good background in both stability and

compatibility for the IFM. The third reason is that, by providing various protocols and driver support, LabVIEW is very friendly to devices of different types and different manufacturers. All these factors allow IFM to work closely with other intelligent devices in the FREEDM system. Furthermore, the expandability of LabVIEW ensures that IFM can be updated to cooperate with novel technologies and protocols in the future.

5.2 System Diagram

The IFM real time protective program has been built on LabVIEW. The program consists of the following blocks: virtual signal generation block, protection calculation units with associated threshold, and timers as shown in Fig.5.1.

For demonstration and testing purposes, a virtual protective section including two lines and a load of three-terminals (as present in Fig. 3.8) is introduced into the program. Three current signals, as the CT output of two line-currents plus the load current, are modeled by 3 virtual signal generators, from which the standard 60Hz sinusoidal waveform is generated. The sampler, simulates as the AMU digitizer and takes 100 samples per cycle from the sinusoidal waveform and sends these samples to differential protection units and over-current protection units separately. The protection unit is basically a mathematical calculation function that continuously calculates the received digital samples based on the protective algorithm. The percentage differential protection concept

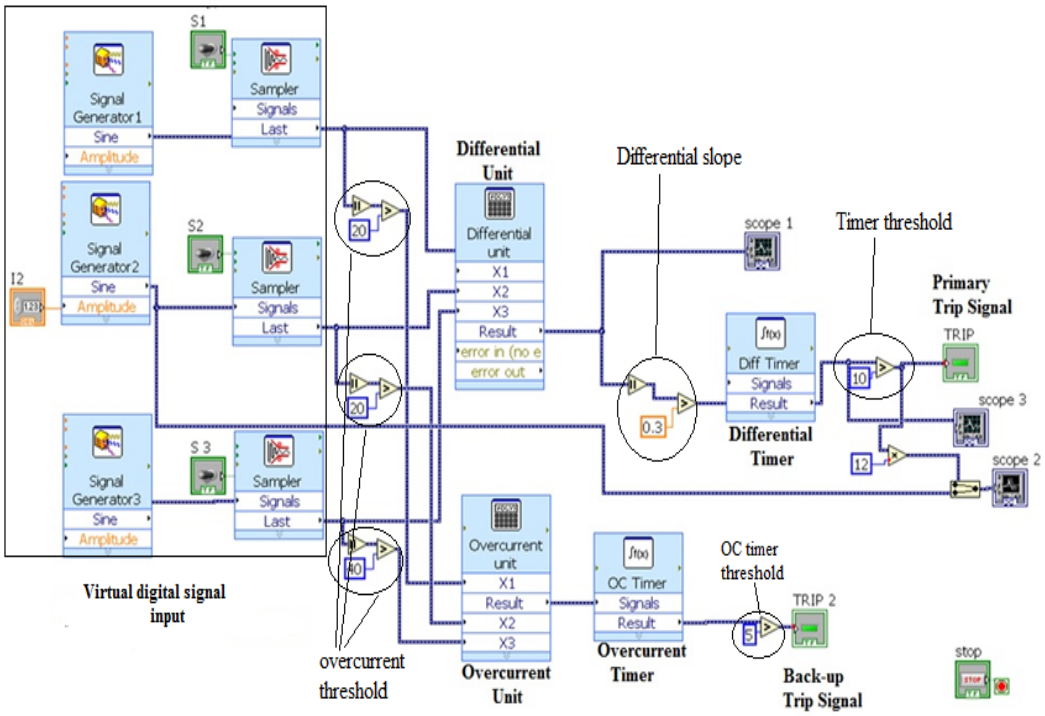

Fig. 5.1. IFM program schematic diagram

is stated in Chapter 3. The mathematic equation applied for the differential calculation unit is: $S = \frac{|\sum_{i=1}^{m} \dot{I}_i| - I_0}{\sum_{i=1}^{m} |\dot{I}_i|}$

Where m equates to the total number of measurement points,

I_i stands for the current value at each point

S is the slope coefficient

I_0 is the minimum operating current

When the slope is calculated, the result is compared with the slope threshold S_0, which is preset as a typical value of 0.3 in the program.

The over current protection unit provides the backup protection. The overcurrent threshold element, which examines the absolute value of the current, is applied prior to the calculating unit to filter out the normal current value. The threshold is implemented by a logic comparison function, which has been set as 20A for source current and 40 A for load current. For the input current that is larger than the threshold value, the threshold element will output the signal “1” to the over-current protection unit. Otherwise the output is 0. The overcurrent protection unit is a mathematical calculation unit that keeps track of all 3 over-current threshold elements. The equation in the over-current unit is:

OC=x1+x2+x3

Where xi is binary output from the threshold element.

When the samples at each winding are less than the threshold value, the overcurrent unit output OC will be 0. Once a high magnitude sample that is greater than the threshold is detected in any winding, the output OC of the overcurrent unit will no longer be 0. Then the signal “1” is generated and it goes to the overcurrent timer.

The output of the protection unit is formed as a binary system, that is: for every sample that is input into the protection unit, the output is either “0”, which stands for no

fault, or “1” which stands for a fault. When the fault judgment is satisfied, the protection unit generates a “1” signal to the timer.

The timer is basically a counter with a small overflow memory which refreshes itself in a small period of time. The refresh time of 100ms is set as default in Labview. It measures the number of samples which indicates the fault by counting the numbers of “1”s in that small time period. When the number of samples is higher than the preset value, the timer sends a trip signal to the FID. The reason for introducing the timer is to eliminate false-trip of IFM due to the error samples occurring during the sampling at AMU, or the data transporting or CT errors. Initially the timer is set to 0. The timer starts counting when a signal “1” is received, indicating a fault. If the outputs of the protection unit keep indicating a fault, the counter of the timer will keeps increasing till the preset threshold, and then a trip signal is generated to the FID. Otherwise, the timer restarts to 0. Thus the preset operation value of timer determines the IFM operating speed. A timer with a lower preset number will improve the protection speed, but it will also increase the risk of false trips. A Timer with large preset number will have a longer trip time but enhances protection system accuracy.

The detailed process in the IFM program follows the flow chart shown in Fig. 5.2. The flow chart starts with the input data, which are the current samples, coming from remote AMUs. These samples then go to the differential unit and the overcurrent unit, which involve mathematical calculation blocks. The two protective units work in parallel: the differential unit provides the primary protection and the over current unit provides the backup protection. The time coordination between the primary protection and the back-up protection is achieved by the timer. The timer counts the number of samples in a time period and compares it with a preset value. If the number is greater than the preset number, it sends a trip signal.

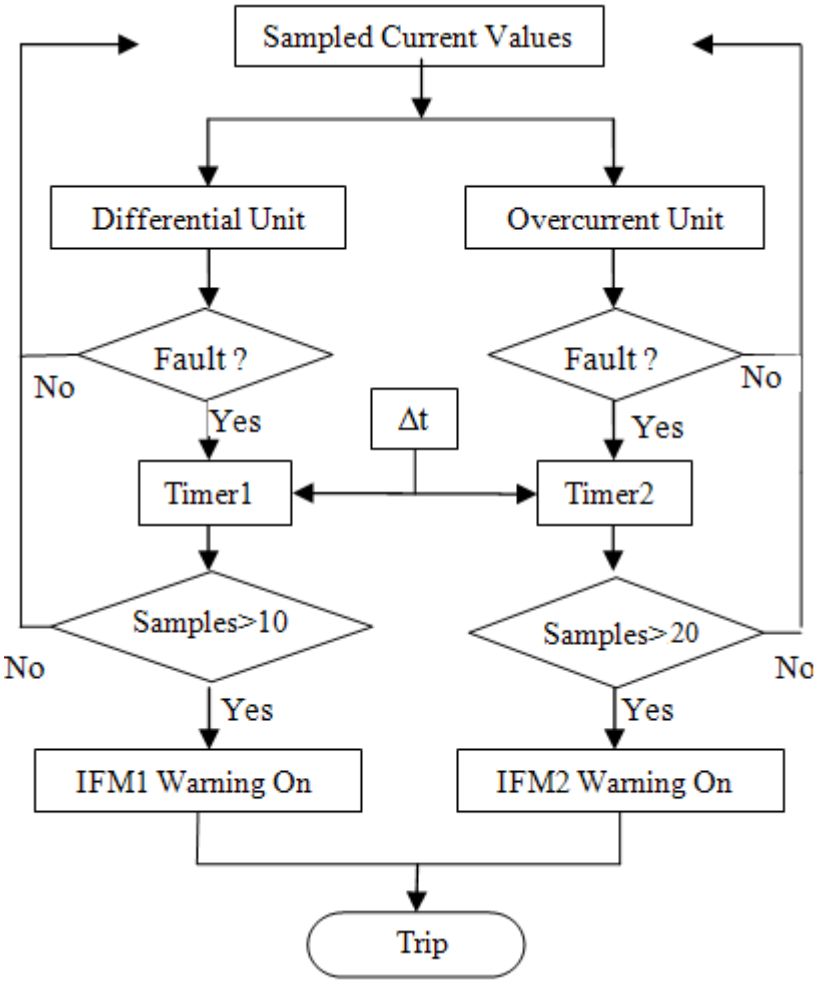

Fig. 5.2. Flow chart of the proposed IFM algorithm

5.3 Protection Algorithm Performance

According to the protection scheme presented in Chapter 3, the IFM program is responsible for providing system status. This chapter evaluates the performance in both operating accuracy and response speed of the IFM algorithm based on the virtual signal generator input. The operating speed of IFM is designed to be less than a cycle.

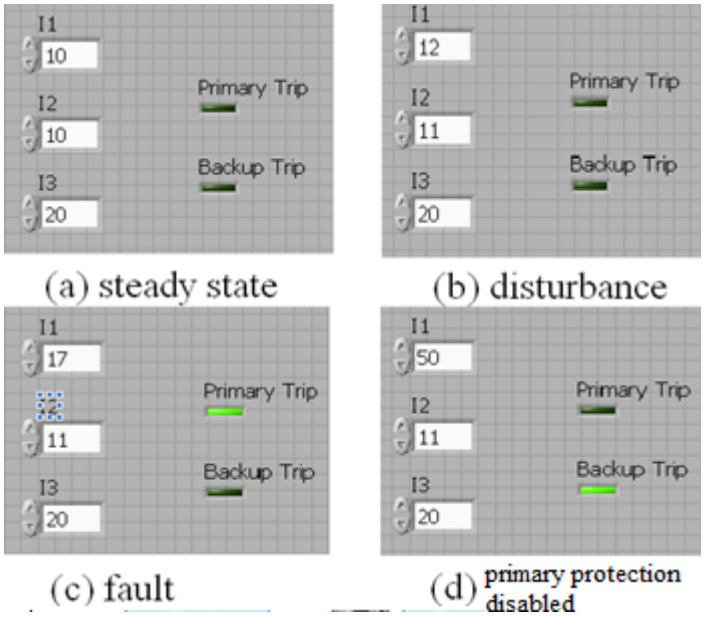

Fig. 5.3. IFM response for various conditions

Fig.5.3 shows the IFM system response under different operating conditions. I1,I2 show the current from the sources, I3 is the load current. The slope is adjusted to 0.15.

(a) When section is running in steady state condition, I1=10, I2=10, I3=20, the sum of the source currents equal the load current, hence there is no tripping command;

(b) When there is a disturbance, I1=12,I2=11,I3=20.The sum of source currents are no longer equal to load current. Output of the differential unit (shown in Fig. 5.4) is between 0.122 to 0.13, which is less than the threshold 0.15, this means that the result is located in the restraining region and IFM does not generate a trip command.

(c) When there is a fault in the section, as in the Fig. 5.3, I1=17, I2=11, I3=20, S=(I1+I2-I3)/(I1+I2+I3)=8/48= 0.167, which is larger than the threshold 0.15. Thus, the differential unit gives out the “1” signal and the timer associated with the differential unit starts counting, Fig.5.5 shows the count number in the timer increases when the fault occurs. When the timer output reaches to the threshold value, 10 in this case, a trip signal is generated by the primary differential unit.

(d) When a 3 phase fault happens and it generates a very large current, I1=50,I2=11,I3=20. Since we set the over current timer faster than the differential timer for critical fault currents, the overcurrent protection operates prior to the primary differential protection.

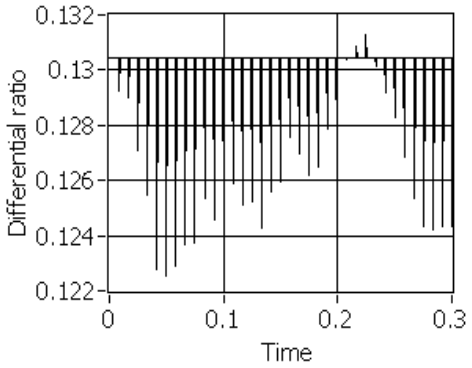

Fig. 5.4. Differential unit output

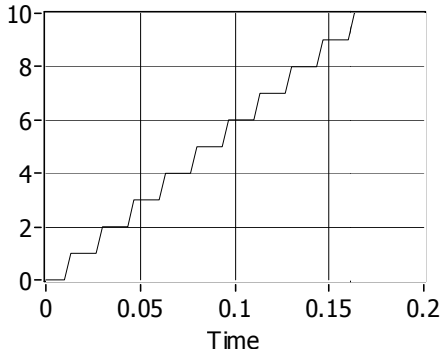

Fig. 5.5. Timer Counting

The time domain process of protection response of Fig. 5.3 is shown in Fig.5.6, showing the waveform for line current and the tripping signal. It can be observed from Fig.5.6 that no trip signal is created during normal operation. When there is a small increase of the current value, still no trip signal is generated as the differential value is lesser than the differential threshold (slope).

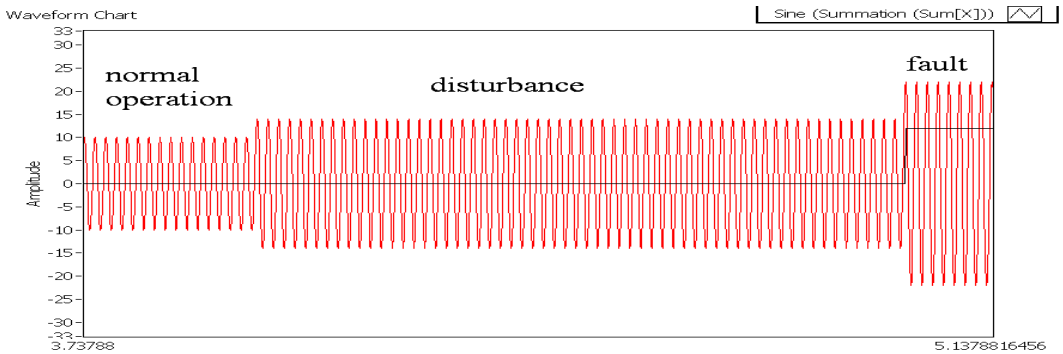

Fig. 5.6. Protection response under disturbance

When the differential result becomes large enough to go beyond the slope threshold, which means that the result is moving out of the restraining region on the characteristic map, a trip signal is generated and sent to the FID.

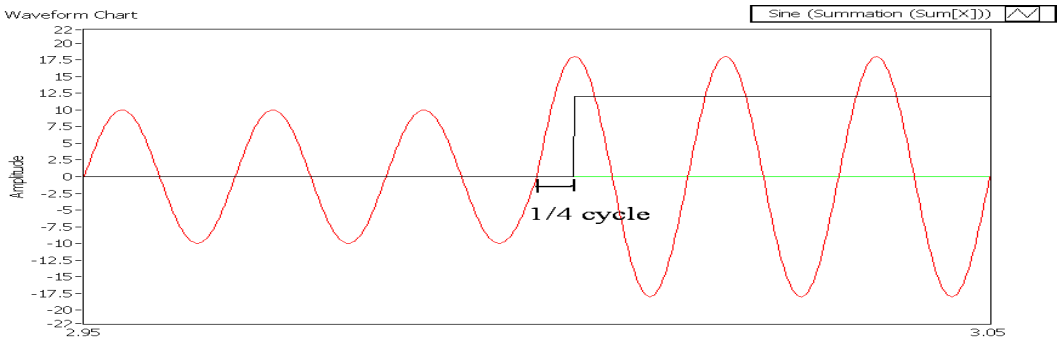

Fig. 5.7. Response with sampling speed of 20 samples/cycle

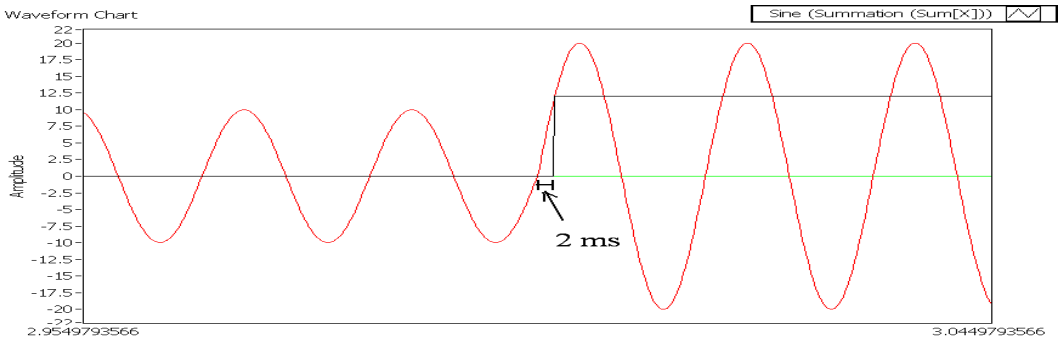

Fig. 5.8. Protection response with sampling speed of 100 samples/cycle

Fig.5.7 and Fig.5.8 clearly shows the primary protection speed. In Fig.5.7, the system is running with 20 samples/cycle and differential timer evaluates 10 samples before tripping. In Fig.5.8, the system is running with 100 samples/cycle and timer evaluates 10 samples before tripping. Hence, we can observe that the trip speed is dependent on the timer, which counts fault samples, and AMU sampling speed, which is the number of samples AMU's which the communication medium allows per cycle.

Fig.5.9 shows the protection response of an overcurrent protection system with primary protection disabled. Since the overcurrent timer is preset as 20 samples, twice as large as the differential timer, the response time is about 6ms.

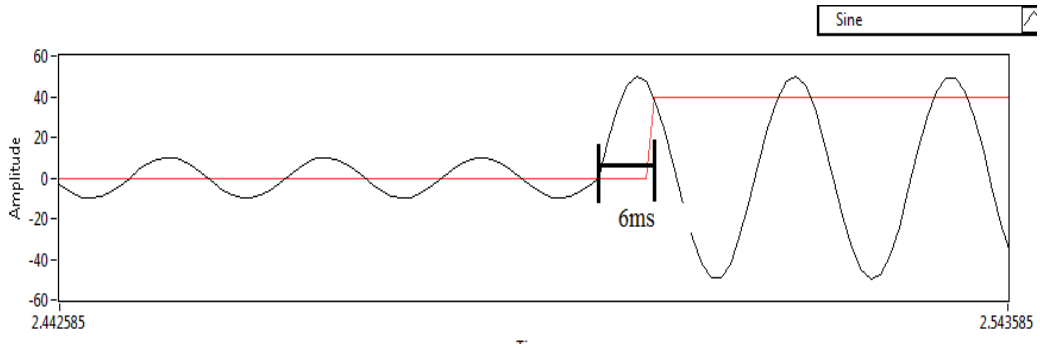

Fig. 5.9. overcurrent protection response for a critical fault

Another advantage of this protection system is that it is based on the instantaneous sample point instead of traditional RMS calculations. In FREEDM zone, with the SST and FCL employed, fault current could be high frequency, non-sinusoidal waveform with high penetration of harmonics which is not easy to deal with by using existing protection methods. However, this IFM algorithm identifies it clearly and trips it fast as observed in Fig. 5.10. The non-sinusoidal fault is modeled by adding square waveforms onto normal sinusoidal waveform. As a non-sinusoidal fault occurs, the IFM trips 2ms later, the same speed as a normal sinusoidal fault.

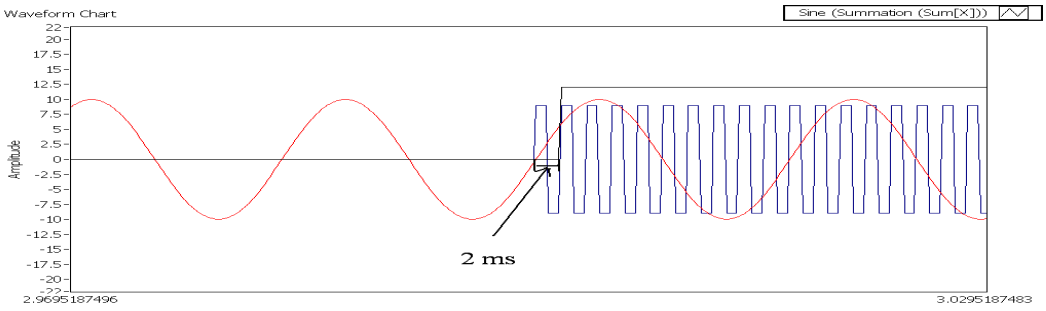

Fig. 5.10. Protection response with square wave fault

5.4 Differential Unit Performance for Multi-Terminal Zones

The previous analysis is based on the simplest 3-terminal system, in which the differential unit only needs to take care of 3 inputs. In the FREEDM system, it's not likely that only one load is present in a zone. There will be several loads in a zone, A sub protective zone of multi-terminals (shown in 5.11), including two sources and several

loads, is analyzed in this part to test the differential protective algorithm performance with load, or terminal number changes.

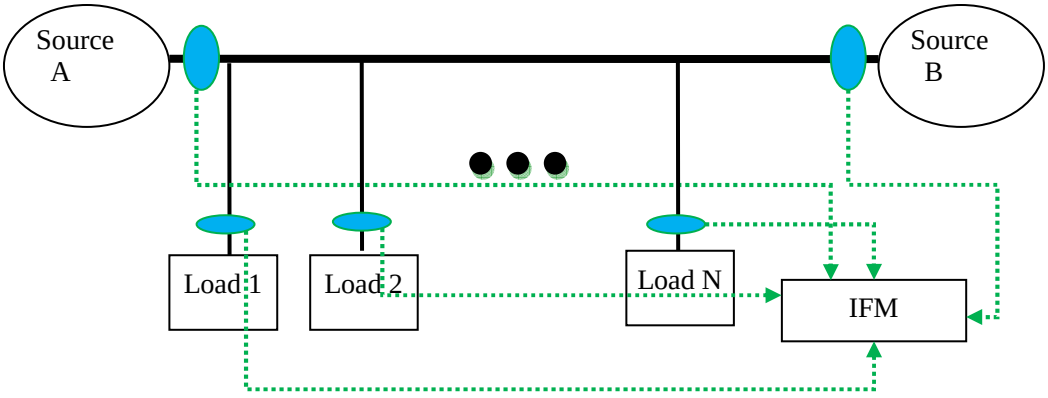

Fig. 5.11. Virtual system of multi-terminal system

5.4.1 Multi-terminal program diagram

Several signal generators are applied in this case to model (shown in Fig. 5.12) the multiple-input of AMUs located at different terminals instead of 3 signal generators that are applied in Fig. 5.1. Notice that only the differential unit is included in the diagram, the overcurrent unit, which works independently with every individual input, will not be affected by the numbers of inputs.

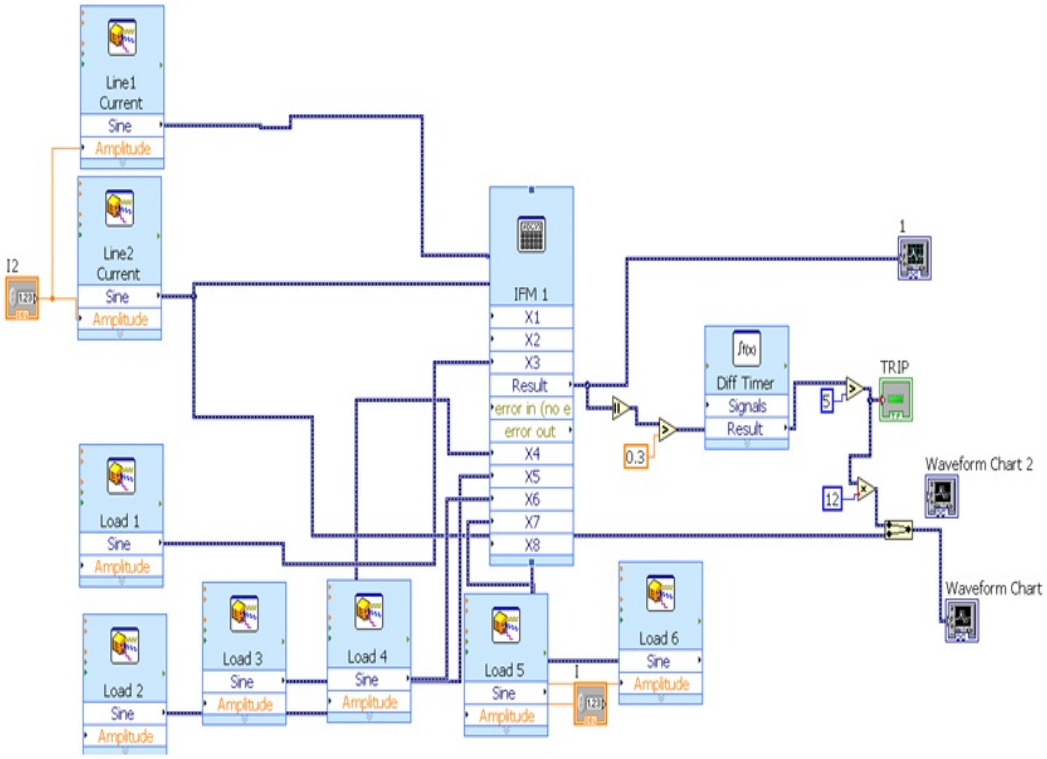

Fig. 5.12. Multi terminal system schematic diagram

5.4.2 Numeric study of port number:

The parameters and assumptions in Fig. 5.12 are fixed as follows: All the load currents are 10A and are supplied by two equal sources. A fault occurs on one of the load lines and doubles the current on that particular line. The other load current is not affected for the small time period. The differential operation slope is set at 0.3 originally, which is a common value for differential protections.

The system is studied with 1 load initially: a load rating of 10A is supplied by two sources equally. Therefore, the current flow at each source is 5A. When a fault happens at the load, it is assumed that the load current is suddenly doubled. Under such circumstances, the differential relay gives a trip signal at the preset threshold slope of 0.3. Then a new load, which is identical to the previous load, is added to test the protection system performance under the same operating condition. When the fault doubles the load current and the IFM is in the restraining region, we reset the slope to a new value that is sensitive enough to detect the fault and record the new slope value. Similar tests are repeated for 6 loads and the result of the test are shown in Table 5.1.

The minimum operating slope in Table 5.1 is 0.13, which means that when there are 6 loads and total of 8 terminals the system may not determine the fault with 0.13 slope or higher slope setting.

Table 5.1. Test result of multi-terminal system

Terminals	Original system response	Minimum operation slope
3	Trip	>0.3
4	Trip	>0.3
5	Trip	0.3
6	No Trip	0.24
7	No Trip	0.19
8	No Trip	0.13

As in the Table 5.1, 6 loads, with 8 terminals, which is the maximum number of inputs for the program, because this is limited by the input ports of the mathematical calculation unit. However, a system with more than 8 inputs can be achieved by using multiple formula calculation units cooperating together. The only problem of increasing the ports is that it will decrease the algorithm sensitivity (slope ratio), which is typically within the range of 10%-30% for security reason. The slope itself can be easily adjusted to meet the sensitivity of fault determination. However, a protection scheme with very low slope ratio will be very sensitive and may result in mis-trip in the case of CT saturation or other abnormal conditions. On the other hand, the sensitivity is also dependent on the magnitude of fault current, If the fault current is large enough, the sensitivity will not be a problem. As the test reveals, the number of ports will not affect the algorithm speed. However, the differential slope needs to be adjusted to the port number for the specific protective zone to obtain the best performance.

CHAPTER 6

IFM WITH AMU HARDWARE

This chapter presents the whole protection system that includes the IFM program, AMU hardware, associated data communication and synchronizations. The IFM program is built on LabView, the AMU is a micro controller that is based on PICDEM.net 2 development platform[26]. The communication system is based on the transmission control protocol (TCP) and synchronization is done by a GPS clock. The physical test bed, stands for a scaled single FREEDM zone, which is described in Chapter 4.

The system prototype overview is shown in Fig. 6.1. The data acquisition system is implemented by a micro-controller with Ethernet communication embedded [27]. One SEL 2407 satellite-synchronized GPS clock provides continuous pulses to all three boards, and this is input to the micro controller board to generate an interrupt.

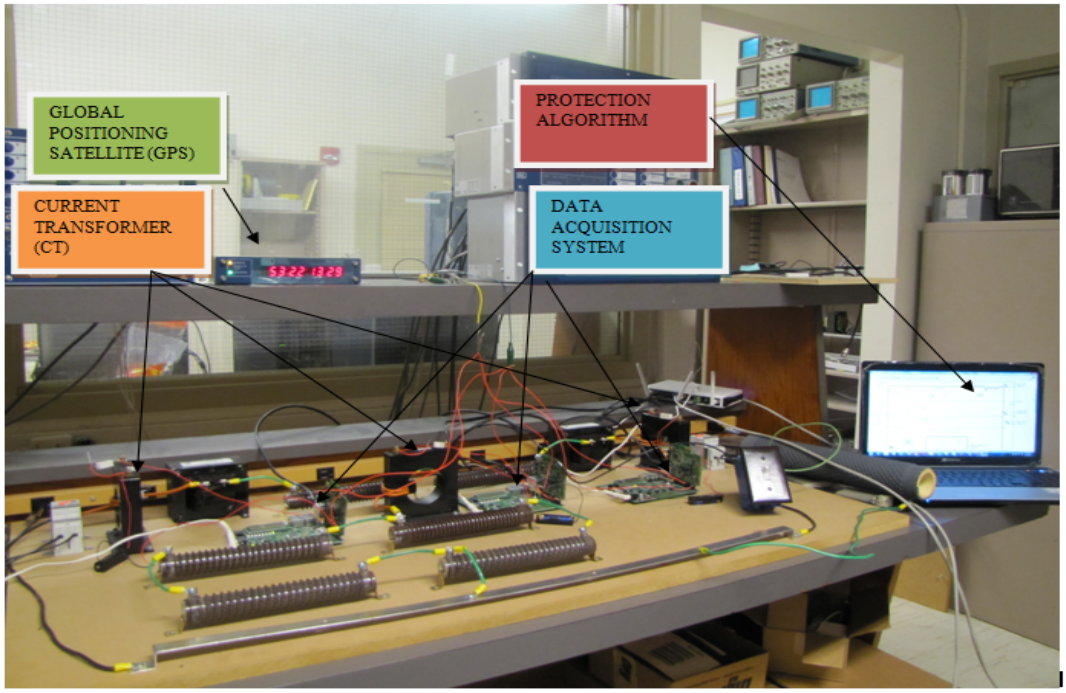

Fig. 6.1. Full protection test system prototype

Once the transmit buffer has data in it, this data is transmitted to the computer through the Ethernet output from the micro-controller, which is routed to the computer using an

Ethernet switch. The IFM program that captures these data and executes both differential and over-current protection algorithm is running on the computer. The communication and synchronization details as well as the micro-controller configuration are discussed in Arvind Thirumalai's thesis – "Design of Data Acquisition System and Fault Current Limiter for an ultra fast protection system".

6.1 Data sampling:

The data sampling connection diagram is shown in Fig. 6.2. A 0.3 ohm resistor is connected across the secondary terminals of each current transformer and the voltage across the resistor is the input to each micro-controller board. Since the micro controller is unable to measure a negative voltage signal, a DC bias circuit, basically a 1.5V battery, is added between the resistor and the ground port of the micro controller.

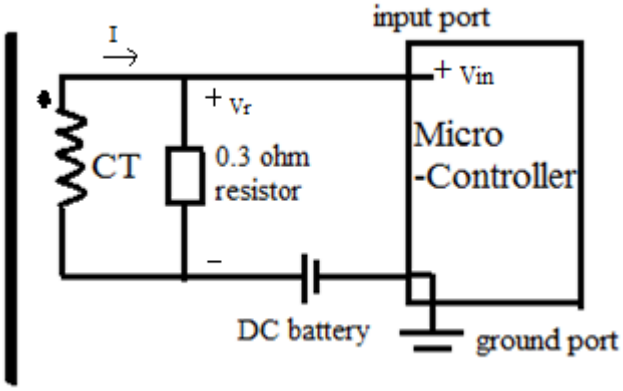

Fig. 6.2. Data sampling connection diagram

With the DC bias circuit, the input voltage signal will be a sinusoidal waveform with a positive DC bias so that the micro controller can make samples, and all the sampled values will be positive numbers. As the trigger pulses form the GPS clock is configured at 1k pulses per second, the sampling speed of the micro controller is defined as 1k samples per second.

As in Fig. 6.2, when the current at the secondary of the CT flows with the reference direction, the voltage on the sampling resistor Vr will be a positive value. Otherwise Vr will be a negative value. Assuming the equivalent DC bias value is V_{DC}, the signal value of input current with the CT reference direction is $V_{in}=V_{DC}+|Vr|$, and the signal value of input current against the CT reference direction is $V_{in}= V_{DC} - |Vr|$. As a result, the digitized current signal that is larger than V0 is with the reference direction. Thus, the direction of input current is determined.

6.2 IFM program update

The IFM program is extended to work together with AMUs which implements the digitizing and sampling task. Compared to the program discussed in Chapter 5, the major change is that the virtual signal input block is replaced by the communication block, which implements the data communication between the IFM program and the remote AMUs hardware. The data process block is added for the digital signal processing. The added function for a single family zone is shown in Fig. 6.3. The full schematic is shown in Fig. 6.4.

The TCP communication block is composed of the TCP connection function, the TCP read function, and the error and warning function. These functions are LabView basic communication functions. The TCP connection function opens a TCP network connection with the IP address and remote TCP port number. When the IP address and TCP port numbers are defined, it will start the TCP command in the backstage. The TCP network connection between the computer and the micro-controller is established. The TCP read function is a function that reads bytes from a TCP network connection, returning the results in data out. It is applied to capture data from TCP packages outcomes from the TCP communication and output string format data that can be processed by LabVIEW platform to the main program.

The error and warning function merge errors together, converting any connection errors to warnings and then triggering the TCP disconnection function to stop the program .

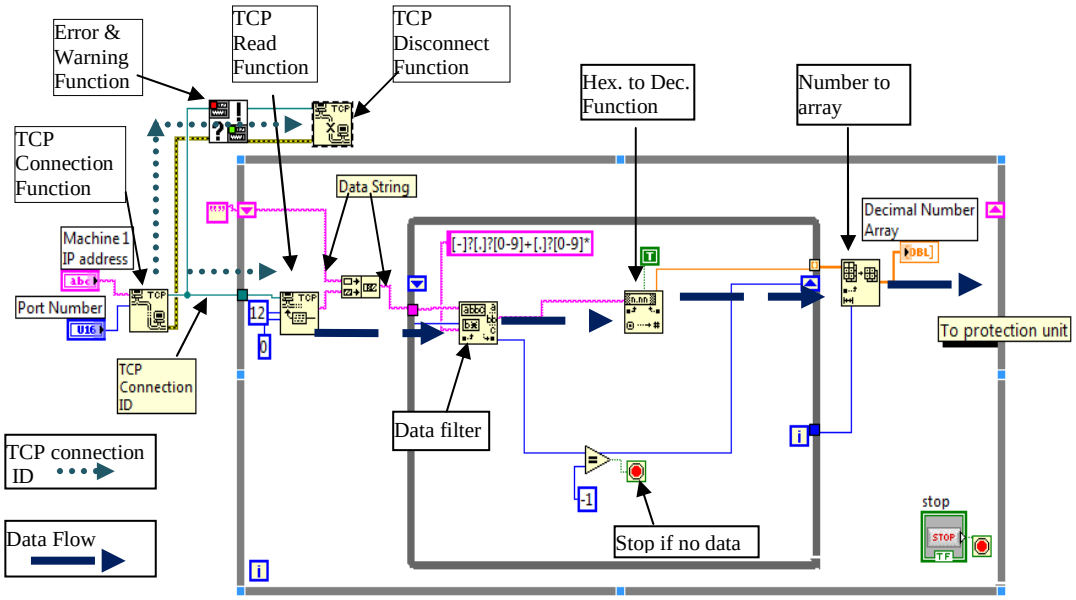

Fig. 6.3. Added block for single AMU input.

As in 6.3, the TCP connection ID contains the IP address and the TCP port number, TCP read function and TCP disconnection function. The data flow of the IFM program starts at the TCP read function, which outputs the current data in string format, and then, it goes to the next block - data process block. The data process block is a while loop that continuously processes the data obtained at the communication block and feeds the processed number array data to the protection block, which can only calculate the data in decimal number array format. The data filter extracts the hexadecimal numbers from the data string, and then the numerical translate function transfers the hexadecimal number into the decimal number, and the array function is applied to build up a number array for the continuous number outputs from the While loop so that the IFM block can process these numbers. The reason that the data process block is introduced is that the

data comes from the AMUs in hexadecimal string format due to the micro-controller's limitation, and the data needs to be converted into the decimal data in integer number format so that the IFM block can directly process the values with the mathematical calculation unit.

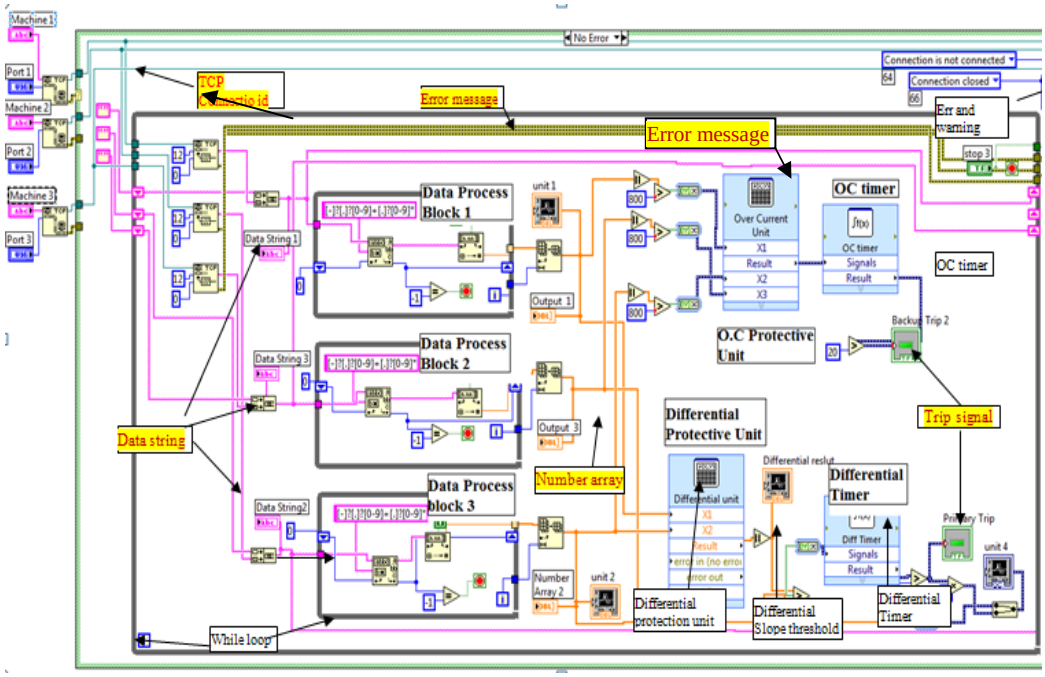

Fig. 6.4. Full IFM program

With the TCP communication block added, the IFM program is able to obtain the data from the remote, distributed AMUs via TCP communication. Fig. 6.5 shows the data obtained from a program control panel.

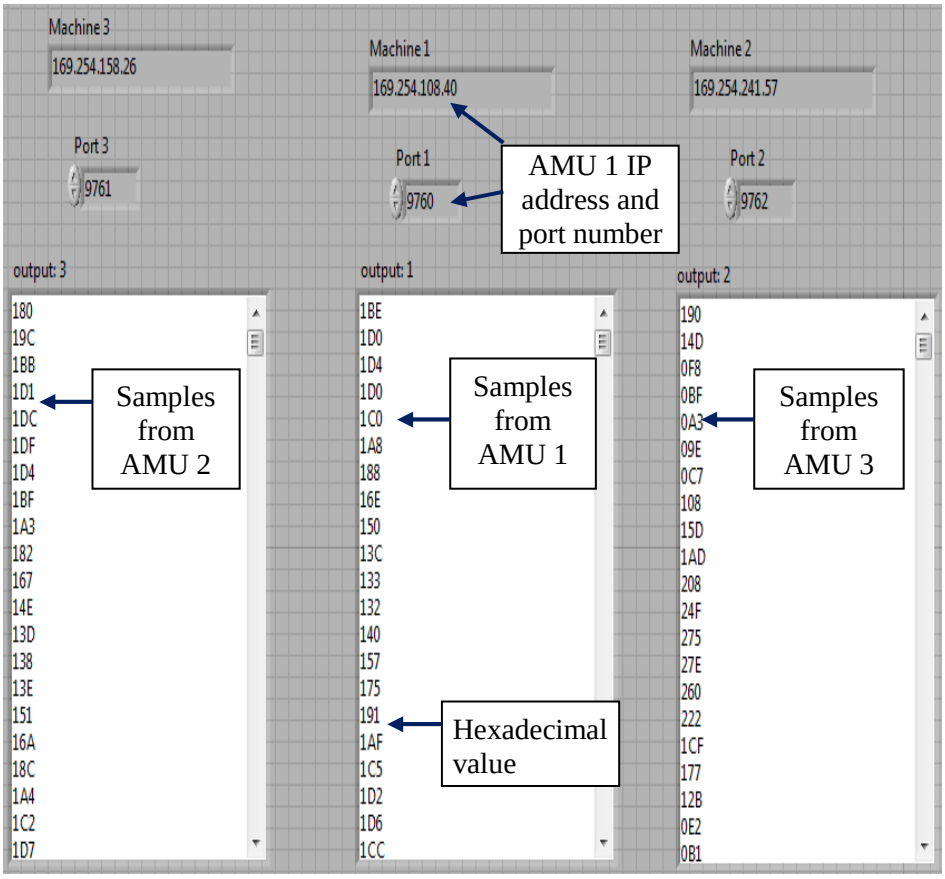

Fig. 6.5. Screen-print of LabVIEW controlling panels

Note that the data shown in Fig.6.5 are the direct outputs of three AMUs distributed in the hardware loop. The data is in hexadecimal number system which is the default output of the micro-controller.

Fig. 6.6 shows the output data as a decimal number waveform which is converted by data process block.

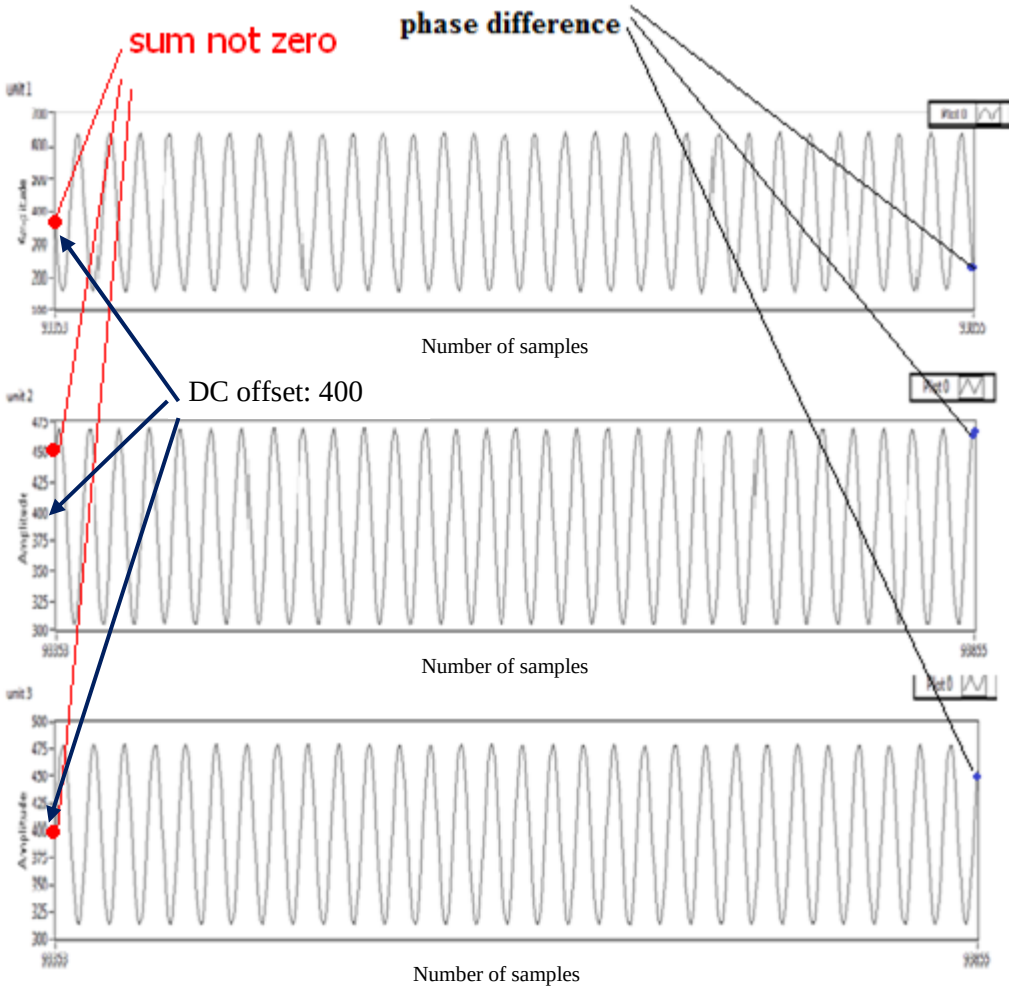

Fig. 6.6. A/D output from data processing block

Notice that the plots in Fig. 6.6 start and stop at the same time instant. The waveform displayed starts at sample number 93353 and ends in number 93855, which indicates the sample numbers. Hence it is inferred that the same sample points are collected individually from each board and examined here. It can be clearly seen that the waveforms are sine waves with few distortion, harmonics, and error sample values.

Then this data goes to the protection block for protective algorithm calculation as discussed in chapter 5. The only change is the DC bias component is eliminated in the differential calculation unit by reducing the DC offset value, 400 as shown in Fig. 6.6, in each winding.

6.3 Peak-peak calculation

A peak detector is a VI component inherited in Labview library to find amplitude of peaks or valleys in the input signal for a small period time. It's connected to the digital data processing block which output of digital value of current from the AMUs (the program chart is shown in Fig. 6.4). In this case, two peak detectors are worked in parallel to obtain the peak and valley separately. After that, the peak to peak result is calculated as the peak minus the valley. At the last, the peak to peak result is output to the protection calculation unit.

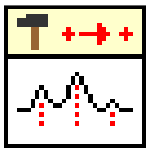

Peak detector

With the peak detector, the data obtained in Fig. 6.6 become to the data in Fig. 6.7

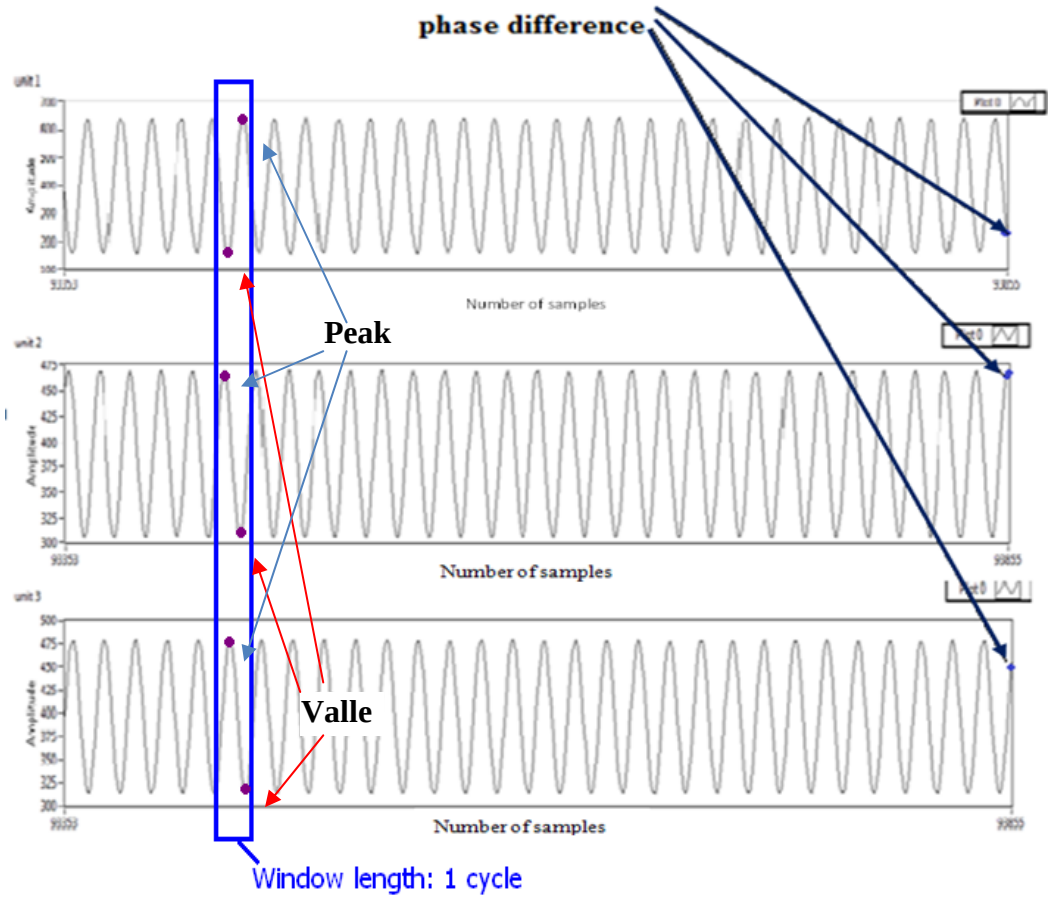

Fig. 6.7. Peak-valley detector working principle

6.4 Differential protection result

As described in chapter 5, the original idea is that the differential unit will directly calculate the instantaneous sample points from AMUs. However, this requires perfect synchronization, which means that all the sampling points received at the differential unit have to be exactly collected at the same time. This requirement causes the problem. As in Fig. 6.6, it's clear that the outputs from the three boards are not perfectly time synchronized. Outputs from units 2 and 3 differ from each otherr by 1 ms, this time difference is good to the differential protection algorithm. But unit 1 varies by 8 ms from unit 3, and 6 ms from unit 2, which are not acceptable. The reason of mis-

synchronization laid on the TCP communication that it takes slightly different time to transfer data from the AMU to the IFM through the Ethernet communication.

These mis-synchronized waveforms will lead to incorrect tripping signal generation by the differential protection algorithm. For the input data of Fig. 6.5., the output of differential unit swings from 0.1 to 0.5 as time varies, as shown in Fig 6.8, while 0.3 is the slope threshold. As a result, the IFM will give wrong trip signal every cycle for normal operation, so the differential protection system will not work properly. Ideally, the output of differential unit shall be always less than 0.1, usually very close to zero.

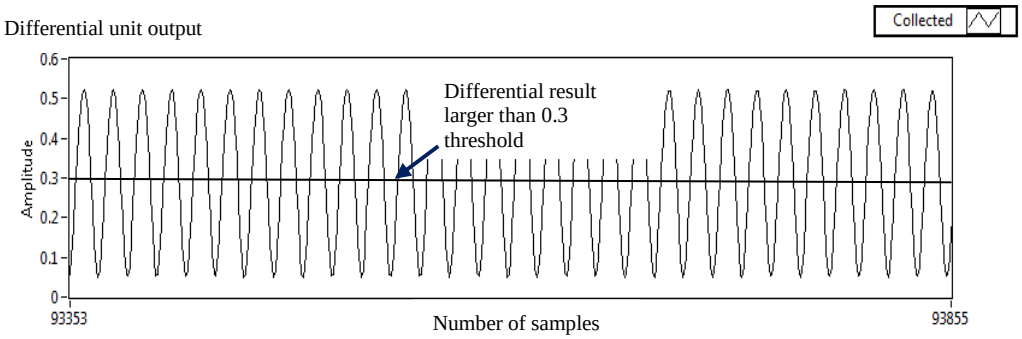

Fig. 6.8. Differential unit output

Since the instantaneous comparison is not feasible, an alternative way is applied. That is to compare the peak to peak value in one cycle instead of each sampling point. The protection algorithm was modified in such a way that, a peak to peak measurement block is added, so the digital data points will be recorded until every packet completes its data transmission to the computer. The microcontroller has been programmed in such a way to send 17 samples in one packet, so each packet received from every microcontroller will be one full cycle of the sine wave. Thus, there should be two peaks, including the positive and negative half cycle, and a peak-peak value in every packet. Then, the differential unit calculates the peak to peak values from each data packet from the AMU. In other words, the input of the differential unit was replaced from

instantaneous samples to the peak to peak value of samples in a cycle. In this way, the synchronization input data that go to the differential unit is achieved. Notice that the system delay will be more than 1 cycle. The peak-to-peak signal for one unit and the trip signal generated are shown in Fig. 6.9.

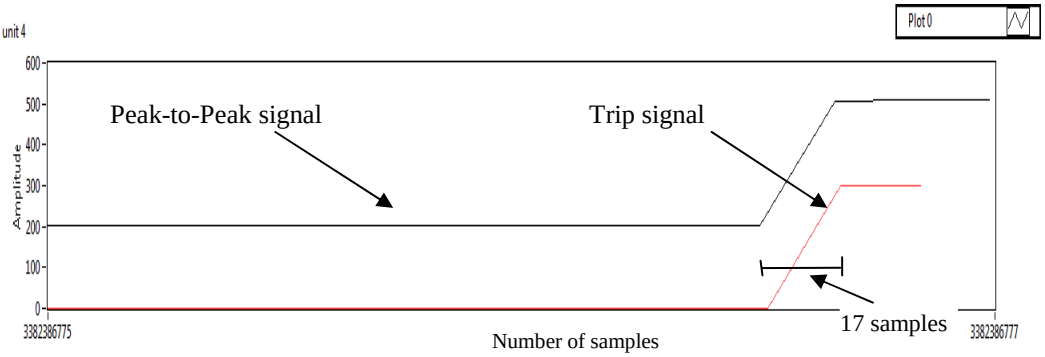

Fig. 6.9. Peak-to-Peak signal with differential unit output

As shown in Fig. 6.9, the curve below is the output of the trip signal and the curve on top is the peak-to-peak value of one source current. It has to be noted that, the sample number in the horizontal axis are packed in a 17 sample packet. Hence the system is updating with every 17 samples, which results in increasing the slope. Fig. 6.10 shows the differential unit output. Initially, the system is in normal condition, and the peak to peak value is 200. When a fault is created on the test-bed circuit, the peak-to-peak waveform rises to approximately 500 and the trip signal is generated. This confirms instantaneous trip signal generation by the protection algorithm.

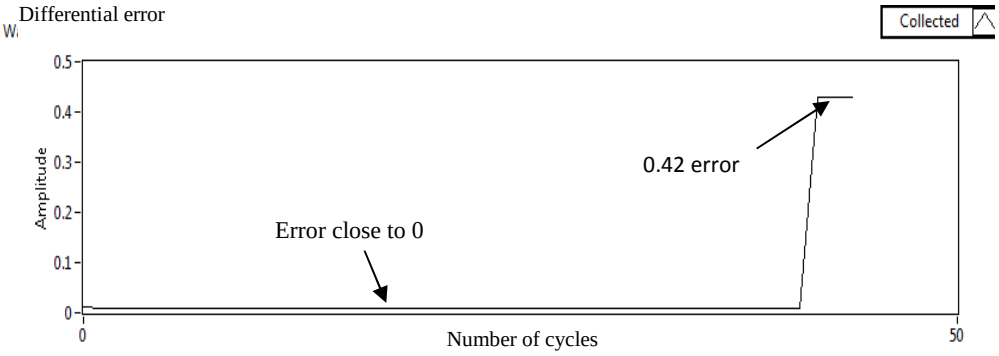

Fig. 6.10. Differential unit output

Fig. 6.10 shows the output from the differential unit. Compared to the differential unit output in Fig. 6.7: in the absence of a fault, the output of a differential unit is very close to 0. When a fault occurs, the output differential unit raises to 0.43, which is larger than the threshold (0.3) value, instantaneously, as in Fig. 6.10. This confirms the successful operation of the protection system.

The trip signal generated is instantaneous when the fault is determined. However, compared to the physical system, the trip signal was generated after IFM program obtained 17 samples in a packet, which is one cycle time period. Hence the response time of the peak-to-peak based differential protection system is around one cycle.

Another possible choice is the RMS value method, which is more popular in practical application. However, this method was not executed because the square root and mathematical complexities associated with the RMS computation in real time data process is very resource consuming. In order to implement it, a dedicated, powerful computer processor is needed.

6.5 Over-current Unit

Unlike the differential unit, the overcurrent unit does not have any time synchronization requirement hence it is self-dependent. The overcurrent protection scheme only depends on the magnitude of the signal of each AMU. In this case, the differential protection unit is disabled. The output of the overcurrent protection algorithm in the event of a fault generated using the switch and the DC trip signal is shown in Fig. 6.11, 6.12, 6.13 (the time scale indicates sample numbers, 1ms for every sample).

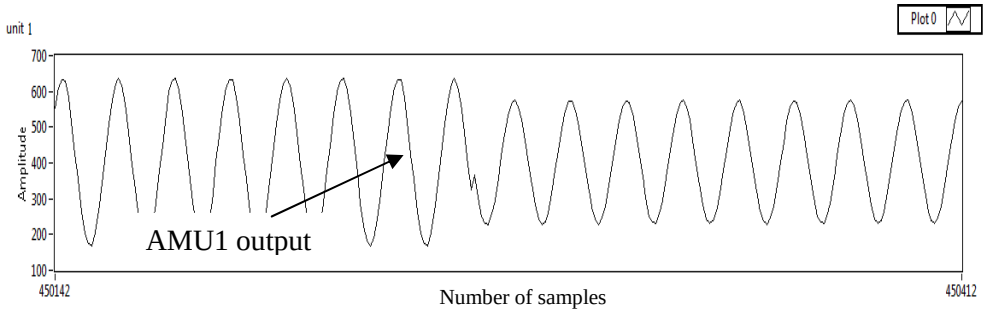

Fig. 6.11. Overcurrent protection unit 1 output during a fault

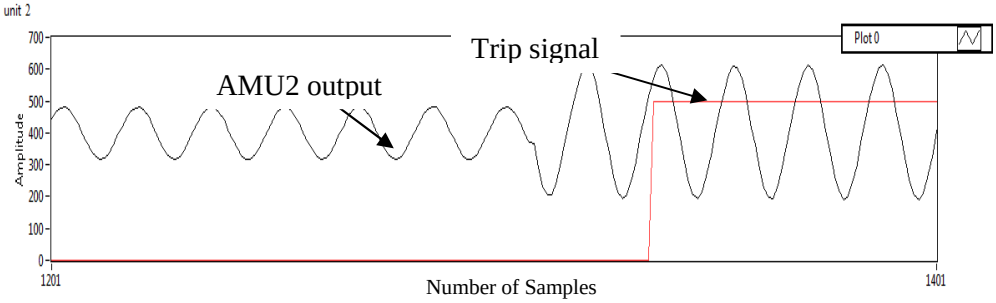

Fig. 6.12. Overcurrent protection unit 2 output during a fault

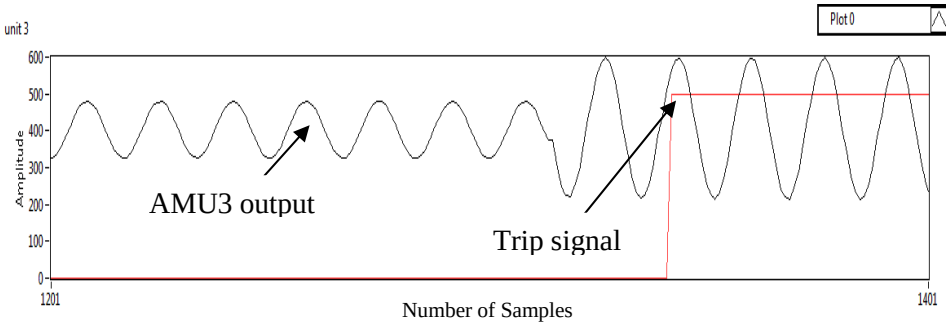

Fig. 6.13. Overcurrent protection unit 3 output during a fault

It can be observed from Fig. 6.12 and 6.13 that a trip signal is generated just after 1.7 cycles after the fault initiation, which is 0.7 cycles after the primary protection response time. Thus the overcurrent unit provides backup protection if the primary function fails.

CHAPTER 7

IFM WITH NI COMPACT-RIO SYSTEM

The NI compact-Rio micro-controller system based on advance EtherCAT [28] communication is applied in this chapter to solve the communication issue. EtherCAT (Ethernet Control Automation Technology), as a part of the IEC 61158, is a high-performance, industrial communication protocol for deterministic Ethernet, which means the delay and response time is deterministic. Thus a deterministic distributed data acquisition system can be expected. The hardware connection is shown in Fig. 7.1.

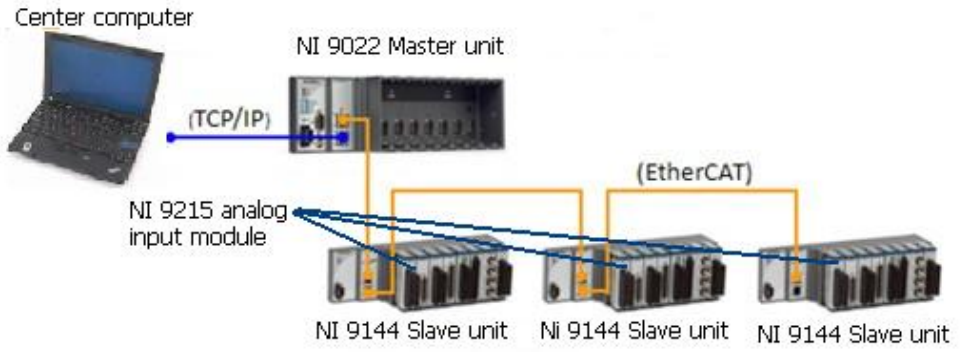

Fig. 7.1. Protection system connection architecture with NI hardware

Every slave AMU consists of a NI 9144 controller and a NI 9125 data acquisition module. The NI 9144 controller is an 8-slot rugged chassis with EtherCAT capability and compatibility with various data acquisition modules, distributed data input and an output module for data acquisition. The NI 9215 data acquisition module is a high-accuracy, high-performance analog measurements input with 8 channels, 16-bit resolution and sampling speed up to 10k samples per second. Compared to the AMU discussed in Chapter 6, one major advantage is that NI-9215 is capable of measuring the negative voltage signals, which means the data obtained is inherent with the plus or minus sign. Thus, no DC bias circuit is needed. The direction of current is defined with the positive

input port. Another advantage is that the AD conversion time is reduced to 4.4us, which is negligible.

The master AMU is a NI 9022 micro controller. The NI 9022 embedded real-time controller is part of the high-performance CompactRIO programmable automation controller (PAC) platform. It features an industrial 533 MHz Freescale MPC8347 real-time processor for deterministic, reliable real-time applications and contains 256 MB of DDR2 RAM and 2 GB of nonvolatile storage for holding programs and logging data. In this application, it acts as a time source for synchronization and manages the EtherCAT communication.

The EtherCAT uses the same frame as Ethernet. A frame is the basic data packet unit for data transportation, an Ethernet frame, as in Fig. 7.2, contains a header, which is designated to the destination address and the source address, body, which data that needs to be transported, and tail, which checks information for cyclic redundancy.

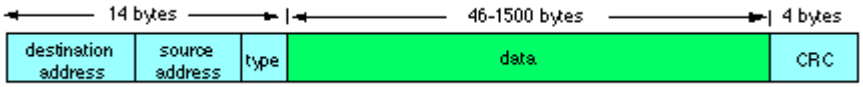

Fig. 7.2. Ethernet frame [28]

Unlike the radius network topology of Ethernet, the connection topology of EtherCAT technology is in series, as shown in Fig. 7.3, the master unit sends out a frame to slave unit 1. When the frame arrives at slave 1, it stops for a while, loads the digital samples at that slave, and then it goes to the next slave unit and stops to load the data exchange. At the end of the slave unit, the frame goes back to the master unit without stopping. Then all the data obtained from the slave units are unloaded to at Master unit. As the data from different slave units is on the same frame, perfect synchronization is achieved. The highest speed of the EtherCAT communication is 1k frames per second.

Thus, the communication delay of EtherCAT is less than 1ms, which is much faster than the regular Ethernet communication which has tens of milliseconds or more delay.

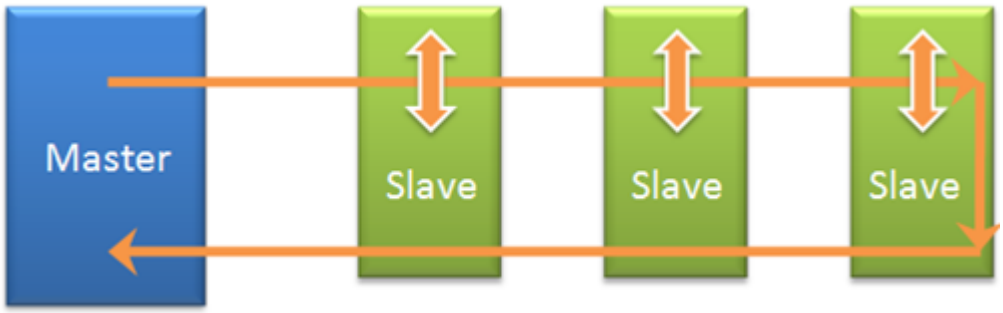

Fig. 7.3. EtherCAT data transfer. [29]

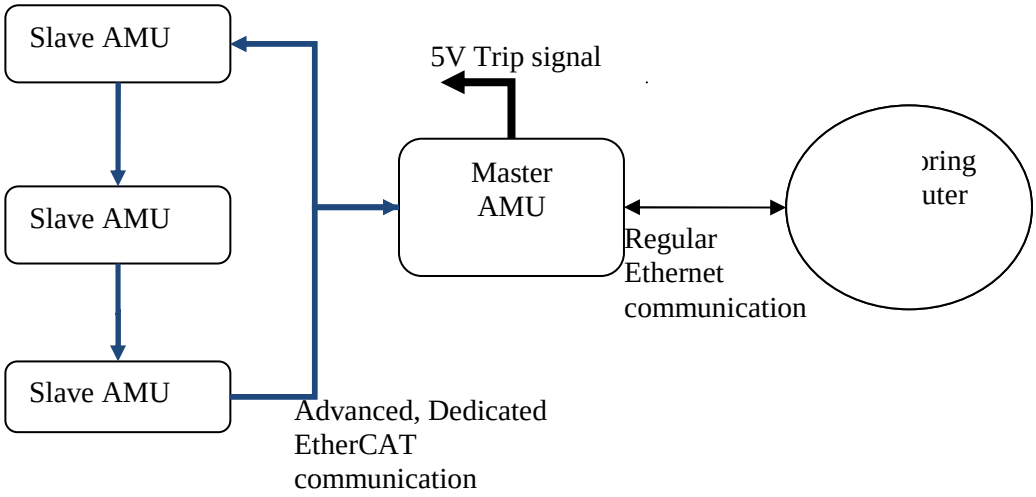

Fig. 7.4. EtherCAT system prototype

In the new protection system, there are 3 slave AMU units, connected to 3 CTs, doing the data acquisition job, 1 master unit, connected to the slave AMUs, implementing the data synchronization between several AMUs and the center computer for protection and monitoring purpose. The communication between the master AMU and the slave AMU is the dedicated, deterministic and reliable EtherCAT communication. The communication between the master AMU to the computer is the regular Ethernet communication.

7.1 Test with single zone test bed

This test is running on the same test bed discussed on Chapter 3 and Chapter 6. The IFM algorithm is updated to work with the compact-rio system, The IFM program is running on the master AMU instead of the computer in order to reduce the communication segment lag between the master AMU and the computer. In this way, the delay caused by slow Ethernet can be eliminated.

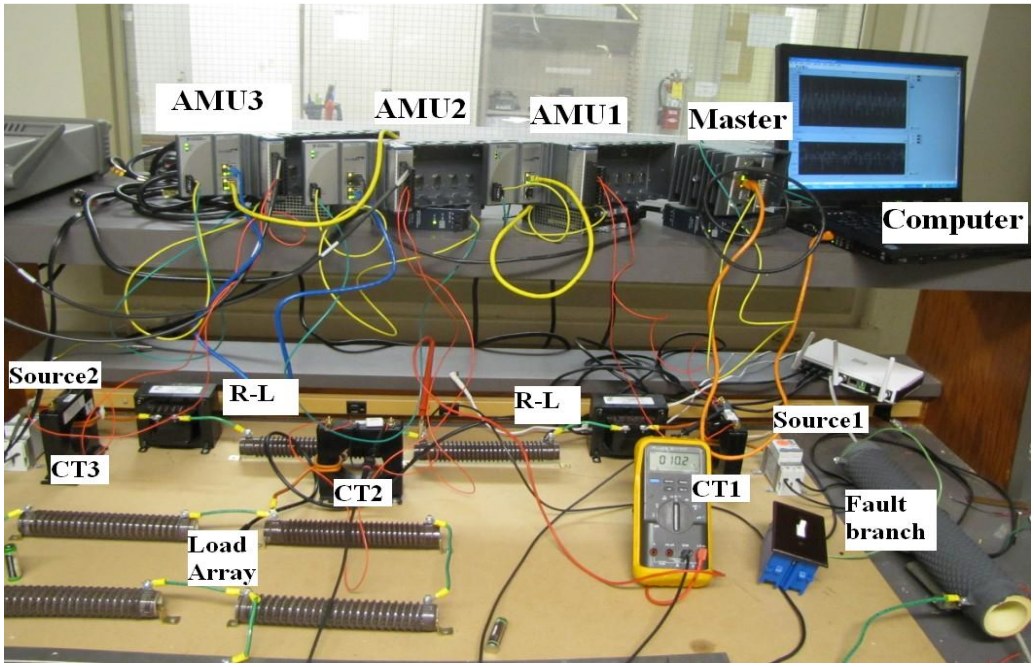

Fig. 7.5. Picture of the new protection system with test bed

The IFM program, which is the same as in Chapter 6, gathers the samples from the EtherCAT frame and calculates the received samples with the protective algorithm. Meanwhile, the timer of the IFM program is set to 3, which means if the last 3 measuring time points indicate a fault, a trip signal (step-up signal) will be generated and sent to the circuit breakers.

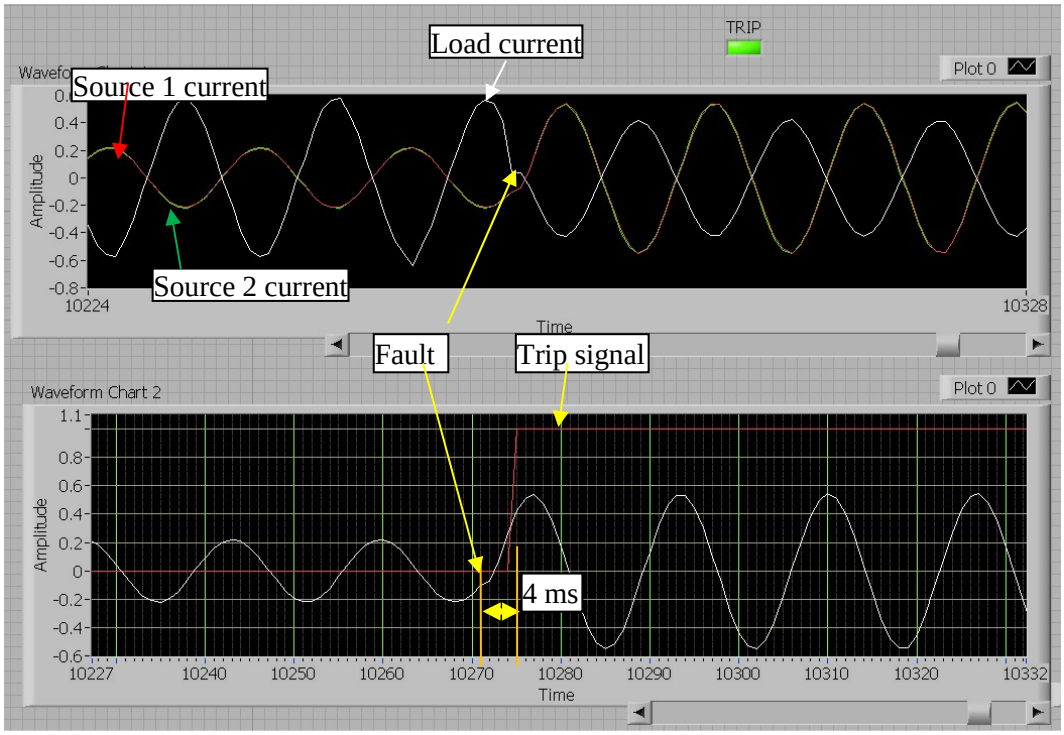

Fig. 7.6. Fault inside zone

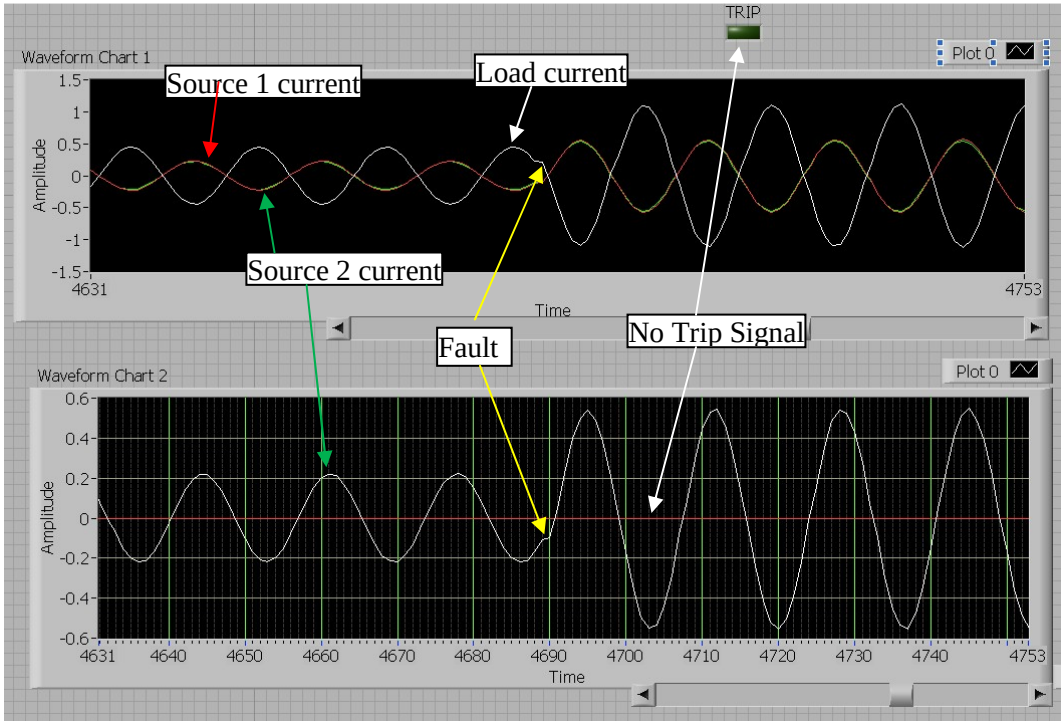

Fig. 7.7. Fault outside zone

The system is tested on the same test-bed described in Chapter 4 and Chapter 6.

The result is shown in the Fig.7.6 and Fig.7.7, the upper chart shows the current

information from source 1, load and source 2, notice that they are perfectly synchronized; the lower chart shows the trip signal along with the source 2 current waveform. When a fault was initialized inside the zone as in Fig. 7.6, the source current increases significantly, and the differential unit starts to send the “fault == true” signal to the timer, and 4 ms later, a trip signal is generated. In Fig. 7.7, when a fault happened out of the zone, the current waveform is seminar to Fig. 7.6, however, as IFM do not see a fault inside the zone, no trip signal is generated. Hence, the real time monitor and operation function is achieved.

Currently, only 3 slave units, which stands for 3 measurement points are included for demonstration purpose. According to a National Instrument application engineer, the same result can be expected for a system with more than 16 salve units which are sufficient for a FREEDM protection zone and that will be a part of future work.

7.2 Protection system reliability statistic analysis

The test in 7.1 has been repeated for 100 times for statistic analysis purpose. The results are measured by an oscilloscope. The tests result is shown in Fig. 7.8.

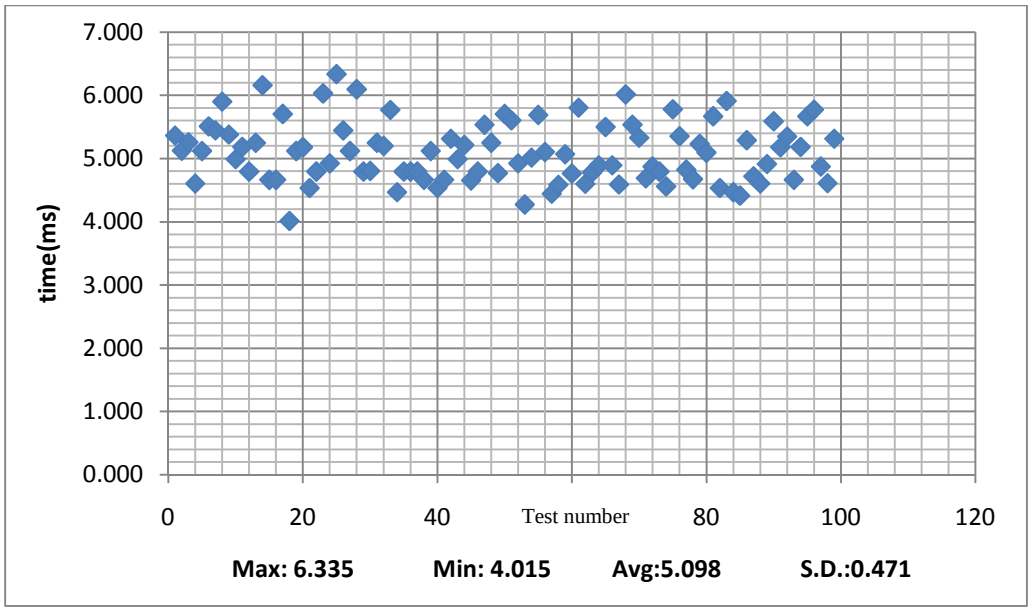

Fig. 7.8. Statistic experiment result

As the experiment results stated in the Fig. 7.8, the average operation time of the protection system is 5.119ms, the maximum operation delay is 6.336, the minimum operation delay is 4.015ms, and the standard deviation is 0.486. The maximum percentage time error is calculated as:

(maximum delay – minimum delay) / average delay = (6.336-4.015)/5.119=45.3%

the maximum time error is not small, but it's still in a reasonable range compare to the commercial relays. As tests conducted in chapter 4, the commercial have similar error around 40%. The time error in operations is mainly due to the uncertain communication and data processing delay.

For the protection system, the key performance indicator is the operation accuracy. So far, the success operation rate observed in the tests is 100%, showing a high operation accuracy and reliability of the system.

7.3 Experimental test on RTDS

The Real Time Digital Power System Simulator (RTDS) technology provides a good tool to study the power system and is widely used for power system real time simulations. The recent additional capability of simulating power electronic switches used in Voltage Source Converters (VSC) on GPC (Gigabyte Processing Card) with significantly smaller time steps makes the detailed modeling of the power electronics devices in the FREEDM possible. The RTDS hardware consisting of a number of parallel processing cards, including cards for running the simulation as well as inter-rack communications (IRC), workstation interface (WIF), and I/O cards. These I/O cards allow real hardware to be interfaced into multiple points within the simulation. The hardware-in-loop function offers the possibility of integrating protection system hardware in the simulation.

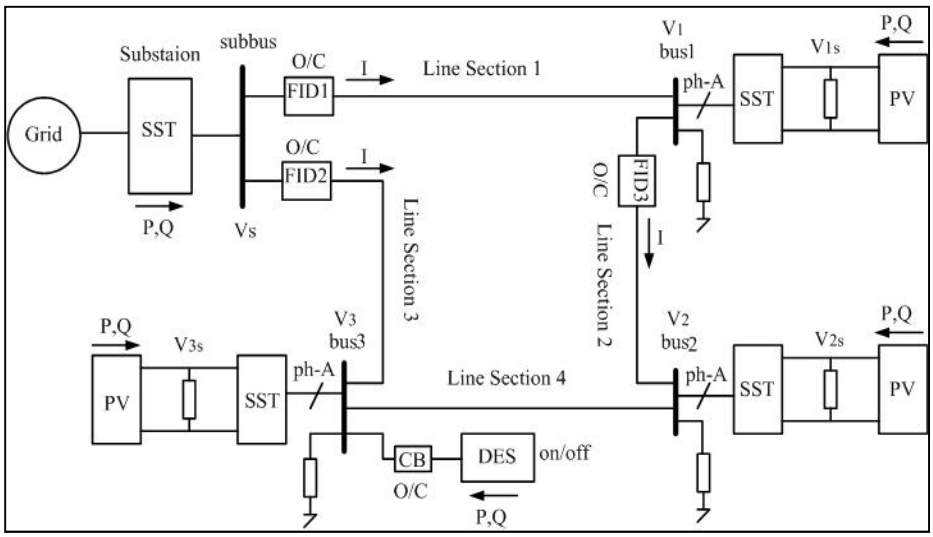

Fig. 7.9. RTDS Virtual FREEDM system diagram [30]

A comprehensive digital FREEDM system model (Virtual FREEDM) includes the novel features of the electronics component such as SST, DES and PV are modeled in detail on RTDS by Florida State University (FSU) [29], shown in Fig. 7.9. The Real-time analog signal which reflects the FREEDM system simulation result can be observed at

the output port and it is connected to the protection system. This ensures the feasibility of a complete study and evaluation of how the protection system cooperates with the FREEDM hardware loop by utilizing the existing virtual RTDS lab. to facilitate the interfacing of newly developed protection equipment.

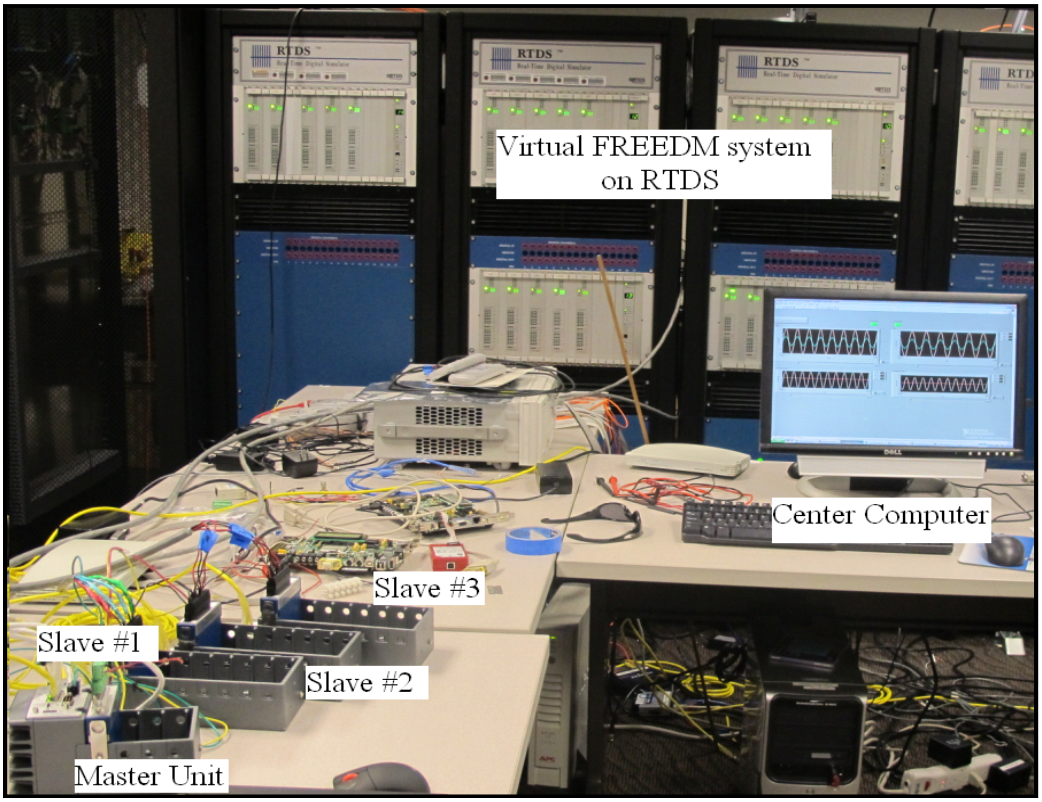

Fig. 7.10. Experimental Version

Fig. 7.10 shows the experiment scope in the RTDS laboratory scope. The experimental system diagram and connection diagram are shown in Fig. 7.11. As the RTDS computation block simulates the virtual FREEDM, the analog I/O block outputs the current and voltage signal of virtual CTs and VTs in the simulation simultaneously. And the slave unit is connected to the corresponding analog I/O part respect to the virtual CTs in the simulation, so the current information in the virtual system is captured. Then, the slave units send the digitized current value to the master unit where the IFM algorithm is running. When the fault is simulated in the virtual FREEDM, the trip-signal

is generated from the master unit and sent back to RTDS, and then the RTDS clears the fault by interrupting the circuit breaker in the virtual system. Faults in various locations have been tested, and the protection system clearly distinguishes fault locations in the RTDS.

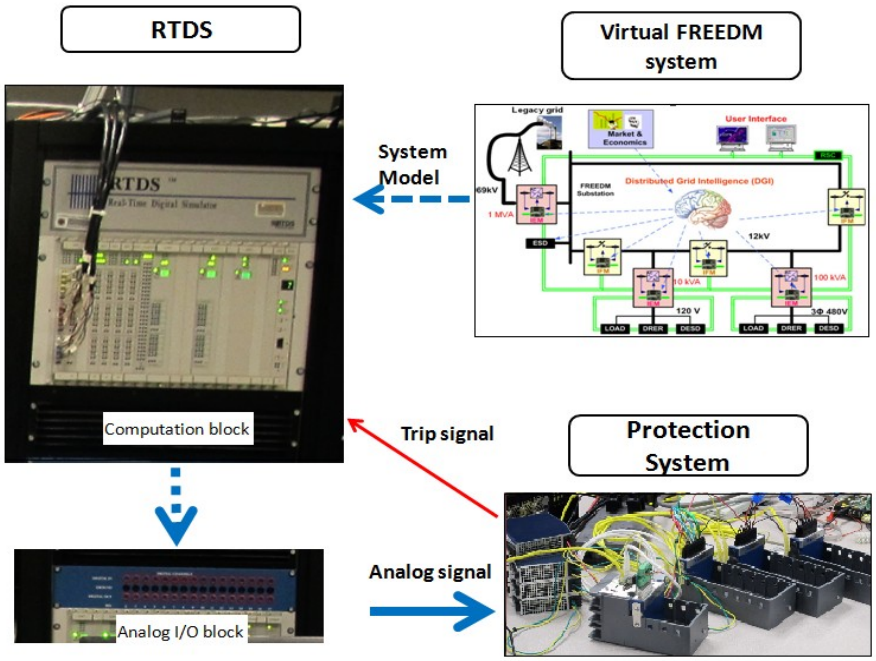

Fig. 7.11. Closed-loop testing diagram

Fig. 7.12. IFM program screen shoot

For the fault happens inside the virtual protective zone of the virtual FREEDM system on RTDS, the IFM program detects the fault and generator a trip signal about 3 ms after fault happens as in Fig.7.12.

For the fault happens out of the zone, The IFM program screen shot is shown in Fig. 7.13. As IFM do not see a fault inside the zone, no trip signal is generated.

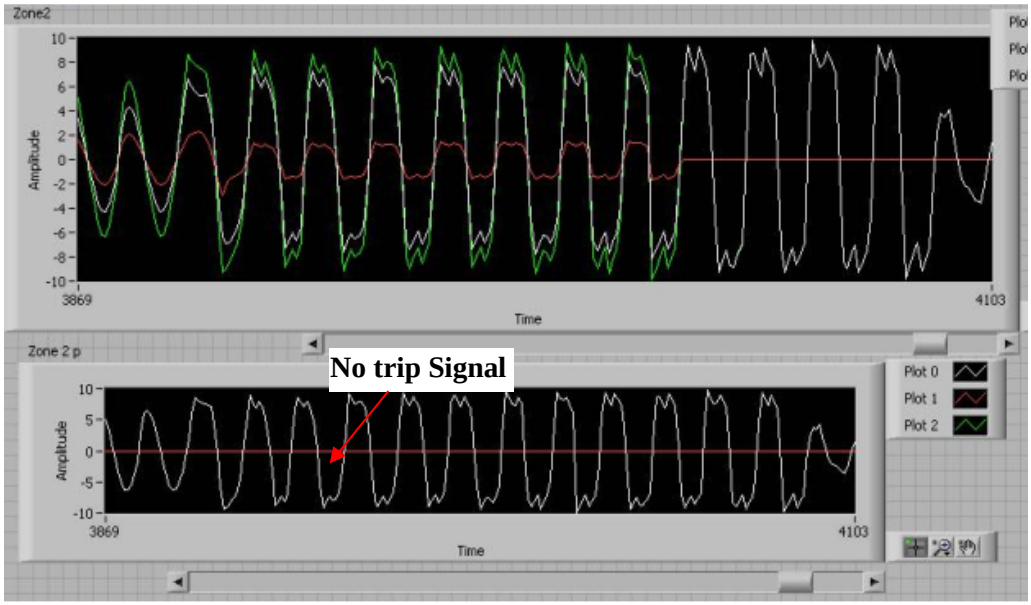

Fig. 7.13. IFM program screen shoot

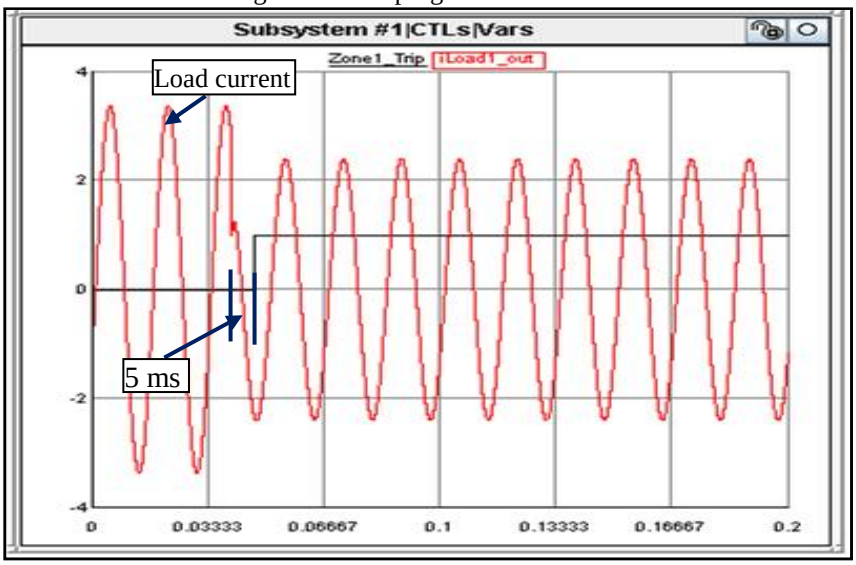

Fig. 7.14. Test result obtained on RTDS

Fig. 7.14 shows the test result obtained on the RTDS. The sinusoidal signal is the load current. Initially, the load is running at rated condition, when a fault happens, the

load current drops suddenly as in Fig. 7.14. And 5ms later, the RTDS receives the trip signal from the protection system. The 5ms is the overall system response time. The overall delay is measured in the following way that starts from the fault happening in the RTDS system to the receiving trip signal returning to the RTDS. All delays of the protection system are included. As discussed in Chapter 5, the IFM program takes 3ms for fault determination, the remaining 2ms is the systematic delay including data sampling, digitizing, data packaging and data communication as well as all devices' physical delay. Thus, a system has the capability to handle the protection requirements of the FREEDM smart grid and the proposed quarter cycle response time is achieved.

CHAPTER 8

CONCLUSIONS AND FUTURE WORK

Main Conclusions

The goal of this research work is to design and develop an ultra fast and reliable protection system for the FREEDM system which is a smart distribution power network. A comprehensive protection strategy, objective oriented designed for the FREEDM system, is proposed. The fault consequence and protection solution is analyzed. The IFM program that ensures a fast and reliable protection for the FREEDM system has been developed. A very fast protection response time is achieved. For the research works done in this project, conclusions can be drawn as follows.

- A comprehensive protection strategy, objective oriented designed for the FREEDM smart distribution system, is proposed. The protection solution is presented.
- A commercial differential and overcurrent relay (SEL 387) is applied on a scaled FREEDM test bed. This result proves the concept of the proposed protection strategy. The response time of existing differential commercial relays is about 2 cycles.
- The IFM real time program is accomplished. It has been tested in a virtual as well as physical environment.
- A hardware system based on micro-controllers with Ethernet communication is implemented. The instantaneous sample calculation is not feasible because the extremely high requirement of time synchronization is not possible due to the delay of physical Ethernet communications. The solution is to use the peak to peak value instead of instantaneous value. This alteration will delay the system response time to a cycle.

- A novel protection hardware based on NI compact-rio with advanced EtherCAT communication is implemented. The new system was tested on both the scaled physical single zone test-bed and verified by the virtual FREEDM system on RTDS.
- An ultra fast protection system response time of 5 ms is achieved, which is the fastest protection system for distribution level electrical system.

Future Work

The future work will be concentrated on the following aspects:

· FREEDM system site test of the proposed protection system.

· Extend the current EtherCAT based system to 8 or more units, which will be sufficient for a protective zone.

· Explore better performance microcontroller or digital signal processors (DSP) [31] which have higher basic frequency or higher bit system for AMUs. This will improve the accuracy of the sampler, and also increases the speed of the sampler which will provide more samples in a cycle.

· Explore the possibility of applying advance protocols, such as the DNP3 [32] IEC 61850 [33] and IEEE 1588 [34] .

REFERENCES

[1] FREEDM system center, available at www.freedm.ncsu.edu. accessible at April 2011

[2] Ravi Akellay, Fanjun Meng, “Distributed Load Balancing for FREEDM system,” IEEE International Conference on Smart Grid Communications, Aug. 2010, pp.7-12.

[3] Hughes, W. L.; Summers, C. S.; Allison, H. J.; “An Energy System For The Future,” Industrial Electronics, May 1963, pp. 108-111.

[4] J. C. Kapur, "Socio-economic considerations in the utilization of solar energy in underdeveloped areas," United Nations Conf. of New Sources of Energy, Rome, Italy, 1981, pp. 5 8-66.

[5] Litos Strategic, “The Smart Grid: An Introduction,” prepared for the U.S. Department of Energy, 2008.

[6] Reuters, “Solar Power 50% Cheaper By Year End - Analysis Reuters,” November 24, 2009.

[7] Alex, Huang, “FREEDM System – A Vision for the Future Grid,” IEEE conference on Power and Energy Society General Meeting, July, 2010.

[8] Karady, G.G., Xing Liu; “Fault Management and Protection of FREEDM Systems,” IEEE Power and Energy Society General Meeting, July, 2010.

[9] Subhashish Bhattacharya, Alex Huang, ect., “Design and Development of Gen-1 Silicon based Solid State Transformer (SST) Converters for 10kVA SST,” FREEDM Annual Conference and NSF Site, 2009.

[10] M. Steurer, O. Vodyakho, D. Neumayr and etc, “Development of Solid State Fault Isolation Devices for Future Power Electronic based Distribution Systems,” FREEDM Annual Conference and NSF Site, 2010.

[11] Energy Industry Background, available at http://globaledge.msu.edu/industries/energy/background/, accessible on April 2011.

[12] Zones Of Protection, available at www.aeusp.com/fundamentals/dvprz, accessible on April, 2011.

[13] Principle of Overcurrent Protection, available at http://www.scribd.com/doc/25082435/Overcurrent-Relays-NEMA-Numbers-51-50, accessible on April, 2011.

[14] IEEE Standard Inverse-Time Characteristic Equations for Overcurrent Relays.

[15] Anderson, P, "Power System Protection," pp. 469, 1999.

[16] N.Zhang, X.Z.Dong, Z.Q.Bo, S.Richards, A. Klimek, "Universal Pilot Wire Differential Protection for Distribution System," IET 9th International Conference on Developments in Power System Protection, pp.224-228, 2008

[17] Hunt, R. ; Adamiak, M. ; King, A. ; McCreery, S. "Pilot protection," IEEE Industry Applications Magazine, Vol. 15, pp 51-60, Sep. 2009.

[18] Introduction to Protective Relaying, available at http://xnet.rrc.mb.ca/janaj/differential_protection, accessible on April, 2011.

[19] Dale Finney, Zhiying Zhang, "Ultra fast distance protection," Developments in Power System Protection conference, 2010.

[20] Abhisek Ukil, Bernhard Deck, and Vishal H. Shah, "Current-Only Directional Overcurrent Relay" IEEE Sensors Journal, Vol. 11, No. 6, June 2011.

[21] George Karady, Hui Zhang, "Concept of FREEDM loop line fault protection," FREEDM Annual Conference and NSF Site, 2009.

[22] Thirumalai, A.; Liu, X.; Karady, G.G., "Ultra fast pilot protection of a looped distribution system," IEEE conference on PowerTech, Trondheim, 2011.

[23] SEL-387E Current Differential and Voltage Relay, available at http://www.selinc.com/sel-387e/, accessible on April 2011.

[24] What is LabVIEW, available at http://www.ni.com/labview/, accessible on April 2011.

[25] Anonymous, SEL-2407 Satellite-Synchronized Clock Instruction Manual, Schweitzer Engineering Laboratories, 2010.

[26] Anonymous, MPLAB C18 C Compiler User's Guide, Microchip Technology Inc., 2002.

[27] A.L.Hoi, R.J. Coomer, “Micro-controller for substation and network automation,” Third International Conference on Future Trends in Distribution switchgear, pp.84-89, 1990.

[28] D. Jansen, H. Buttner, “Real-time Ethernet the EtherCAT solution,” Computing & Control Engineering Journal, March, 2004, pp. 16.

[29] NI co., Intrudction to EtherCAT, available at http://zone.ni.com/devzone/cda/tut/p/id/7299

[30] P. Tatcho, Y. Jian and H. Li, “A real time digital test bed for a smart grid using RTDS,” *IEEE PES General Meeting*, 2011

[31] A. Spanias, V. Atti, “On-line signal processing using J-DSP,” IEEE Signal Processing Letters, 2004, vol. 11, pp. 924-825.

[32] IEEE Standard for Electric Power Systems Communications- Distributed Network Protocol (DNP3), 2010.

[33] IEEE Standard for Electrical Power System Device Function Numbers, Acronyms, and Contact Designations (IEC 61850), 2008.

[34] L.Shuai,L.Yueming. J. Yuefeng, “An Enhanced IEEE 1588 Time Synchronization for Asymmetric Communication Link in Packet Transport Network,” IEEE Communication Letters, vol.14, no.8, pp.764-766

APPENDIX A

SEL 387 RELAY CODE

Level 1
=>2AC /* access to level 2*/

****
Relay system setting
****

CONFIG. SETTINGS
Relay Identifier (39 Characters) /* name*/
RID =FREEDM
?
Terminal Identifier (59 Characters)
TID =Zone1
?
Enable Wdg1 in Differential Element(Y,N,Y1) E87W1 = Y
/* choose Winding differential protective element */

Enable Wdg2 in Differential Element(Y,N,Y1) E87W2 = Y
Enable Wdg3 in Differential Element(Y,N,Y1) E87W3 = Y
Enable Wdg1 O/C Elements and Dmd. Thresholds(Y,N) EOC1 = Y

/* choose Winding overcurrent protective element */
Enable Wdg2 O/C Elements and Dmd. Thresholds(Y,N) EOC2 = Y
Enable Wdg3 O/C Elements and Dmd. Thresholds(Y,N) EOC3 = Y

/* other protective element selection */
Enable Combined O/C Elements(Y,N) EOCC = N
Enable Volts/Hertz Protection(Y,N) E24 = N
Enable Undervoltage Protection(Y,N) E27 = N
Enable Overvoltage Protection(Y,N) E59 = N
Enable Frequency Protection(N,1-6) E81 = N
Enable SELogic Set 1(Y,N) ESLS1 = N
Enable SELogic Set 2(Y,N) ESLS2 = N
Enable SELogic Set 3(Y,N) ESLS3 = N

****
General environment setting
****

GENERAL DATA /* CT input confignation*/

Wdg 1 CT Connection (D,Y) W1CT = Y
Wdg 2 CT Connection (D,Y) W2CT = Y
Wdg 3 CT Connection (D,Y) W3CT = Y
Wdg 1 CT Ratio (1-50000) CTR1 = 20
Wdg 2 CT Ratio (1-50000) CTR2 = 20
Wdg 3 CT Ratio (1-50000) CTR3 = 20
PT Ratio (1-6500) PTR = 2000
Compensation Angle(0-360deg) COMPANG = 0

/ Delta-wye angle compensation*/*

Voltage-Current Winding(1,2,3,12) VIWDG = 12

RESTRICTED EARTH FAULT
Enable 32I(SELogic Equation)
E32I =0

? >

****
Protection scheme setting
****

WINDING 1 ELEMS */* protective element setting for winding 1*/*

PHASE O/C ELEMS
Phase Def-Time O/C Lvl 1 PU(OFF,0.25-100A,sec) 50P11P = 1.00
/ overcurrent setting for winding 1*/*

Phase Lvl 1 O/C Delay(0.00-16000.00cyc) 50P11D = 0.25
50P11 Torque Control (SELogic Equation)
50P11TC =0
Phase Inst O/C Lvl 2 PU(OFF,0.25-100.00A,sec) 50P12P = OFF
Phase Inst O/C Lvl 3 PU(OFF,0.25-100.00A,sec) 50P13P = 0.50

/ instant overcurrent setting for winding 1*/*
Phase Inst O/C Lvl 4 PU(OFF,0.25-100.00A,sec) 50P14P = 4.00
Phase Inv-Time O/C PU(OFF,0.50-16.00A,sec) 51P1P = 4.00
Phase Inv-Time O/C Curve(U1-U5,C1-C5) 51P1C = U2
Phase Inv-Time O/C Time-Dial(0.50-15.00) 51P1TD = 3.00
Phase Inv-Time O/C EM Reset(Y,N) 51P1RS = Y
51P1 Torque Control (SELogic Equation)
51P1TC =1

? >

WINDING 2 ELEMS */* Off OC unit for winding 2*/*

PHASE O/C ELEMS
Phase Def-Time O/C Lvl 1 PU(OFF,0.25-100A,sec) 50P21P = OFF

WINDING 3 ELEMS

PHASE O/C ELEMS
Phase Def-Time O/C Lvl 1 PU(OFF,0.25-100A,sec) 50P31P = 1.00

MISC. TIMERS

Trip Duration Delay (4.000-8000.000 cyc) TDURD = 9.000

TRIP LOGIC */* trip logic equations*/*

TR1 =50P11T + 51P1T + 51Q1T + OC1 + LB3

? >

CLOSE LOGIC

52A1 =IN101

? >

EVENT TRIGGER */* Event Trigger logic equations*/*

ER =/50P11 + /51P1 + /51Q1 + /51P2 + /51Q2 + /51P3

? >

OUT101 =TRIP1 */* Output Contact Logic*/*

? >

E87W1 = N E87W2 = N E87W3 = N
EOC1 = Y EOC2 = Y EOC3 = Y EOCC = N
E24 = N E27 = N E59 = N
E81 = N
ESLS1 = N ESLS2 = N ESLS3 = N

W1CT = Y W2CT = Y W3CT = Y
CTR1 = 20 CTR2 = 20 CTR3 = 20
PTR = 2000 COMPANG = 0 VIWDG = 12 TPVI = N

E32I =0

50P11P = 1.00 50P11D = 0.25 50P11TC =1
50P12P = OFF
50P13P = 0.50 50P14P = 4.00

Press RETURN to continue
51P1P = 4.00 51P1C = U2 51P1TD = 3.00 51P1RS = Y
51P1TC =1

50Q11P = OFF 50Q12P = OFF
51Q1P = 6.00 51Q1C = U2 51Q1TD = 3.00 51Q1RS = Y
51Q1TC =1

50N11P = OFF 50N12P = OFF
51N1P = OFF
DATC1 = 15 PDEM1P = 7.00 QDEM1P = 1.00 NDEM1P = 1.00

50P21P = OFF 50P22P = OFF
50P23P = 0.50 50P24P = 3.50
51P2P = 3.50 51P2C = U2 51P2TD = 3.50 51P2RS = Y
51P2TC =1

50Q21P = OFF 50Q22P = OFF
51Q2P = 5.25 51Q2C = U2 51Q2TD = 3.50 51Q2RS = Y
51Q2TC =1

Press RETURN to continue

50N21P = OFF 50N22P = OFF
51N2P = OFF
DATC2 = 15 PDEM2P = 7.00 QDEM2P = 1.00 NDEM2P = 1.00

50P31P = 1.00 50P31D = 0.00 50P31TC =1
50P32P = OFF
50P33P = 0.50 50P34P = 4.00
51P3P = 4.00 51P3C = U2 51P3TD = 1.30 51P3RS = Y
51P3TC =1
50Q31P = OFF 50Q32P = OFF
51Q3P = OFF
50N31P = OFF 50N32P = OFF
51N3P = OFF
DATC3 = 15 PDEM3P = 7.00 QDEM3P = 1.00 NDEM3P = 1.00
TDURD = 9.000 CFD = 60.000

****
Output setting
****

TR1 =50P11T + 51P1T + 51Q1T + OC1 + LB3 */*trip logtic setting*/*
TR2 =51P2T + 51Q2T + OC2
TR3 =50P31 + 51P3T + OC3
TR4 =87R + 87U
ULTR1 =!50P13
ULTR2 =!50P23
ULTR3 =!50P33
ULTR4 =!(50P13 + 50P23 + 50P33)
52A1 =IN101
52A2 =IN102
52A3 =IN103

*/*recloser setting*/*

CL1 =CC1 + LB4 + /IN104
CL2 =CC2 + /IN105
CL3 =CC3 + /IN106
ULCL1 =TRIP1 + TRIP4
ULCL2 =TRIP2 + TRIP4
ULCL3 =TRIP3 + TRIP4
ER =/50P11 + /51P1 + /51Q1 + /51P2 + /51Q2 + /51P3

*/*output setting*/*

OUT101 =TRIP1
OUT102 =TRIP2
OUT103 =TRIP3
Press RETURN to continue
OUT104 =TRIP4
OUT105 =CLS1
OUT106 =CLS2
OUT107 =CLS3

=>>sho 1
Group 1 */* setting for stradgy group 1*/*

****
Overcurrent Protection Setting
****

/ select winding*/*

RID =FREEDM
TID =OC
E87W1 = N E87W2 = N E87W3 = N
EOC1 = Y EOC2 = Y EOC3 = Y EOCC = N
E24 = N E27 = N E59 = N
E81 = N
ESLS1 = N ESLS2 = N ESLS3 = N

/ disable differential unit, enable overcurrent unit*/*

W1CT = Y W2CT = Y W3CT = Y
CTR1 = 200 CTR2 = 200 CTR3 = 200
PTR = 2000 COMPANG = 0 VIWDG = 12 TPVI = N
E32I =0
50P11P = 1.50 50P11D = 1.50 50P11TC =1
50P12P = 2.00 50P12TC =1
Press RETURN to continue
50P13P = OFF 50P14P = OFF

51P1P = OFF
50Q11P = OFF 50Q12P = OFF
51Q1P = OFF
50N11P = OFF 50N12P = OFF
51N1P = OFF
DATC1 = OFF
50P21P = 1.00 50P21D = 1.50 50P21TC =1
50P22P = 2.50 50P22TC =1
50P23P = OFF 50P24P = OFF
51P2P = OFF
50Q21P = OFF 50Q22P = OFF
51Q2P = OFF
50N21P = OFF 50N22P = OFF
51N2P = OFF
DATC2 =
Press RETURN to continue
50P31P = 1.00 50P31D = 1.50 50P31TC =1
50P32P = 2.30 50P32TC =1
50P33P = OFF 50P34P = OFF
51P3P = OFF
50Q31P = OFF 50Q32P = OFF
51Q3P = OFF
50N31P = OFF 50N32P = OFF
51N3P = OFF
DATC3 = OFF
TDURD = 4.000 CFD = 60.000
TR1 =50P11T + 51P1T + 51Q1T + OC1 + LB3
TR2 =51P2T + 51Q2T + OC2
TR3 =50P31 + 51P3T + OC3
TR4 =87R + 87U
ULTR1 =!50P13
ULTR2 =!50P23
ULTR3 =!50P33
Press RETURN to continue
ULTR4 =!(50P13 + 50P23 + 50P33)
52A1 =IN101
52A2 =IN102
52A3 =IN103
CL1 =CC1 + LB4 + /IN104
CL2 =CC2 + /IN105
CL3 =CC3 + /IN106
ULCL1 =TRIP1 + TRIP4
ULCL2 =TRIP2 + TRIP4
ULCL3 =TRIP3 + TRIP4
ER =/50P11 + /51P1 + /51Q1 + /51P2 + /51Q2 + /51P3
OUT101 =TRIP1
OUT102 =TRIP2
OUT103 =TRIP3
OUT104 =TRIP4
OUT105 =CLS1

OUT106 =CLS2
OUT107 =CLS3

/ enable differential unit, enable overcurrent unit*/*
Enable Wdg1 in Differential Element(Y,N,Y1) E87W1 = Y
Enable Wdg2 in Differential Element(Y,N,Y1) E87W2 = Y
Enable Wdg3 in Differential Element(Y,N,Y1) E87W3 = Y
Enable Wdg1 O/C Elements and Dmd. Thresholds(Y,N) EOC1 = Y
Enable Wdg2 O/C Elements and Dmd. Thresholds(Y,N) EOC2 = Y
Enable Wdg3 O/C Elements and Dmd. Thresholds(Y,N) EOC3 = Y
Enable Combined O/C Elements(Y,N) EOCC = N
Enable Volts/Hertz Protection(Y,N) E24 = N
Enable Undervoltage Protection(Y,N) E27 = N
Enable Overvoltage Protection(Y,N) E59 = N
Enable Frequency Protection(N,1-6) E81 = N
Enable SELogic Set 1(Y,N) ESLS1 = N
Enable SELogic Set 2(Y,N) ESLS2 = N
Enable SELogic Set 3(Y,N) ESLS3 = N

****
Input transformer setting
****

GENERAL DATA
Wdg 1 CT Connection (D,Y) W1CT = Y
Wdg 2 CT Connection (D,Y) W2CT = Y
Wdg 3 CT Connection (D,Y) W3CT = Y
Wdg 1 CT Ratio (1-50000) CTR1 = 20
Wdg 2 CT Ratio (1-50000) CTR2 = 20
Wdg 3 CT Ratio (1-50000) CTR3 = 20
PT Ratio (1-6500) PTR = 2000
Compensation Angle(0-360deg) COMPANG = 0
Voltage-Current Winding(1,2,3,12) VIWDG = 12

RESTRICTED EARTH FAULT
Enable 32I(SELogic Equation)
E32I =0

? >

****
Winding setting
****

WINDING 1 ELEMS

PHASE O/C ELEMS
Phase Def-Time O/C Lvl 1 PU(OFF,0.25-100A,sec) 50P11P = 1.00

Phase Lvl 1 O/C Delay(0.00-16000.00cyc) 50P11D = 0.25
50P11 Torque Control (SELogic Equation)
50P11TC =1

? 1
Phase Inst O/C Lvl 2 PU(OFF,0.25-100.00A,sec) 50P12P = OFF
Phase Inst O/C Lvl 3 PU(OFF,0.25-100.00A,sec) 50P13P = 0.50
Phase Inst O/C Lvl 4 PU(OFF,0.25-100.00A,sec) 50P14P = 4.00
Phase Inv-Time O/C PU(OFF,0.50-16.00A,sec) 51P1P = 4.00
Phase Inv-Time O/C Curve(U1-U5,C1-C5) 51P1C = U2
Phase Inv-Time O/C Time-Dial(0.50-15.00) 51P1TD = 3.00
Phase Inv-Time O/C EM Reset(Y,N) 51P1RS = Y
51P1 Torque Control (SELogic Equation)
51P1TC =1

? >

WINDING 2 ELEMS

PHASE O/C ELEMS
Phase Def-Time O/C Lvl 1 PU(OFF,0.25-100A,sec) 50P21P = OFF

WINDING 3 ELEMS

PHASE O/C ELEMS
Phase Def-Time O/C Lvl 1 PU(OFF,0.25-100A,sec) 50P31P = 1.00

MISC. TIMERS
Trip Duration Delay (4.000-8000.000 cyc) TDURD = 9.000

TRIP LOGIC

TR1 =50P11T + 51P1T + 51Q1T + OC1 + LB3

? >

CLOSE LOGIC

52A1 =IN101

? >

EVENT TRIGGER

ER =/50P11 + /51P1 + /51Q1 + /51P2 + /51Q2 + /51P3

? >

OUTPUT CONTACT LOGIC

OUT101 =TRIP1

? >

*/*status view*/*

E87W1 = N E87W2 = N E87W3 = N
EOC1 = Y EOC2 = Y EOC3 = Y EOCC = N
E24 = N E27 = N E59 = N
E81 = N
ESLS1 = N ESLS2 = N ESLS3 = N

W1CT = Y W2CT = Y W3CT = Y
CTR1 = 20 CTR2 = 20 CTR3 = 20
PTR = 2000 COMPANG = 0 VIWDG = 12 TPVI = N

E32I =0

50P11P = 1.00 50P11D = 0.25 50P11TC =1
50P12P = OFF
50P13P = 0.50 50P14P = 4.00

Press RETURN to continue
51P1P = 4.00 51P1C = U2 51P1TD = 3.00 51P1RS = Y
51P1TC =1

50Q11P = OFF 50Q12P = OFF
51Q1P = 6.00 51Q1C = U2 51Q1TD = 3.00 51Q1RS = Y
51Q1TC =1

50N11P = OFF 50N12P = OFF
51N1P = OFF
DATC1 = 15 PDEM1P = 7.00 QDEM1P = 1.00 NDEM1P = 1.00

50P21P = OFF 50P22P = OFF
50P23P = 0.50 50P24P = 3.50
51P2P = 3.50 51P2C = U2 51P2TD = 3.50 51P2RS = Y
51P2TC =1

50Q21P = OFF 50Q22P = OFF
51Q2P = 5.25 51Q2C = U2 51Q2TD = 3.50 51Q2RS = Y
51Q2TC =1

Press RETURN to continue

50N21P = OFF 50N22P = OFF
51N2P = OFF
DATC2 = 15 PDEM2P = 7.00 QDEM2P = 1.00 NDEM2P = 1.00

50P31P = 1.00 50P31D = 0.00 50P31TC =1
50P32P = OFF
50P33P = 0.50 50P34P = 4.00
51P3P = 4.00 51P3C = U2 51P3TD = 1.30 51P3RS = Y
51P3TC =1
50Q31P = OFF 50Q32P = OFF
51Q3P = OFF
50N31P = OFF 50N32P = OFF
51N3P = OFF
DATC3 = 15 PDEM3P = 7.00 QDEM3P = 1.00 NDEM3P = 1.00
TDURD = 9.000 CFD = 60.000

****

Output setting

****

TR1 =50P11T + 51P1T + 51Q1T + OC1 + LB3
Press RETURN to continue
TR2 =51P2T + 51Q2T + OC2
TR3 =50P31 + 51P3T + OC3
TR4 =87R + 87U
ULTR1 =!50P13
ULTR2 =!50P23
ULTR3 =!50P33
ULTR4 =!(50P13 + 50P23 + 50P33)
52A1 =IN101
52A2 =IN102
52A3 =IN103
CL1 =CC1 + LB4 + /IN104
CL2 =CC2 + /IN105
CL3 =CC3 + /IN106
ULCL1 =TRIP1 + TRIP4
ULCL2 =TRIP2 + TRIP4
ULCL3 =TRIP3 + TRIP4
ER =/50P11 + /51P1 + /51Q1 + /51P2 + /51Q2 + /51P3
OUT101 =TRIP1
OUT102 =TRIP2
OUT103 =TRIP3
Press RETURN to continue
OUT104 =TRIP4
OUT105 =CLS1
OUT106 =CLS2
OUT107 =CLS3

=>>sho 1
Group 1

****

Overcurrent protection setting
****

RID =FREEDM
TID =OC
E87W1 = N E87W2 = N E87W3 = N
EOC1 = Y EOC2 = Y EOC3 = Y EOCC = N
E24 = N E27 = N E59 = N
E81 = N
ESLS1 = N ESLS2 = N ESLS3 = N

W1CT = Y W2CT = Y W3CT = Y
CTR1 = 200 CTR2 = 200 CTR3 = 200
PTR = 2000 COMPANG = 0 VIWDG = 12 TPVI = N
E32I =0
50P11P = 1.50 50P11D = 1.50 50P11TC =1
50P12P = 2.00 50P12TC =1
Press RETURN to continue
50P13P = OFF 50P14P = OFF
51P1P = OFF
50Q11P = OFF 50Q12P = OFF
51Q1P = OFF
50N11P = OFF 50N12P = OFF
51N1P = OFF
DATC1 = OFF
50P21P = 1.00 50P21D = 1.50 50P21TC =1
50P22P = 2.50 50P22TC =1
50P23P = OFF 50P24P = OFF
51P2P = OFF
50Q21P = OFF 50Q22P = OFF
51Q2P = OFF
50N21P = OFF 50N22P = OFF
51N2P = OFF
DATC2 =
Press RETURN to continue
50P31P = 1.00 50P31D = 1.50 50P31TC =1
50P32P = 2.30 50P32TC =1
50P33P = OFF 50P34P = OFF
51P3P = OFF
50Q31P = OFF 50Q32P = OFF
51Q3P = OFF
50N31P = OFF 50N32P = OFF
51N3P = OFF
DATC3 = OFF
TDURD = 4.000 CFD = 60.000
TR1 =50P11T + 51P1T + 51Q1T + OC1 + LB3
TR2 =51P2T + 51Q2T + OC2
TR3 =50P31 + 51P3T + OC3
TR4 =87R + 87U

ULTR1 =!50P13
ULTR2 =!50P23
ULTR3 =!50P33
Press RETURN to continue
ULTR4 =!(50P13 + 50P23 + 50P33)
52A1 =IN101
52A2 =IN102
52A3 =IN103
CL1 =CC1 + LB4 + /IN104
CL2 =CC2 + /IN105
CL3 =CC3 + /IN106
ULCL1 =TRIP1 + TRIP4
ULCL2 =TRIP2 + TRIP4
ULCL3 =TRIP3 + TRIP4
ER =/50P11 + /51P1 + /51Q1 + /51P2 + /51Q2 + /51P3
OUT101 =TRIP1
OUT102 =TRIP2
OUT103 =TRIP3
OUT104 =TRIP4
OUT105 =CLS1
OUT106 =CLS2
OUT107 =CLS3

APPENDIX B

IFM ALOGRITHEM ON LABVIEW

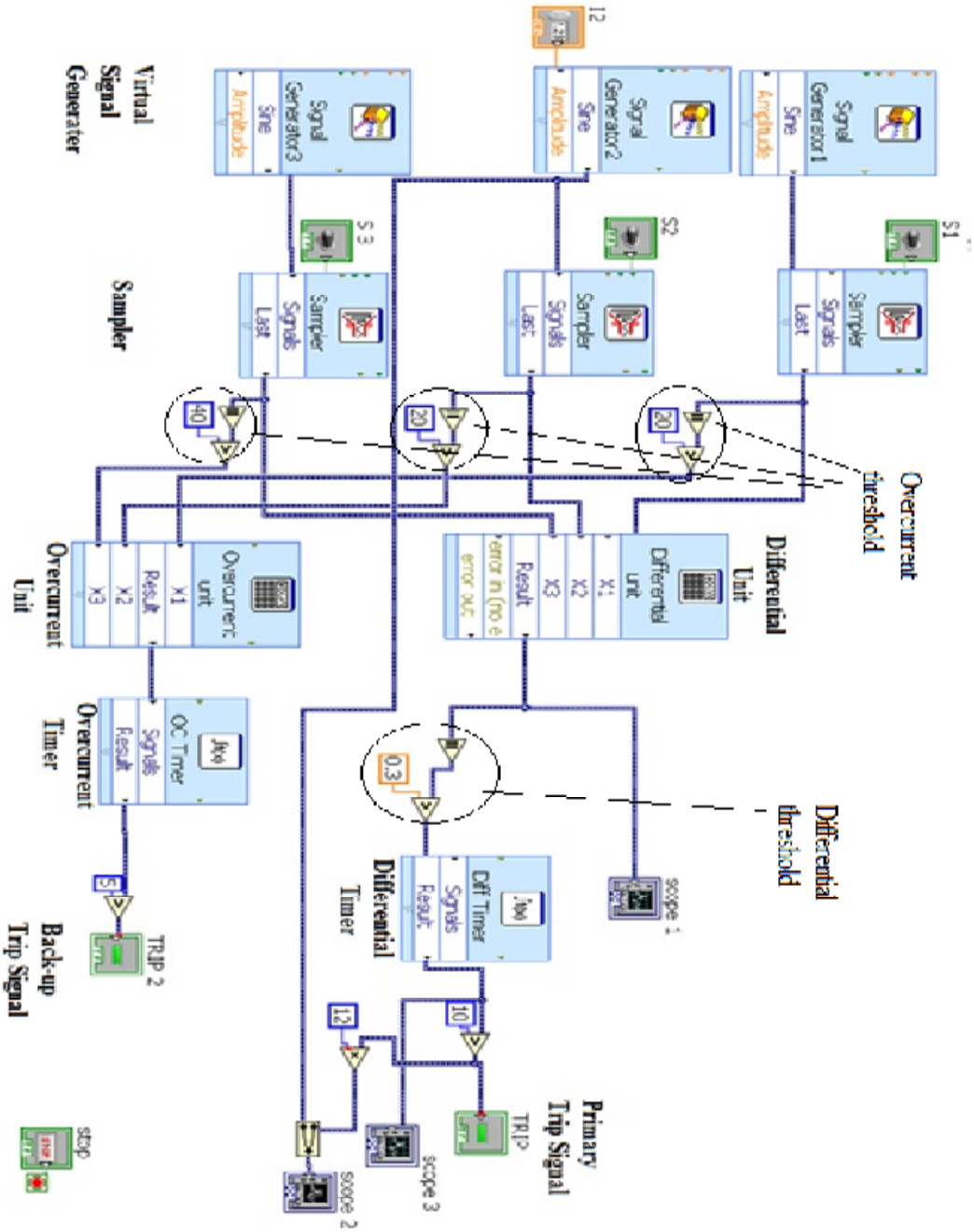
Virtual Signal Generater
Signal Generator1
Signal Generator2
Signal Generator3
Sine
Amplitude
12
S1
S2
S3
Sampler
Signals
Last
Sampler
40
20
20
Overcurrent threshold
Differential Unit
Differential unit
X1
X2
X3
Result
error in
error out
Differential threshold
0.3
scope 1
Overcurrent Unit
Overcurrent unit
Result
Overcurrent Timer
OC Timer
Diff Timer
Differential Timer
5
TRIP 2
Back-up Trip Signal
10
12
TRIP
Primary Trip Signal
scope 3
scope 2
stop

APPENDIX C

FULL LABVIEW CODE FOR AMU

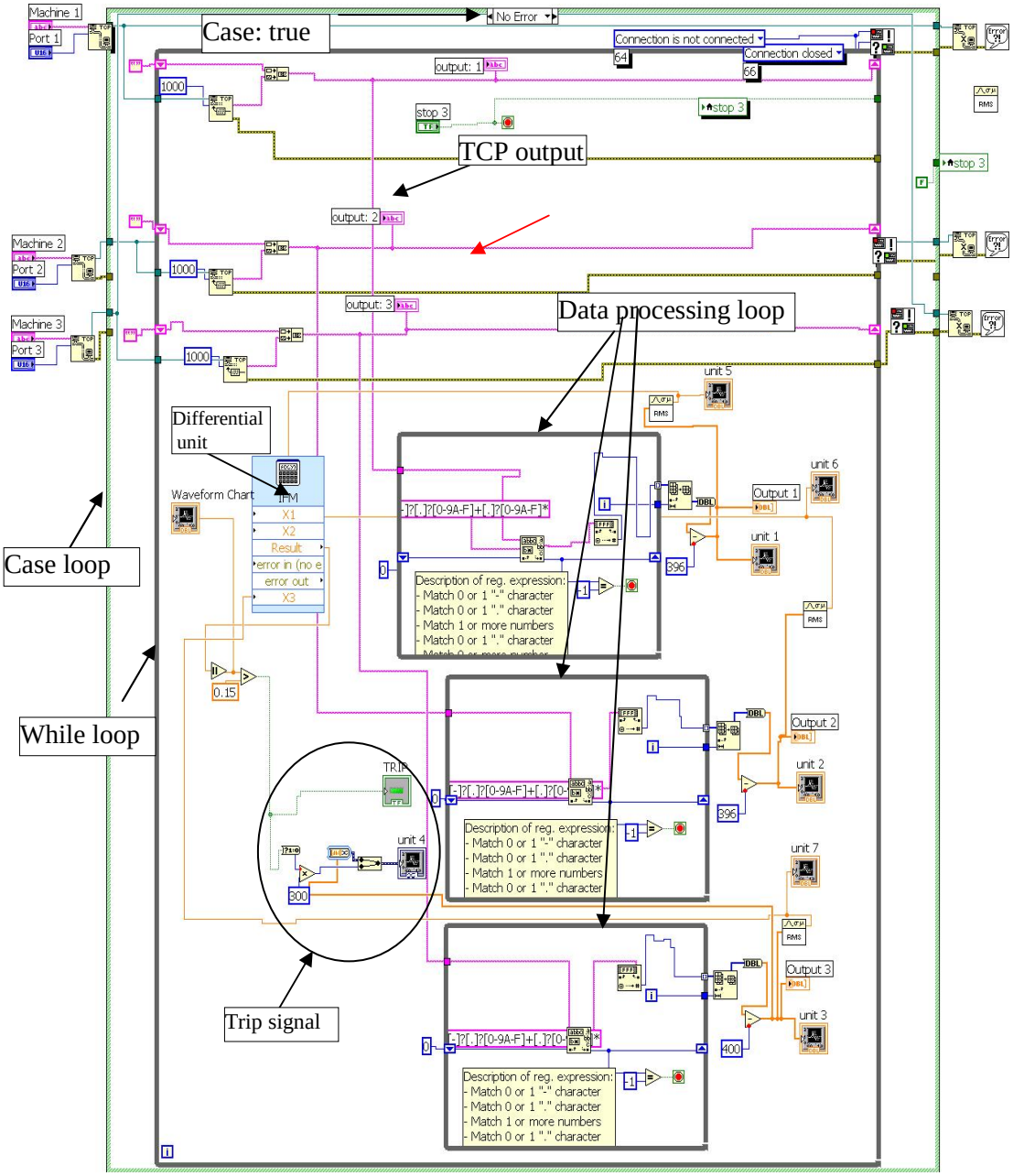
Case: true
TCP output
Data processing loop
Differential unit
Case loop
While loop
Trip signal
Machine 1
Port 1
Machine 2
Port 2
Machine 3
Port 3
No Error
Connection is not connected
Connection closed
output: 1
output: 2
output: 3
stop 3
1000
Waveform Chart
IFFM
X1
X2
Result
error in (no e
error out
X3
0.15
800
400
396
unit 1
unit 2
unit 3
unit 4
unit 5
unit 6
unit 7
Output 1
Output 2
Output 3
TRIP
Description of reg. expression:
- Match 0 or 1 "-" character
- Match 0 or 1 "." character
- Match 1 or more numbers
- Match 0 or 1 "." character

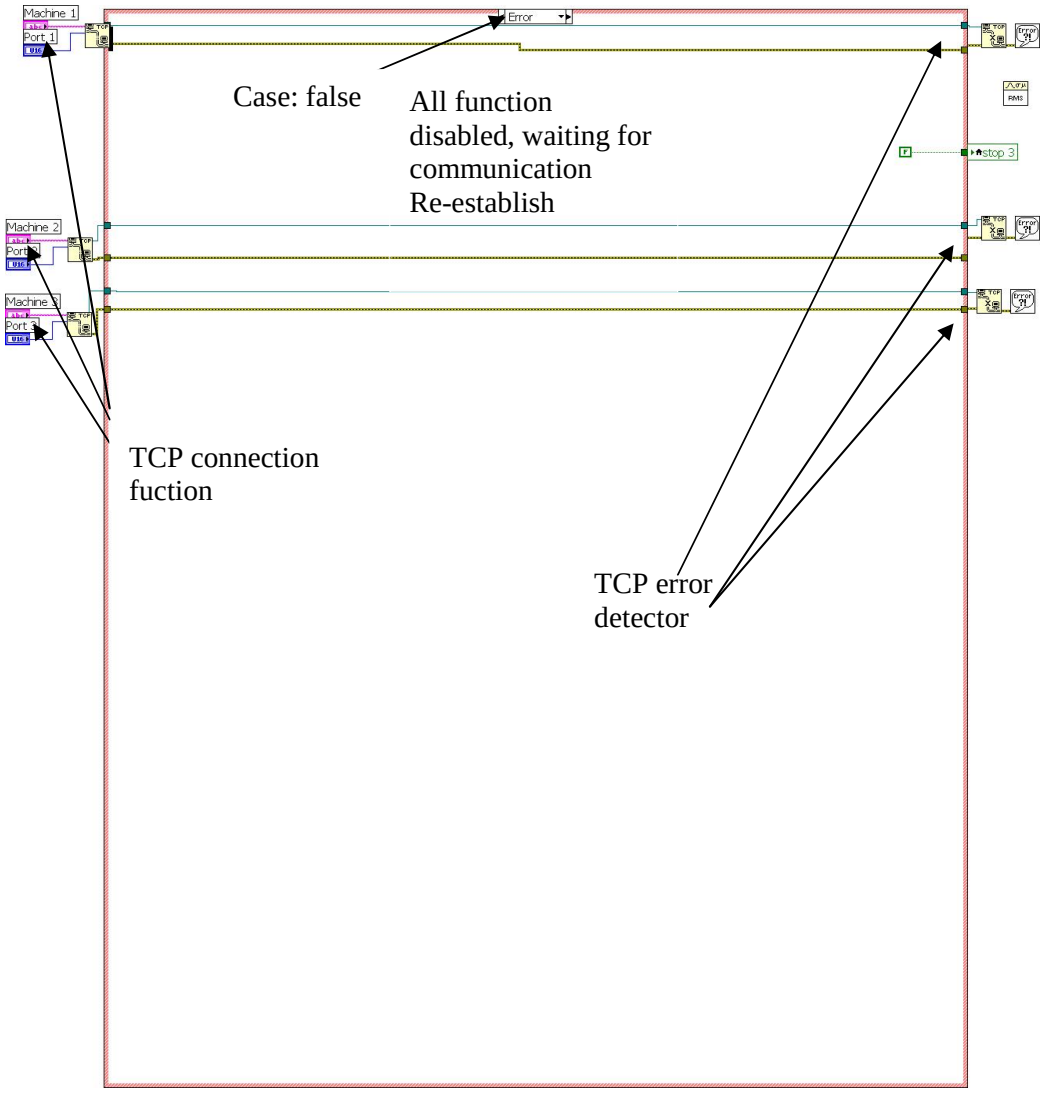
Machine 1
Port 1
Error
Case: false
All function
disabled, waiting for
communication
Re-establish
stop 3
Machine 2
Port 2
Machine 3
Port 3
TCP connection
fuction
TCP error
detector